

Review

# Mechanochemistry: A Green Approach in the Preparation of Pharmaceutical Cocrystals

Mizraín Solares-Briones <sup>1</sup>, Guadalupe Coyote-Dotor <sup>1</sup>, José C. Páez-Franco <sup>1</sup>, Miriam R. Zermeño-Ortega <sup>2</sup>, Carmen Myriam de la O Contreras <sup>2</sup>, Daniel Canseco-González <sup>3</sup>, Alcives Avila-Sorrosa <sup>4</sup> , David Morales-Morales <sup>5,\*</sup>  and Juan M. Germán-Acacio <sup>1,\*</sup> 

- <sup>1</sup> Red de Apoyo a la Investigación, Coordinación de la Investigación Científica-UNAM, Instituto Nacional de Ciencias Médicas y Nutrición SZ, Ciudad de México, C.P. 14000, Mexico; misolb13@gmail.com (M.S.-B.); ibtcoyotedg@gmail.com (G.C.-D.); paez@ic.unam.mx (J.C.P.-F.)
- <sup>2</sup> Facultad de Ciencias Químicas, Universidad Autónoma de Chihuahua, Circuito Universitario No. 1, Nuevo Campus Universitario, Apdo. Postal 1552, Chihuahua, C.P. 31125, Mexico; mrzermeno@uach.mx (M.R.Z.-O.); cdelao@uach.mx (C.M.d.I.O.C.)
- <sup>3</sup> CONACYT-Laboratorio Nacional de Investigación y Servicio Agroalimentario y Forestal, Universidad Autónoma de Chapingo, Texcoco de Mora, C.P. 56230, Mexico; jdcanseco@conacyt.mx
- <sup>4</sup> Instituto Politécnico Nacional, Escuela Nacional de Ciencias Biológicas, Departamento de Química Orgánica, Carpio y Plan de Ayala S/N, Colonia Santo Tomás, Ciudad de México, C.P. 11340, Mexico; aavilas@ipn.mx
- <sup>5</sup> Instituto de Química, Universidad Nacional Autónoma de México, Circuito Exterior, Ciudad Universitaria, Ciudad de México, C.P. 04510, Mexico
- \* Correspondence: damor@unam.mx (D.M.-M.); jmga@ic.unam.mx (J.M.G.-A.)



**Citation:** Solares-Briones, M.; Coyote-Dotor, G.; Páez-Franco, J.C.; Zermeño-Ortega, M.R.; de la O Contreras, C.M.; Canseco-González, D.; Avila-Sorrosa, A.; Morales-Morales, D.; Germán-Acacio, J.M. Mechanochemistry: A Green Approach in the Preparation of Pharmaceutical Cocrystals. *Pharmaceutics* **2021**, *13*, 790. <https://doi.org/10.3390/pharmaceutics13060790>

Received: 17 April 2021

Accepted: 10 May 2021

Published: 25 May 2021

**Publisher's Note:** MDPI stays neutral with regard to jurisdictional claims in published maps and institutional affiliations.



**Copyright:** © 2021 by the authors. Licensee MDPI, Basel, Switzerland. This article is an open access article distributed under the terms and conditions of the Creative Commons Attribution (CC BY) license (<https://creativecommons.org/licenses/by/4.0/>).

**Abstract:** Mechanochemistry is considered an alternative attractive greener approach to prepare diverse molecular compounds and has become an important synthetic tool in different fields (e.g., physics, chemistry, and material science) since is considered an ecofriendly procedure that can be carried out under solvent free conditions or in the presence of minimal quantities of solvent (catalytic amounts). Being able to substitute, in many cases, classical solution reactions often requiring significant amounts of solvents. These sustainable methods have had an enormous impact on a great variety of chemistry fields, including catalysis, organic synthesis, metal complexes formation, preparation of multicomponent pharmaceutical solid forms, etc. In this sense, we are interested in highlighting the advantages of mechanochemical methods on the obtaining of pharmaceutical cocrystals. Hence, in this review, we describe and discuss the relevance of mechanochemical procedures in the formation of multicomponent solid forms focusing on pharmaceutical cocrystals. Additionally, at the end of this paper, we collect a chronological survey of the most representative scientific papers reporting the mechanochemical synthesis of cocrystals.

**Keywords:** mechanochemistry; green reactions; pharmaceutical cocrystals

## 1. Introduction

Grant et al., reported that the intrinsic activity of a drug is immensely influenced by its molecular structure and its supramolecular arrangement [1]. Most of the 90% of marketed pharmaceutical products are sold as solid forms: tablets, capsules, suppositories, etc. [2]. The drug efficacy largely depends on their physicochemical and materials properties in the solid state, because its performance can be affected by different crystalline states [1]. It is said that approximately 80% of all drug molecules exhibit polymorphism [3]. Is for this reason that pharmaceutical companies invest enormous amounts of money in the development of high-throughput experimental technologies to determine the crystalline diversity of a drug [4–8]. Crystallization methods in the pharmaceutical industry represent one of the most recurrent practices in the separation and purification of an active pharmaceutical ingredient (API). After partial or total synthesis of an API, crystallization is considered the most efficient purification process compared with liquid-liquid extraction

or chromatography [9]. Thus, in to ensure purity of the crystal, shape, and size of the crystal distribution, and the crystal habit of a drug, the proper choice of solvent plays an important role [10,11].

Drugs may exhibit different solid forms, and this diversity may modify their physico-chemical and biological properties, such as melting point, thermal stability, solubility and dissolution rate, and bioavailability [12–18]. For instance, nearly 40% of the approved drugs and 90% of the developmental pipeline drugs show low solubility [17,19,20]. The determination of the different solid/crystalline forms adopted by an API during its development process is fundamental since it may have a great impact in its scale-up, formulation, and clinical trials; and in some cases, may avoid patent litigations among the pharmaceutical companies [16,18,21].

Drug efficacy depends at least on three pharmaceutical and pharmacological factors: potency (dose), solubility, and permeability [22–24]. By itself, potency is an intrinsic property of the molecule and is difficult to manipulate, however, solubility and permeability can be modulated. The biopharmaceutics classification system (BCS) is a guidance to categorize drugs on the basis of its aqueous solubility and intestinal permeability [25]. This protocol classifies drugs in four groups: Class I (high solubility and permeability); Class II (low solubility and high permeability); Class III (high solubility and low permeability); and Class IV (low solubility and permeability) [26,27].

The modulation of the drug permeability can be reached by various methods: (1) metabolism inhibitors [28], (2) ion-pairing and complexing agents [29], (3) lipid and surfactant adjuvants [30], and (4) inhibitors of secretory proteins [31]. In addition, many approaches are employed to enhance low-solubility drug issues, such as: chemical modifications (prodrugs or preparation of salts) [32,33] and development of new dosage forms (cyclodextrin complexes, lipid formulations, drug-carrier formulations: polymers, surfactants, carbohydrates, dendrimers, etc.) [34–38]. The restrictions found in chemical modifications are that prodrug formation may represent an elevated-cost process subsequent to the chemical derivatization and the structural modification can affect the toxicological profile of the molecule [39]. Salt formation largely depends on the ionizable functional groups that the drug has, otherwise the process is difficult and furthermore this procedure sometimes can modify the properties of the parent drug [40]. On the other hand, the limitations encountered in new dosage forms using cyclodextrin complexes are: size compatibility cavity/drug, reversibility of complex, and sometimes cyclodextrins have been related with toxic reactions, however, apparently these issues were more likely due impurities [41]. Additionally, lipid formulations only admit the entrapment of lipophilic drugs, and drugs with high melting point and  $\log p > 2$  are poor candidates [42]. Recurrent hurdles found in drug-carrier formulations include: (1) carriers used frequently are hygroscopic absorbing water destabilizing the system, (2) sometimes high amounts of carrier are required to ensure the molecular mixing, (3) scale-up problems, and (4) thermodynamic instability [35,43].

The formation of multicomponent solid forms is another important approach used for the modulation of drug solubility and dissolution rate properties [44–53]. This approach may offer important drug property improvements (physicochemical and biological), modifying the molecular conformations and intermolecular interactions of the parent API due to incorporation of a second molecular agent (coformer or drug), without affecting its intrinsic activities [48,54,55]. All drugs with solubility issues are candidates to form multicomponent solid forms, contrary to some of the methods mentioned above i.e., salt formation, cyclodextrin complexes, and lipid formulation. Thus, the pharmaceutical industry and the scientific community have proposed an ample view of how we must classify the different solid forms observed in an API, Figure 1. This holistic view is based on scale range-order periodicity and composition diversity, from single to multicomponent forms [14,15,18].

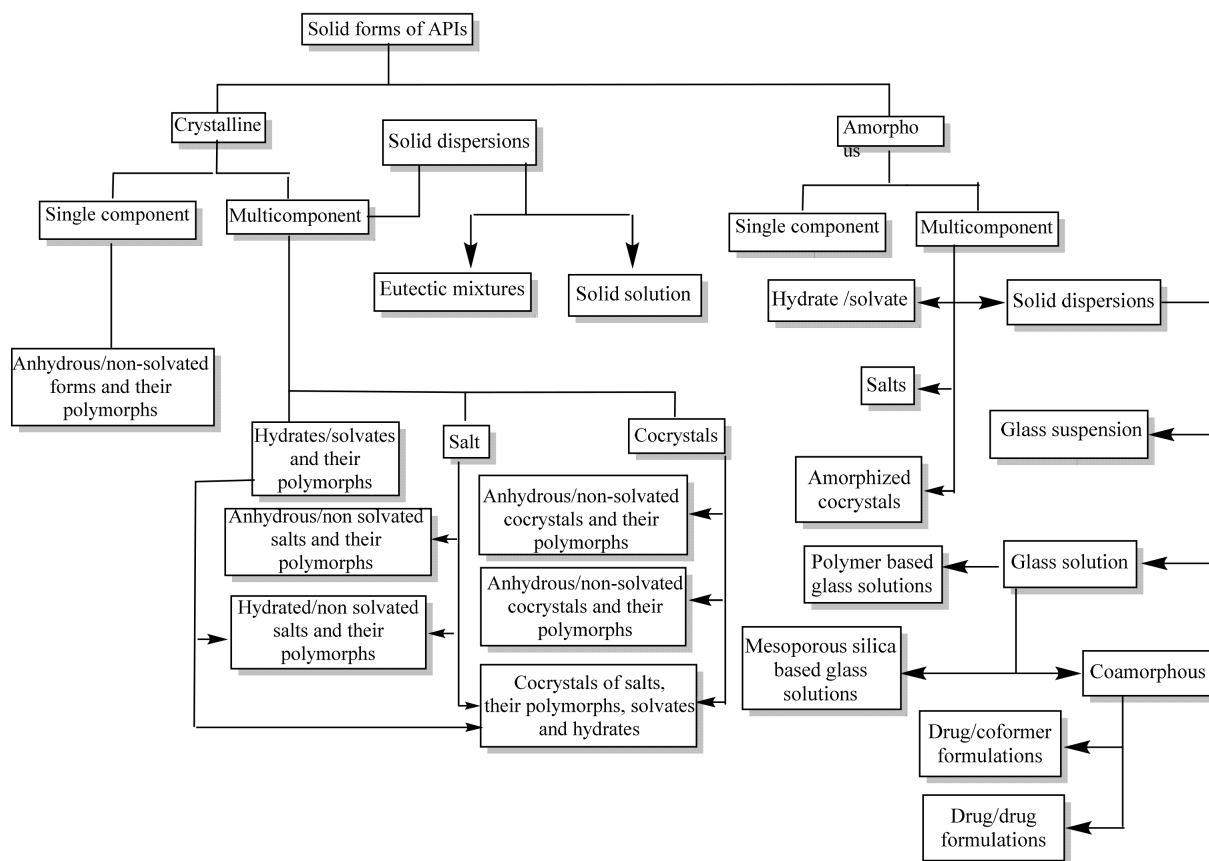


**Figure 1.** Classification of an API depending on its scale range-order periodicity and composition. Adapted with permission from [15], Elsevier, 2017.

Pharmaceutical multicomponent solid systems can solidify in various forms: cocrystals [56–58], salts [59–62], solid eutectic compositions [50,51,63,64], coamorphous [52,53,64–67], polymorphs of cocrystals [68–75], etc.

Pharmaceutical solid forms: cocrystals/multicomponent salts [76,77], 22 eutectic mixtures [50,51,63,64,78], coamorphous [53,64] can be prepared by diverse methods, however, recently solvent free solid-state processes have gained a lot of interest, since they can take place even in the absence or with the minimal amounts of solvent (catalytic amounts).

These free solvent reactions are different compared with the traditional solution reactions (dissolving, heating, and stirring). Mechanochemistry, by itself is an important synthetic tool branch of solid state-chemistry [79,80]. Mechanochemistry is related mainly with the chemical transformation of matter induced by mechanical energy by grinding or milling. Mechanochemistry has emerged as an important green tool of synthesis in diverse fields (e.g., physics, chemistry, material science). Recently, mechanochemistry has had an important impact in a great variety of synthetic fields of the chemistry, including catalysis [81–86], synthesis of organometallic compounds [87–91], organic synthesis [83,92–97], metal complexes preparation [98–100], main-group elements [101,102], porous metal-organic frameworks (MOFs) [81,99,103–107], polymers [108–110], fullerenes [111], multicomponent pharmaceutical materials [53,81,99,105,112–117], etc. Thus, the main focus of this review is to highlight the benefits of mechanochemical reactions in the preparation of pharmaceutical cocrystals. First, the paper will provide the reader with the definition of mechanochemistry, historical aspects, comparisons with other sustainable techniques, etc. Then, the main characteristics of cocrystals, definition, their diverse analytical methods to characterize, diverse synthetic methods, etc., will be described. Finally, a chronological summary of the most relevant papers concerning with their mechanochemical preparation will be presented.

## 2. Mechanochemistry

### 2.1. Definitions, Relevant Historical Aspects, and Applications of Mechanochemistry

The old belief that the success of a chemical reaction depends of the presence of large amounts of a solvent is no longer valid [118]. Recently, enormous interest has been focused on the study of ecofriendly and sustainable reactions, with the aim to perform them under solventless conditions or at least with a minimal utilization of solvents. These kinds of reactions fall in the realm of Green Chemistry, prioritizing high yields and mild conditions [119]. Green Chemistry is a discipline prone to reduce the utilization of environmentally noxious materials and energetic resources. Green Chemistry promotes the development of benign reactions; limiting the use of solvents and finding the optimization of all resources employed (materials, reactants, reagents, solvents, and energy requirements). Green Chemistry is ruled by twelve lineaments [120,121].

On the other hand, solid state-chemistry explores the reactivity of the substances in solid state, through different synthetic methods such as: [92] microwave irradiation [122,123], ultrasound (sonochemistry) [123–125], photochemistry [126–129], mechanochemistry [105,130]. A symbolic representation of these different synthetic methods is depicted in Figure 2 [101].

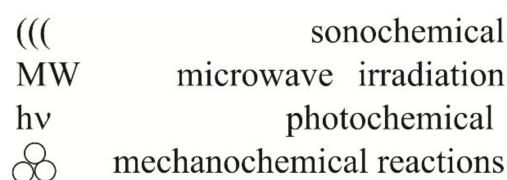


**Figure 2.** Symbolic representations of the different solid state-chemistry synthetic methods. Adapted with permission from [101], Royal Society of Chemistry, 2019.

Mechanochemistry is a term related with the chemical reactivity promoted by diverse mechanical stimulus, (typically friction, impact, collision, grinding). A mechanochemical reaction is defined by the IUPAC as: “a chemical reaction that is induced by the direct absorption of mechanical energy” [131]. Mechanochemistry through the time have received several definitions [132]. Wilhelm Ostwald classified overall the chemistry in diverse fields: thermochemistry, electrochemistry, photochemistry, etc., depending on the energy input [105]. From this classification, it should be noted that Wilhelm Ostwald separated the mechanochemistry as a unique branch of chemistry [133,134]. Later, Walther Nernst (Ostwald’s student) supported this classification [105,135]. However, according to Baláž, the current accepted definition is that of Heinicke that establishes that “mechanochemistry is a branch of chemistry which is concerned with the chemical and physicochemical transformations of substances in all states of aggregation produced by the effect of mechanical energy” [132].

Sometimes tribochemistry (*vide infra*) is confused with mechanochemistry, however, by itself the former term is a branch of the latter, Figure 3 [80]. Tribochemistry (friction, *tribos*), per se is related with chemical reactions occurred between two solid surfaces, within the lubricating material, or between the lubricant and solid surfaces [136,137]. Thus, in general, mechanochemistry it should be considered into four areas: tribochemistry (the chemistry of surfaces in contact), trituration (chemistry induced by grinding and milling), macromolecular mechanochemistry (from breakage of polymer chains to molecular motors and biological motion), and sonochemistry (the chemistry generated from the mechanical consequences of sound), Figure 3 [80].

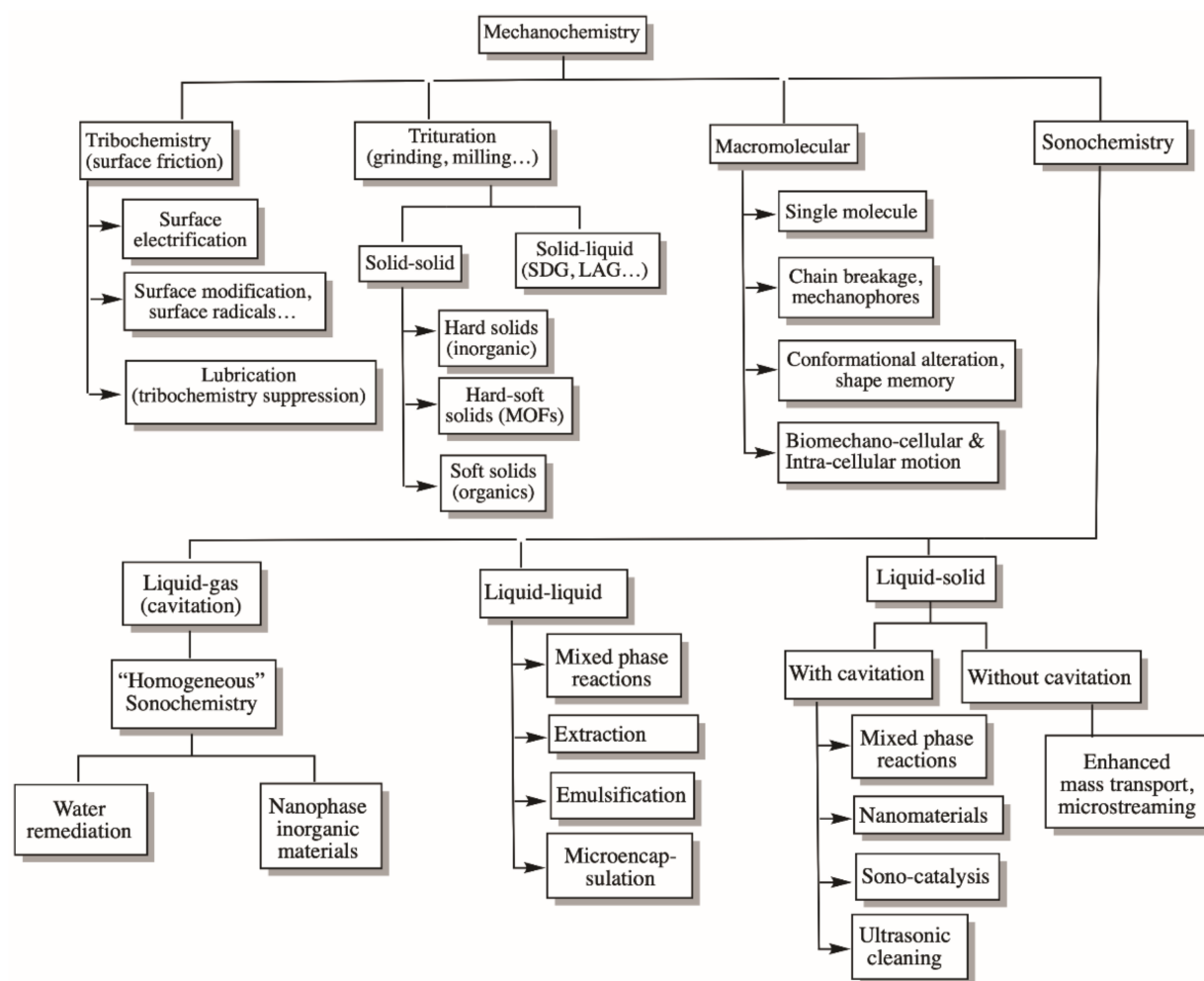


**Figure 3.** Different branches derived from the mechanochemistry. Adapted with permission from [80], Royal Society of Chemistry, 2014. SDG: solvent drop-grinding; LAG: liquid-assisted grinding; MOFs: metal-organic frameworks.

Mechanochemistry can be dated back to the prehistoric times [138], Greek ages [Theophrastus of Ephesus (371–286 B.C.)] [139,140] and at the period between the 19th and the early 20th century [105,113,138,141–143]. Particularly in the 19th and 20th centuries, the pioneering work of Carey Lea (according with Takacs the first mechanochemist) [134,141,144,145] and Faraday can be highlighted [142,143]. For an excellent detailed description of the development of mechanochemistry through the history, “The historical development of mechanochemistry” must be consulted [143].

The recent interest in mechanochemical methods is due to diverse advantages compared with the classical-based dissolution reactions. According to Etter: “the absence or at least the minimal usage of solvents during the course of the reactions, often leads by mechanochemical methods to the phase similar to that obtained by solution crystal growth”, suggesting that the presence of large amounts of solvent is not necessary for the formation of a new phase [105,146–149]. Mechanochemical methods are preferred to be used when the product is not accessible via conventional reactions (classical dissolution) [150–154]. In addition, mechanochemical processes can provide control over the polymorphic outcome, sometimes not obtained in solution [155–162]. In addition, yields can be improved and reactions may proceed faster than in solution [98,163–166]. Furthermore, improved stereochemical control and selectivity can be achieved [167,168]. Additionally, reactions can be carried out to completion, with additional purification steps not necessary [169,170]. Some reactions exhibit a reduced energy consumption due to efficient energy transfer in the mixture reaction (e.g., planetary ball-milling) [171].

Apparently, the first paper describing the formation of a cocrystal using a mechanochemical reaction was reported in 1893 [172]. In this paper was informed the preparation of quinhydrone cocrystals grinding equimolar amounts of *p*-benzoquinone and hydroquinone. After this, the reports of Curtin [173] and Etter [174,175] were established as great contributions to the development in the preparation of cocrystals by mechanochemical procedures.

Kaupp indicated that milling, grinding, shearing, kneading, stirring, pulling, and cutting do not constitute part of the mechanochemistry if this stimulus does not produce a bond breaking [79]. The term mechanochemistry is usually ligated with the rupture and formation of covalent bonds [140], but the “non-covalent mechanochemistry”, ref. [176] is part of interest in the preparation of multicomponent pharmaceutical solid forms. Grinding two chemical substances lead to the modification of the intermolecular interactions altering the solid-state properties of the new solid form. The definition of what is a cocrystal will be discussed in Section 3.1.

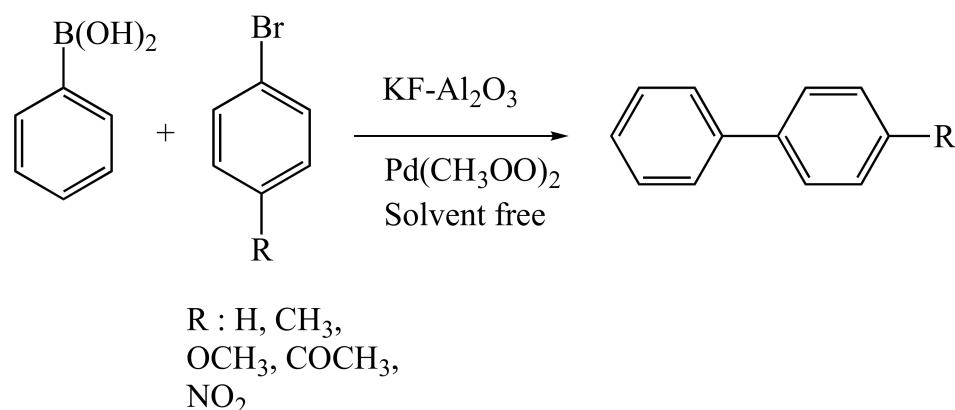
## 2.2. Different Mechanochemical Apparatuses

Grinding may be so simple as manually grinding two chemical reagents in a mortar and pestle. However, it should be noted, that grinding and milling are different techniques, since grinding is the mechanochemical procedure working in a mortar and milling is carried out in ball mills devices [95]. At the laboratory level, ball-milling is employed rather than grinding, when higher energy input is required, more systematic times of reaction (reproducibility) are needed and better mixing (mass and energy transfer) is sought [92]. Grinding with a mortar depends on the vigor and intensity applied during the process being less systematic and sometimes atmospheric conditions can be an adverse factor [101]. The implementation of automatic devices (milling equipment) can circumvent these hurdles [162]. For a detailed description of the diverse types of milling apparatuses and their characteristics (balls mills to vibratory, planetary, mills, and attritors), proper references must be consulted [132,177,178]. According to Mack, at the laboratory level, there are three typical mills (mixer/shaker mills, planetary, twin screw extrusion) [93]. From which mixing/stirring mills and planetary devices are more accessible to obtain (USD 3000–7000) [93]. For an excellent description of the characteristics and differences associated with mixing/stirring mills and planetary devices, the following relevant references must be consulted [93,100,179,180]. Twin-screw extrusion (TSE) is another mechanochemical tool which can provide large-scale preparation of cocrystals (industrial level). [181–183] Additionally, TSE has been used for the scale-up preparation processes in the synthesis of organic compounds [184,185], MOFs [186], and deep eutectic solvents, etc. [187].

## 2.3. Advantages of Reaction Performance among Grinding/Milling and Other Sustainable Methods

Schneider et al., showed the advantages in energy consumption of mechanochemical reactions over other sustainable methods [171]. Thus, in a comparative study of Suzuki-Miyaura reactions (C-C couplings: phenylboronic acid + different aryl bromides) for the production of several biaryls, Scheme 1. Experiments grinding the components with mortar and ball-milling were carried out. Grinding outcomes revealed problems with the reproducibility, not found in ball-milling experiments. In addition, different studies evaluating the energy demand (ball-milling or microwave irradiation) were performed. A third experiment was carried out combining (ball-milling + microwave irradiation, COMB) also seeking to determine the energy consumption. Interestingly, ball-milling experiments required lesser energy demand than microwave assays and the combination of both methods, demonstrating the advantages of mechanochemical synthesis over microwave irradiation. According to the authors, the couplings of the *p*-bromoacetophenone proceed easier than the other substrates due to the fact that the C-Br bond is weaker because of the electron-donating nature of the *p*-substituent, resulting in the best yields in the couplings reactions. Thus, taking this as a model reaction, their yields were evaluated, initially comparing the reaction carried out with a mortar and pestle and in a Pulverisette 7 device (planetary ball mill). From these experiments, it was observed that by grinding in a mortar, the

reaction produced yields greater than 50%, but when the milling equipment was used, the performance depended on the rpm used. Producing yields of ~5%, ~70%, and ~89% for 200, 400, and 800 rpm, respectively. A further comparison of the yields employing ball-milling (Pulverisette 7 (at 800 rpm) BM1 or swing/mixer mill BM2), microwave irradiation (MW1: multimode or MW2: mono-mode) or COMB, the following results were obtained: BM1 (89%); BM2 (45%); MW1 (80%); MW2 (70%); COMB (94%), thus showing the best yields to be produced by the COMB method for this particular Suzuki–Miyaura cross coupling reaction. Although the BM1 procedure required lesser energy demand than the other methods.



**Scheme 1.** Pd-catalyzed C-C coupling reactions (Suzuki–Miyaura).

Another study comparing the efficiency (chemical yield and energy consumption) of ball-milling with different synthetic methods was reported by Thorwirth et al. [188]. The oxidation of primary aromatic amines to azo and azoxy compounds were evaluated by different methods: mechanochemical (planetary and vibratory ball-milling) and solvent-based procedures (microwave, conventional heating, ultrasound). In this case, also the mechanochemical reactions were more efficient in terms of both chemical yield and energy consumption. However, planetary ball-milling was more efficient for a scale-up reactions compared with vibratory milling.

#### 2.4. Preparative Conditions of Mechanochemical Methods of Pharmaceutical Cocrystals

Braga has classified solid-state reactions as [189,190]:

1. Intracrossolid reactions, which proceed amongst molecules within a single-crystal (Topochemical Postulates developed by Schmidt), Figure 4 [191–193].
2. Intersolid reactions, which pertain to the reactivity between solids (mechanochemical reactions), Figure 4.
3. Furthermore, Braga added a third category, solid–gas reactions [189,190].

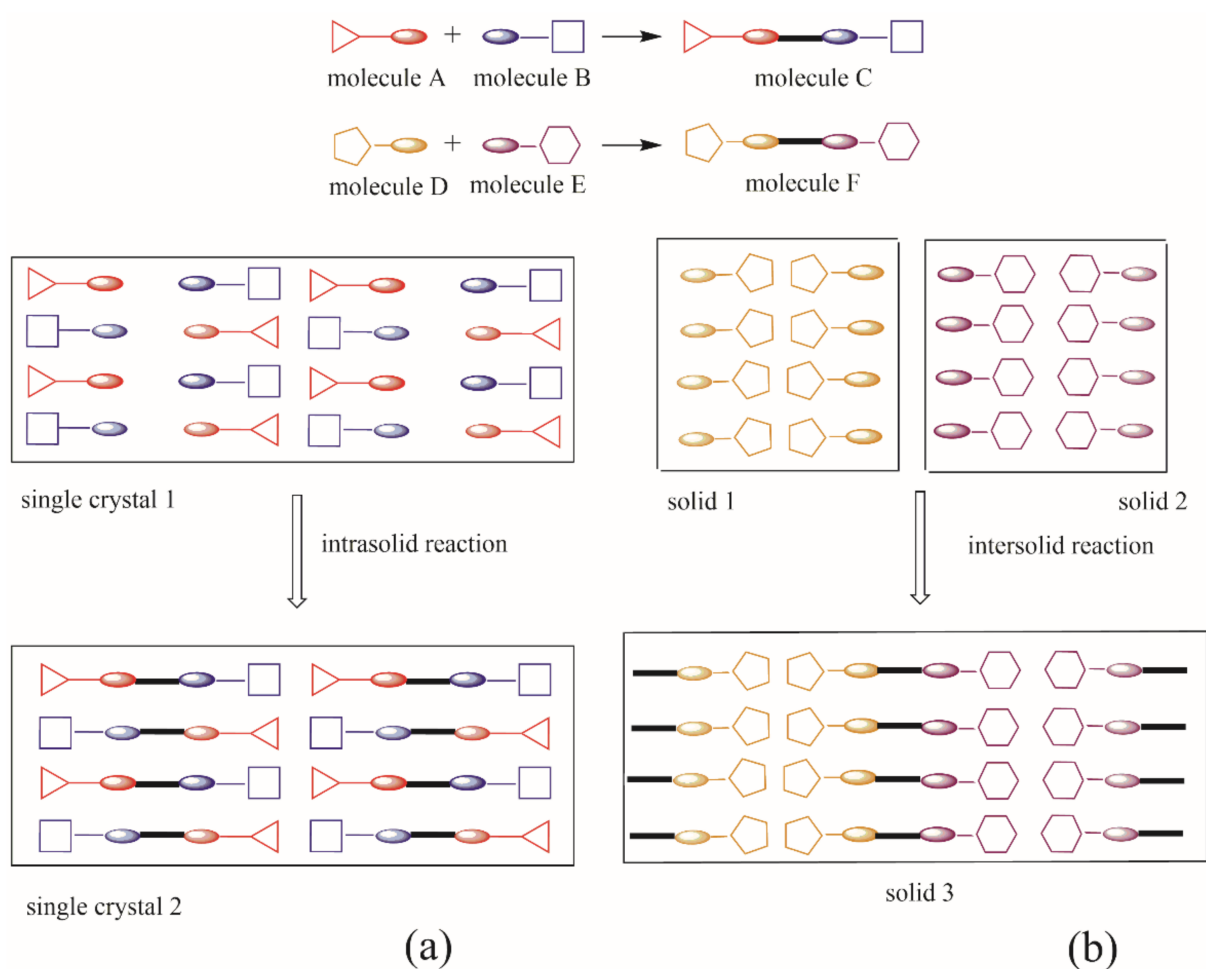


**Figure 4.** Classification of solid–solid reactions: (a) intrasolid and (b) intersolid. Adapted with permission from [189], Wiley, 2004.

However, Bolm indicates that solventless reactions can be categorized into three groups [194]:

1. Reactions between solids (solid–state reactions).
2. Reactions between solids with intermediate local melting.
3. Reactions with at least one liquid reagent.

One of the persistent problems found in the mechanochemical reactions is the lack of understanding in the mechanisms involved. In this context, mechanochemical reactions can be monitored *ex situ* [96,195,196] or *in situ* [84,96,197] using synchrotron XRPD [198–200] and Raman spectroscopy [201–203], in order to get an insight into the different intermediate steps and pathways involved.

The components involved in a typical mechanochemical reaction can be mixed at least by two different conditions: the “dry” manner denominated neat grinding (NG) or by “wet” conditions [105,112,204]. “Dry” conditions is to grind/mill all the components in total absence of solvent, consequently “wet” conditions are carried out when solvent is added in catalytic amounts. Currently, the accepted term used for “wet” conditions is liquid-assisted grinding (LAG), but in some old literature, is also known as kneading [105]. Although LAG was also formerly known as solvent drop grinding (SDG) [154,155].

To the best of our knowledge, the first paper, the improvement in kinetics of cocrystal formation by grinding under “wet” conditions was reported by Jones et al. [205]. Combining cyclohexane-1,3-cis-5-cis-tricarboxylic acid (CTA,  $C_6H_9(COOH)_3$ ) in the presence of 4,4'-bipyridine (4,4'-bipy) (1:1) for 1 h under NG conditions lead to the partial formation of the cocrystal. However, the addition of 0.05 mL of methanol in the mixture and grinding by

20 min lead to a significant acceleration of the reaction to achieve the complete formation of the cocrystal. Another multicomponent system explored was CTA + 4,7-phenanthroline (4,7-phen) (1:2) under NG. After a long period of time grinding, the reaction only occurred partially. However, if the reaction was carried out in the presence of small amounts of methanol, after 5 min, the reaction proceeded almost quantitatively, although traces of the original reactants were detected. Based on these findings, Jones et al., proved that the kinetics of the formation of cocrystals can be improved by LAG.

Jones and Friščić later showed that outstanding benefits can be obtained by LAG over NG in the preparation of cocrystals [81,82,162,206]. For instance, NG has a slight implication in the molecular change of the course of a mechanochemical reaction, contrary to LAG which confers mobility to the components involved. In this regard, LAG imparts additional degrees of freedom (orientational and conformational) to the molecules affecting the reaction outcome. The empirical parameter  $\eta$ ,  $\eta = V(\text{liquid, } \mu\text{L})/m$  (sample, mg) (volume of solvent, and  $m$  represents the weights of cocrystal components) helps to assign a scale to distinguish the different conditions in which the reaction is carried out (NG = 0; LAG  $0 < \eta < 2$ ; slurring  $2 < \eta < 12$  and solution synthesis  $> 12$ ) [81]. This parameter provides an interesting insight of the role of the solvents for the design of experiments that are mediated by the presence of a minimal amount of solvent (catalytic conditions) going through slurring or liquid phase [206].

The importance of  $\eta$  is illustrated by the work of Jones et al., where he explored the polymorph diversity of the cocrystal caffeine:anthranilic acid (caf:ana) using VALAG (variable amount liquid-assisted grinding) [207]. The screening experiments varying the amount of the solvent used ( $\eta$  parameter range 0.05–0.5) and utilizing 15 solvents of different polarity, revealed that polar solvents (4 of 15): acetonitrile, nitromethane, ethylene glycol, and 1,6-hexanediol yielded one cocrystal polymorphic form. It should be noted that experimental conditions (grinding time, frequency, and ball-to-powder weight ratio) were maintained fixed. However, the utilization of non-polar solvents (11 of 15) led to the formation of two or more different cocrystal polymorphs. Thus, globally, Jones et al., concluded that polymorphic control of the cocrystal can be achieved by the polarity of the solvent used and fixing the  $\eta$  parameter. With this work, Jones demystified the common belief of “one liquid for one specific polymorphic form”.

POLAG (polymer assisted grinding) is another relevant mechanochemical technique for the screening of new pharmaceutical solid forms. As mentioned above in the introduction, for drug-carrier formulations, polymers are used as excipients, mainly to stabilize highly activated molecular structures [43]. In this context, Matzger has explored new crystalline forms using primarily polymers as nucleation inducers for the discovery of new polymorphs [208]. According with Matzger, polymers (are crystallization directors) have the capacity to promote selectively the formation of one polymorph over another [209,210]. Jones et al., continued in this line using POLAG, where by means of mechanochemical reactions using polymers; these materials can direct the formation of specific polymorphs [162,211]. Jones et al., described the preparation of three different cocrystals previously reported in the literature caffeine: citric acid (caf:ca) [212] phenazine and mesaconic acid (phe:ma) [213] and caf:ana [69] by POLAG. The polymer used as catalyst was polyethylene glycol (PEG) varying its molecular weight from 200 to 10,000.

The cocrystal caf:ca (1:1) can be obtained by LAG (grinding with water) or by NG (only when caf hydrated + ca dehydrated is used). [212] In the second system phe:ma, produced with LAG, a dramatical increase in the cocrystallization process is observed. In addition, for the third system caf:ana, the product can be obtained by NG or LAG, however, LAG promotes cocrystal polymorphism. Additionally, in the system caf:ana, using POLAG yielded a different polymorphic form compared with NG. In general, according with the findings in the three systems, using POLAG (adding PEG) produced similar results to those observed with LAG. However, depending on the amount of polymer added in the mechanochemical procedure, this promotes or inhibits the formation of the cocrystal. For instance, in the system caf:ca, using PEG 10,000 in low amounts (1–5%), the presence of the

characteristic peak of caf at  $2\theta = 12^\circ$  is noted by powder X ray diffraction (PXRD). However, by increasing the amount of PEG 10,000 to 10% the peak of caf at  $2\theta = 12^\circ$  is considerably reduced, but at higher percentages of PEG 10,000 (60%), the intensity of this peak increased again. Experiments using other PEGs (200, 300, 400, 3000, 6000, 10% of polymer), and increasing the times of milling, revealed in the PXRD patterns a considerably reduction of the peaks corresponding to the starting materials. Besides, in general, in the three systems, the polymer chain length did not affect the mechanochemical formation of the cocrystal, revealing POLAG as an excellent method for the control of the powder particle size.

Recently, Germann et al., reported the first in situ PXRD monitored mechanochemical cocrystallization (caffeine:glutaric acid; caf:glu) employing POLAG. [214] The authors introduced the  $\delta$  parameter for POLAG (equivalent to  $\eta$  parameter used in LAG) [81] to compare the reactions in terms of the amount of grinding additive. In this work, they explored the use of diverse PEGs and different  $\delta$  values.

So far, two forms of the system caf:glu (1:1) have been reported: Form I which is metastable and converts to Form II under high humidity conditions, (CSD refcodes: EXUQUJ ( $P2_1/c$ ) and EXUQUJ01 ( $P\bar{1}$ )), Figure 5. [155,215] However, after the transformation of Form I into Form II, the latter system remains stable for three days before inevitably undergoing conversion to caffeine hydrate. Both forms of caf:glu 1:1 ( $P2_1/c$  or  $P\bar{1}$ ) can be prepared by slow evaporation techniques or NG and LAG [155]. By using NG, Form I can be exclusively produced, but by using LAG, both forms can be obtained. Form I is obtained by LAG using non-polar solvents (hexane or heptane) whilst Form II was formed preferably employing polar solvents (acetonitrile or dichloromethane).

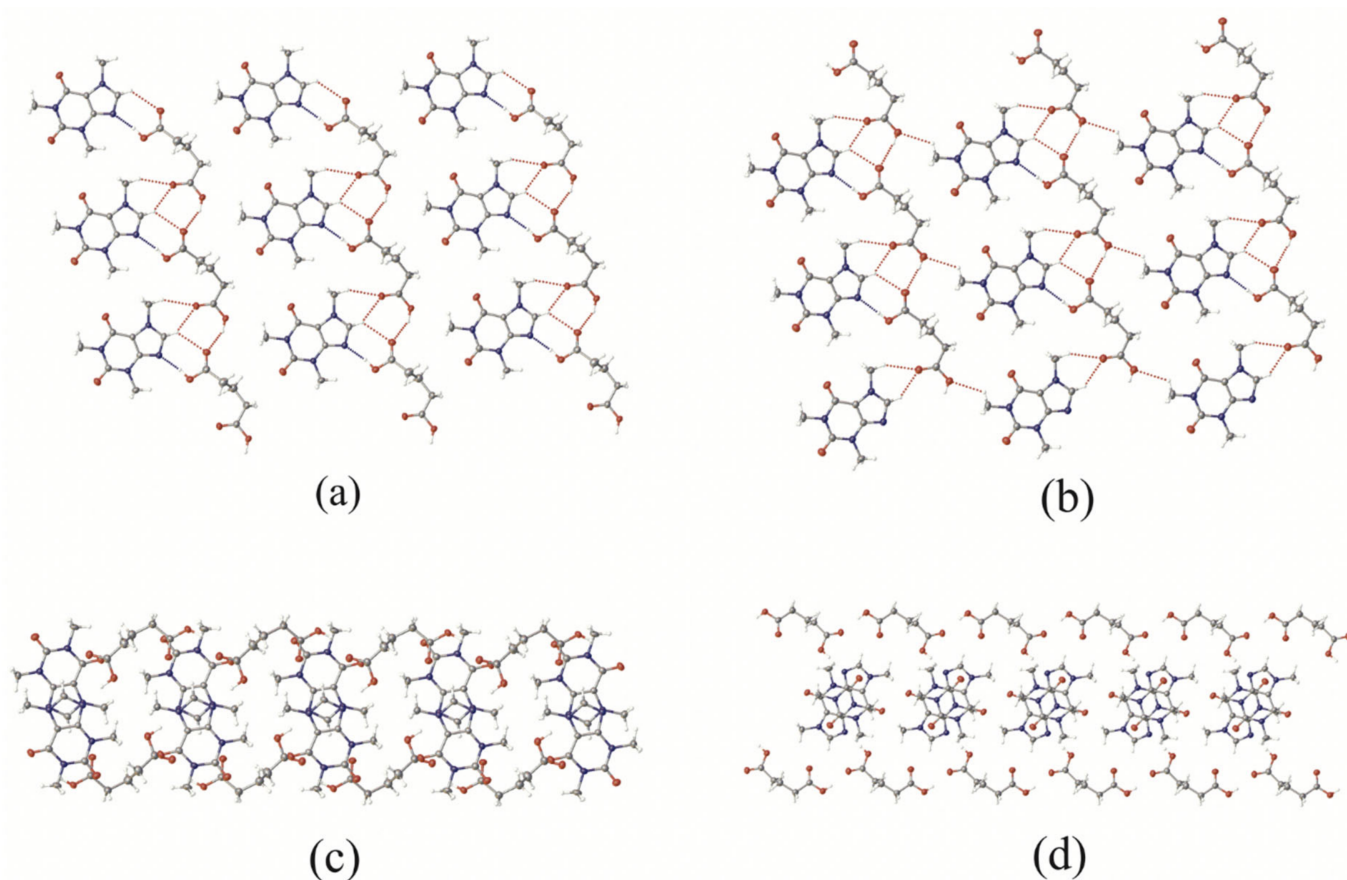


**Figure 5.** Sheets of caf:glu (1:1) ribbons. (a) Form I and (b) Form II. Stacked ribbons of caf:glu (1:1): (c) Form I and (d) Form II. CSD refcodes: Form I; EXUQUJ ( $P2_1/c$ ) and Form II; EXUQUJ01 ( $P\bar{1}$ ).

The first milling experiments carried out in this work used NG and LAG (acetonitrile,  $\eta = 0.05 \text{ mL}\cdot\text{mg}^{-1}$ ). In NG, Form I was formed in the first 7 min of reaction. LAG

experiments were faster than NG reactions. In LAG, firstly, Form I was formed as an intermediate, but subsequently, Form II appeared as the final product. LAG experiments adjusting  $\eta$  to higher values (0.12 and 0.17 mL·mg<sup>-1</sup>) exhibited that while this parameter is augmented, the overall rate is generally increased. The findings with POLAG ( $\delta = 0.05$ ; PEG 3000) showed the formation of Form I after 4 min, reaching completion after approximately 30 min. Enhancing  $\delta$  (0.12 and 0.5) apparently has no direct influence in the cocrystallization efficiency. In POLAG conditions ( $\delta = 0.05$ ; PEG 10,000), the increment in the polymer chain length has no influence in the overall reaction, however, apparently the cocrystallization was slightly slower. At higher amounts of polymer PEG 10,000 ( $\delta = 0.05$ ) at 60 min of reaction, unreacted starting materials were detected.

Interesting results were obtained through qualitative comparison of the rates of cocrystallization by determining the start of the reaction (induction time) and the 50% conversion point performed in NG, LAG, and POLAG experiments. Overall, POLAG and NG showed NG to be almost two times faster. Additionally, in POLAG, the reaction rate was not influenced by the molecular weight of the polymer additives. However, in LAG, the reaction rate was enhanced when  $\eta$  was increased. In addition, the authors indicated that in this reaction, only small quantities of polymer were necessary to have a catalytic role. This work represented an important advance in the influence of the  $\delta$  parameter in the cocrystal formation as it was mentioned with VALAG.

Another variant of LAG is known as ion liquid-assisted grinding (ILAG), where a salt is added during the grinding as an additive. For instance, the addition of small amounts of salts (NO<sub>3</sub><sup>-</sup> or SO<sub>4</sub><sup>2-</sup>) in the preparation of the MOF [Zn<sub>2</sub>(ta)<sub>2</sub>(dabco)] (ta: terephthalate; dabco: 1,4-diazabicyclo [2.2.2]octane), under ILAG conditions, accelerated the formation of the MOF compared with LAG. [216] The authors suggested that under ILAG conditions, the formation of the MOF [Zn<sub>2</sub>(ta)<sub>2</sub>(dabco)] goes through an anion-templating mechanism.

Besides, in 2018, Mukherjee et al., described the formation of the cocrystals caf:ca and caf:glu using ILAG [217]. It must be noted, that for the preparation of the MOF [Zn<sub>2</sub>(ta)<sub>2</sub>(dabco)] by ILAG [216], the grinding was made in the presence of inorganic salts, however, in the formation of the systems caf:ca or caf:glu, different imidazolium-based ionic liquids (IL) were employed. The caf:ca system (1:1) has two cocrystal polymorphs (CSD ref codes: KIGKER (P $\bar{1}$ ), KIGKER01 (P2<sub>1</sub>/c); Form I and Form II), Figure 6 Form I can be produced by LAG (grinding with water) or NG (only when is used caf hydrated + ca dehydrated) [212]. Form II has only been obtained by slow evaporation in a chloroform/methanol solution [218]. As it was described previously, Form I also can be isolated by POLAG [211]. With this rationale, Mukherjee et al., explored ILAG in an attempt to emulate the results obtained with POLAG, by employing a series of ILs, Figure 7, instead of varying chain lengths of polymers (PEGs). Various ILs were used modifying the substitution on the imidazolium cation (different alkyl chain lengths) or by changing the anions (different hydrogen bonding ability) to determine their influence in the final crystallization outcome.

Experiments in both systems (caf:ca and caf:glu) were carried out in a mortar and pestle in stoichiometric ratio of components (1:1) and adding c.a. 40  $\mu$ L of the ILs (15 min). The formation of both cocrystal systems was monitored by PXRD.

From the results obtained in the system caf:ca, the authors suggest that independently, the different nature of ILs were employed (hydrophobicity/hydrophilicity), this did not affected the outcome since only the formation of the Form I was observed. However, a different case was observed in the cocrystal system caf:glu. As mentioned above, Form I in caf:glu is obtained by LAG using non-polar solvents. Additionally, Jones et al., reported that the employment of POLAG (increasing the chain lengths of polymers increasing non-polar effect) provides a selective control in the formation of Form I. [219] From this, it has been hypothesized that in both LAG and POLAG, the presence of a non-polar slip plane (200) in Form I absent in Form II, interacts favorably with non-polar liquids. Based on these results, Mukherjee et al., carried out ILAG experiments using hydrophobic and non-polar ILs to stabilize the non-polar slip plane (200) favoring the formation of Form I.

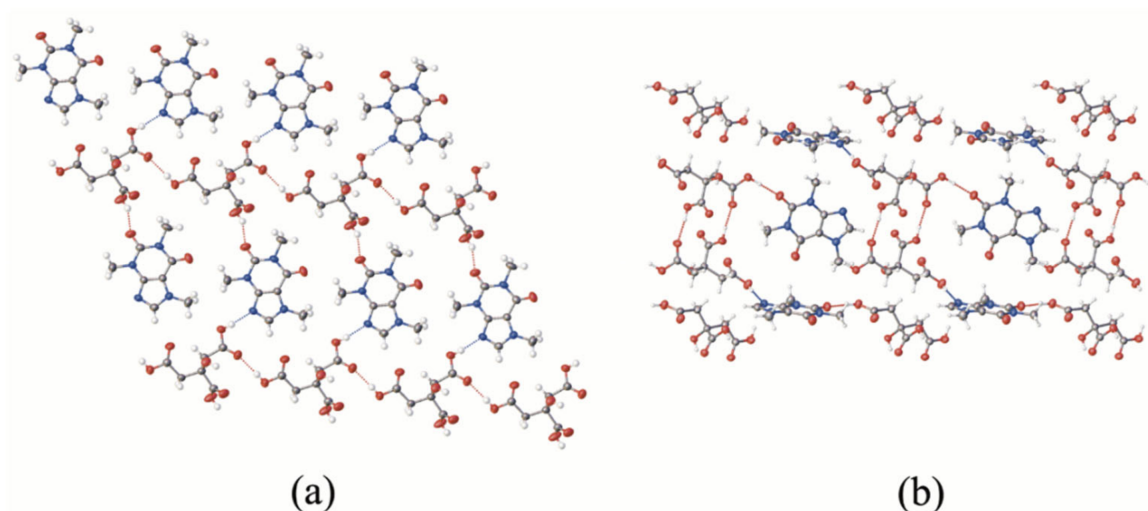


**Figure 6.** Sheets of caf:ca (1:1) ribbons. (a) Form I and (b) Form II. CSD refcodes: Form I; KIGKER (P1) [216] and Form II; KIGKER01 (P2<sub>1</sub>/c).

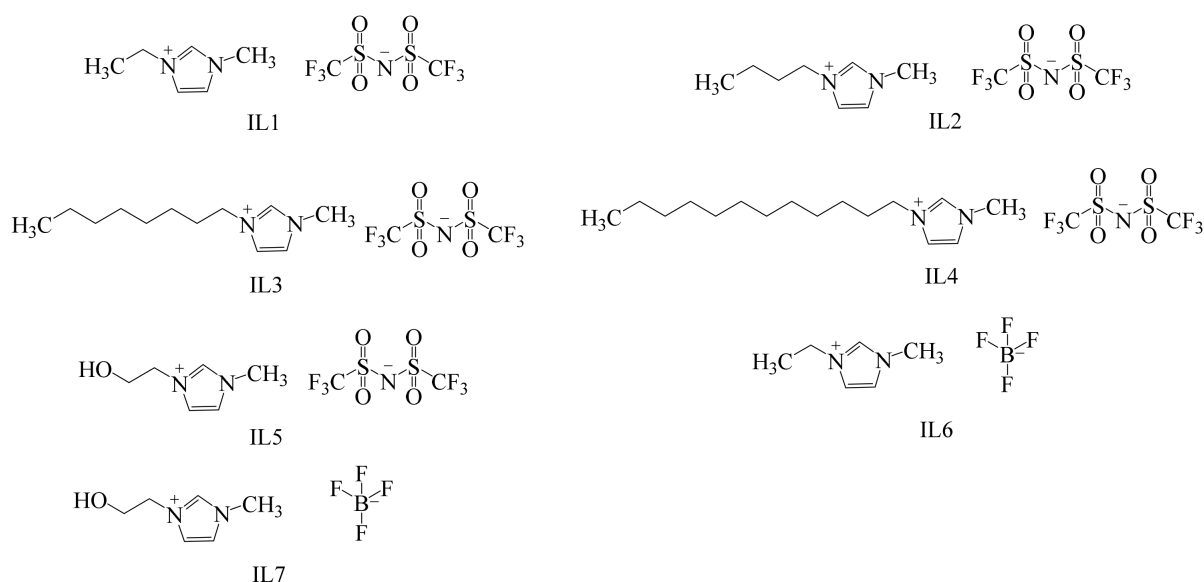


**Figure 7.** ILs employed in ILAG experiments.

Mukherjee et al., described that employment of all these ILs led to the crystallization of Form I, however the increase in alkyl chain length in the ILs affected the rate of formation. In particular, the use of IL5 promotes the formation of Form I, however, IL7 leads to Form II (polymorph control), by the simple change of the anion, but showed traces of the Form I. With this work, Mukherjee et al., demonstrated that slight modifications in the ILs used in ILAG may promote polymorphic control over cocrystals.

Finally, VATEG (variable temperature grinding) is another subclass of LAG. Here, the monitoring of the temperature changes observed during a mechanochemical process is a relevant factor to reveal reaction kinetics and mechanisms involved [162]. However, VATEG has been scarcely explored and few papers have been reported [220,221]. One of the main hurdles to explore VATEG in ex situ experiments is to monitor the reaction at a given temperature, because it is necessary to interrupt the mechanochemical process to extract a sample for analysis [162]. However, real-time in situ monitoring techniques, in particular variable-temperature synchrotron powder X-ray diffraction, have shown remarkable results to overcome this obstacle. One case study of variable-temperature in situ investigations will be discussed in Section 2.5 [222].

### 2.5. Mechanistic Aspects in Cocrystal Formation Applying Mechanochemistry

Despite the benefits of mechanochemical reactions in the preparation of cocrystals, there is an incipient knowledge behind its formation mechanism. The cocrystal mechanism using mechanochemical methods remains unclear, for this reason, many models have been proposed.

According to Jones and Frišćić, the cocrystal formation cannot be assumed as a single mechanism process [117]. At least three different models are accepted to explain these mechanistic aspects: molecular diffusion [117], eutectic formation [223], and mediation by an amorphous phase [224]. These models have a common point, all of them propose the presence of an intermediate bulk phase (gas, liquid, or amorphous form) during the mechanism. Detailed examples explaining these models have been reported [117].

First, under NG conditions using the molecular diffusion model, it is likely to occur when one or both components exhibit considerable vapor pressure in the solid state. In fact, some reactions can proceed simply by contact between the starting chemical reagents, even in the total absence of mechanochemical action. Rastogi et al., reported mechanochemical reactions between picric acid and some aromatic hydrocarbons, where the mechanism is proceeding through surface migration and diffusion via vapor phase [225].

In addition, Kaupp contributed with important advances into the mechanistic aspects via molecular diffusion through NG cocrystallization (intersolid reactions), Figure 8 [226]. Using an atomic force microscope, he proposed a three staged mechanism starting from crystal solid species A and B, which give rise to the new product C, Figure 8.

1. Molecule migration. The first stage is the reconstruction of the solid phase, suggesting directional long-range migrations of molecules, where component A invades the planes or channels of component B (or vice-versa). The incipient formation of C distorts the original crystal structures of A and B, producing a mixed A-B-C phase.
2. Product-phase formation. The concomitant appearance of component C in the mixed phase A-B-C favors spatial discontinuity in particles A and B due to strain and crystal defects.
3. Crystal disintegration. In this step, is suggested a chemical and geometrical mismatch between components A and B, produced by the appearance of C causing a disintegration of the particles. The grinding/milling process produces fresh surfaces available for further reaction to completion.

Jones and Frišćić suggested that Kaupp's model although is related for a solid–solid intercrystalline reaction, it may be adopted to explain the formation of cocrystals or multi-component salts, Figure 8 [117,227].

Additionally, Scott et al., emphasized that some NG reactions between two solids may proceed via an eutectic intermediate (observation of a liquid phase) [228]. According to Chadwick et al., the cocrystal formation (grinding in a mortar) starting from benzophenone and diphenylamine is through an eutectic phase. The authors indicated that the action of the grinding creates a high interfacial area between the starting components facilitating the eutectic form. This induces nucleation and the eventual formation of the cocrystal phase [223].

The cocrystal formation via NG mediated by an amorphous phase is most likely to proceed when the components are non-volatile, especially with solids with strong intermolecular interactions (hydrogen bonds) [117]. Rodríguez-Hornedo et al., demonstrated that grinding carbamazepine and saccharin below the expected glass transition of the final mixture outcome induces an amorphous phase formation. But conversely, when the components are ground at higher temperature of the expected glass transition of the mixture, it would lead to a metastable polymorphic form. The storage of this amorphous form at room temperature slowly tends to cocrystallize. Under high relative humidity conditions (75%), this amorphous phase increases its molecular mobility and complementarity between the components, leading to the cocrystal formation. The amorphous phase intermediate is considered a high energy and high molecular mobility species.

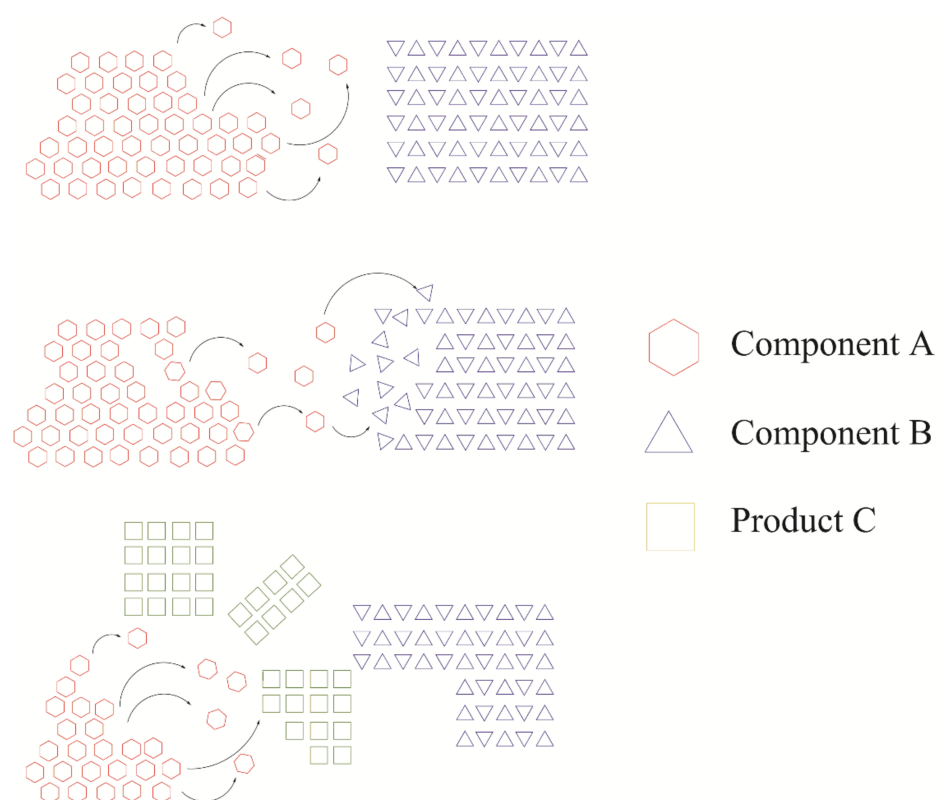


**Figure 8.** Schematic representation of cocrystal formation mechanism applying grinding/milling in a binary system. Adapted with permission from [117], American Chemical Society, 2009.

Regarding LAG, the cocrystal formation mechanism is not fully understood [227]. In fact, it has been suggested that the liquid is a lubricant facilitating the molecular diffusion among the components [117,206]. Where the parameter  $\eta$  and polarity of solvent employed plays an important role in the cocrystal formation as it was mentioned with VALAG [207]. Additionally, the parameter  $\eta$  has a strong influence on the possible mechanisms, intermediates, or different polymorphic outcomes in a cocrystallization reaction [229].

It has been suggested that many milling parameters may affect the rates of product formation: milling frequency [203,230], milling time [231], filling degree of the jar [232,233], milling ball diameter and the beaker size [164,234,235], degree of milling ball filling [164], energy input [236,237], and material of jar [231].

Furthermore, variable-temperature in situ studies have shown that reaction rates are temperature-dependent and that slight changes in temperature generally influence the mechanism [222]. Using as a model of synthesis, the preparation of the coordination polymer ( $\text{CdCl}_2$  + cyanoguanidine in dry conditions), the authors showed that an increment of  $45^\circ\text{C}$  in the bulk reaction temperature accelerates the rate reaction (6-fold). The increment in the bulk reaction temperature could be reached by increasing the number of ball impacts, or when are used heavier balls (7 to 9 mm). Raising of the temperature has an important influence in the reactant consumption rate, as well as a change in reaction mechanism. In this context, the authors explain that the accepted model mechanisms for milling reactions in the preparation of inorganic materials (“hot-spot” and “magma-plasma”) [238–240], apparently do not properly fit for softer materials such as coordination polymers or cocrystals. According with these results, at temperatures near room temperature, the mechanism goes through an amorphous phase intermediate. However, at higher temperatures, the mechanism proceeds by the rapid formation of an intermediate. Thus, it has been suggested that at elevated temperatures, the mobility of the amorphous intermediate is higher, thus facilitating the formation of the final product via crystallization of the intermediate.

Recently, Friščić et al., demonstrated the appearance of the cocrystal polymorph (Form II) in the system nicotinamide and adipic acid (nic:adi) [229]. It must be noted that the nic:adi cocrystal form has been reported to exist in two stoichiometric relations 1:1 and 2:1 [241]. Milling nic and adi in a 1:1 stoichiometric proportions using acetonitrile ( $\eta = 0.125 \mu\text{L}\cdot\text{mg}^{-1}$ ) led to the formation of Form I. Having the milling reaction performed using two stainless steel (ss) balls (7 mm) in a poly(methyl methacrylate) (PMMA) material jar.

Repeating the previous experiment, but using ss jars instead of the PMMA jars lead to the formation of the Form II. The molecular structure of Form II was established by the combination of PXDR and solid state nuclear magnetic resonance (for more details about this technique see Section 3.3) analyses. Besides, in order to verify that the control of the polymorphic outcome depends on the choice of the jar material, experiments under NG and LAG in the presence of different solvents at a fixed  $\eta$  parameter ( $0.125 \mu\text{L}\cdot\text{mg}^{-1}$ ) were performed. The solvents chosen were  $\text{H}_2\text{O}$ , methanol and  $\text{MeNO}_3$ . Hence, in LAG reactions, the formation of Form I was preferably observed when PMMA jars were used. Further, Form II tends to be formed when ss jars were employed, Figure 9. In both cases, NG and LAG experiments, the reactions performed with  $\text{H}_2\text{O}$  were slower, and a mixture of products (Form I and Form II) was observed. These results thus prove that the milling jar material has an important effect in the polymorphic outcome.

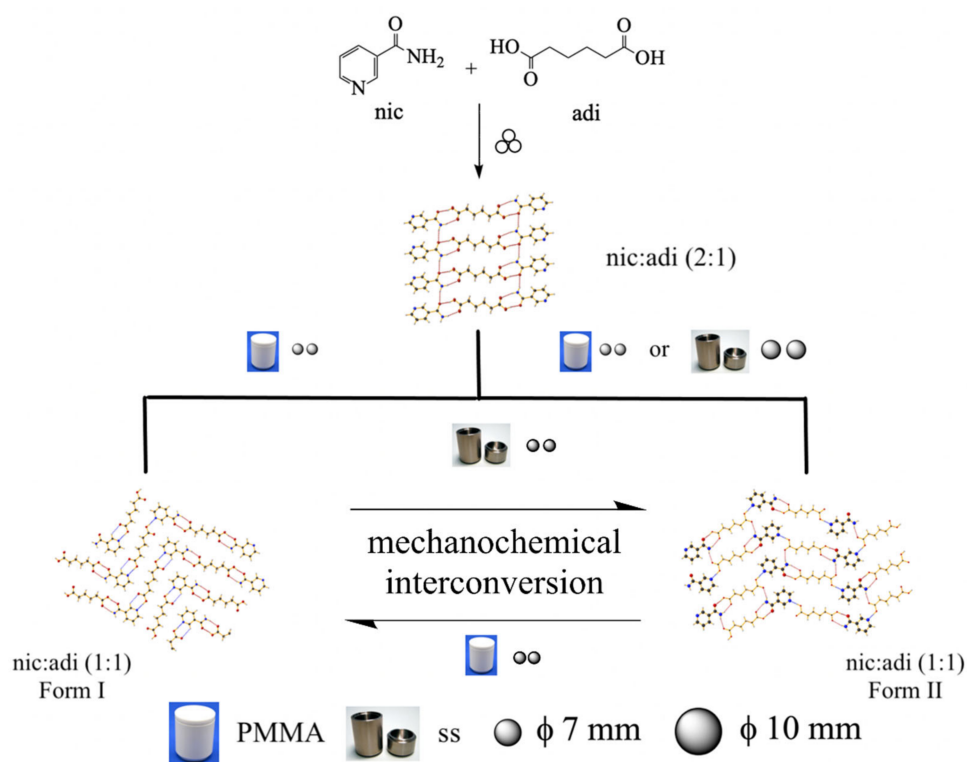


**Figure 9.** Schematic representation of the different solid forms in the cocrystal system nic:adi. These processes can be controlled by the choice of milling assembly. Adapted with permission from [229], Royal Society of Chemistry, 2020.

The mechanochemical interconversion, Figure 9, can be achieved milling a sample of Form I initially prepared using a ss jar and a pair of ss balls of 7 mm diameter each in the presence of acetonitrile  $\eta = 0.125 \mu\text{L}\cdot\text{mg}^{-1}$ . From this milling (60 min), Form I can be interconverted to Form II (Form I  $\rightarrow$  Form II). In the case of the reverse process, i.e., Form II  $\rightarrow$  Form I, starting from Form II milling in a PMMA jar under identical conditions, Form I was produced after 2 h, but this reaction was slower and traces of the Form II were detected. It should be noted that the transition enthalpy for the metastable Form II with respect to

Form I was determined by differential scanning calorimetry DSC ( $\Delta H = +2.3(3) \text{ kJ}\cdot\text{mol}^{-1}$ ). For further details about the DSC technique, consult Section 3.3.

In addition, three different experiments were studied by in situ PXDR. In the first one, (A) PMMA jars and two ss balls of 7 mm diameter were used. Then, in the second and third experiments (B and C), PMMA jars were used, but in experiment B ss balls of 7 mm diameter were added, while in experiment C, two zirconia balls of 10 mm diameter were used. It should be noted that the total balls weight in experiment A, B, and C were 2.8, 5.6, and 5.8 g, respectively.

In the three experiments, the formation of nic:adi (2:1) as the first reaction intermediate was detected, Figure 9. For the experiment A, initially the formation of nic:adi (2:1) is observed and gradually Form I is produced as a final product after 85 min of milling. Further, in experiment B (where balls weight was increased), the reaction proceeded from the intermediate nic:adi (2:1) and the subsequent formation of the Form II and finally produce Form I. The increase in balls weight in experiment B led to an increase in the reaction rate due to a higher energy input. Based on these results, both reaction sequences can be explained under the Ostwald's rules of stages. These rules describe that: "states that in a crystallization, the system moves to equilibrium from an initial high-energy state through minimal changes in free energy, and thus implying that the least stable polymorph must be the first isolated in any crystallization" [242]. In this context, experiment C showed unexpected results, since the reaction sequence observed was first the formation of nic:adi (2:1) and then Form II (metaestable polymorph) via the thermodynamically more stable phase (Form I). This completely challenges Ostwald's rules of stages. With this work on mind, Frišćić et al., elegantly demonstrated that the polymorphic outcome of the cocrystal system nic:adi is strongly influenced by the nature of the jar material and the balls used.

In another interesting investigation, Guerain et al., demonstrated that cocrystal polymorphism can be observed in the system S or RS-ibuprofen (S-ibp or RS-ibp) with nicotinamide (nic). [243] According to the authors, the polymorphic outcome depends on the synthetic method used. It should be noted that previously both cocrystal S-ibp:nic and RS-ibp:nic were reported by Berry et al. [244] and Guerain et al., synthesized both cocrystals using the following methods: (1) milling under dry conditions, (2) melting at 100 °C and then the mixture was cooled down and then recrystallized (isothermal and non-isothermal processes), and (3) slow evaporation (ethanol). From the results obtained by PXRD or Raman spectroscopy (for further information about this technique, consult Section 3.3), in both cocrystals obtained from methods 1 and 3, the spectral and diffraction information obtained are almost identical. However, the analytical information obtained from method 2 exhibited differences compared with 1 and 3. It is noteworthy that the analytical results observed in the solid form (hereafter Form B) produced by methods 1 and 3 are in agreement with that reported by Berry et al. [244]. This evidence indicated that the solid form obtained from method 2 (Form A) is a cocrystal polymorph of the Form B. Hence, additional PXRD experiments were performed with the products of the room temperature and 100 °C procedures. According to the diffraction results, both cocrystals obtained by methods 1 and 3 remained as Form B until melting. After cooling down from the melting process, both cocrystals were found to be in an amorphous form. The solid form obtained from method 2 corresponds to Form A being slightly different from Form B. This Form A is transformed into Form B at 65 °C, and above 80 °C, the solid form is melted. Further analytical studies by DSC and Raman spectroscopy were performed. The Raman analysis revealed a subtle polymorphic transformation not detected in DCS experiments. Despite DSC techniques being the more suitable technique to analyze phase transitions, non-detection of the polymorphic transformation was observed, suggesting that both Forms are slightly different from an energetically point of view. Since the polymorphic transformation was not detected by DSC, analysis by low-wave number Raman experiments under similar thermal conditions employing the same calorimetric technique (DSC) led to the observation of two-step successive mechanism. From recrystallization experiments (method 2, isothermal and non-isothermal), it was first observed the formation

of Form A via a nano/microcrystalline state. Being the second step, the transformation of Form A into Form B. It was observed that transformation of Form A into Form B upon heating via the two-step mechanism exhibited very weak changes in the hydrogen bond networks of the participant intermediates. This work thus demonstrated the crucial role of the H-bonding organizations on the cocrystal formation mechanisms.

Finally, in another interesting study, Dudek et al., prepared, by ball-milling using methanol as an additive, a ternary cocrystal system starting from a binary cocrystal system. Evaluation of the possible pathways involved suggests a non-concerted mechanism [245]. The components involved were barbituric acid (BA), thiobarbituric acid (TBA), and 1-hydroxy-4,5-dimethyl-imidazole 3-oxide (HIMO), Figure 10. Using the binary cocrystal system BA:TBA; 1:1 as model, [246] and comilled with HIMO, the reaction was monitored by ssNMR (for further information about this technique, consult Section 3.3), Figure 10. Based on the results obtained, two mechanistic pathways were assumed. Pathway 1 involving a concerted process, in which, as HIMO is forming the new solid form (HIMO:TBA), BA is simultaneously departed in a synchronized manner. Additionally, the non-concerted Pathway 2, where it is proposed that in the intermediate stage the three components are completely separated and subsequently HIMO:TBA is formed.

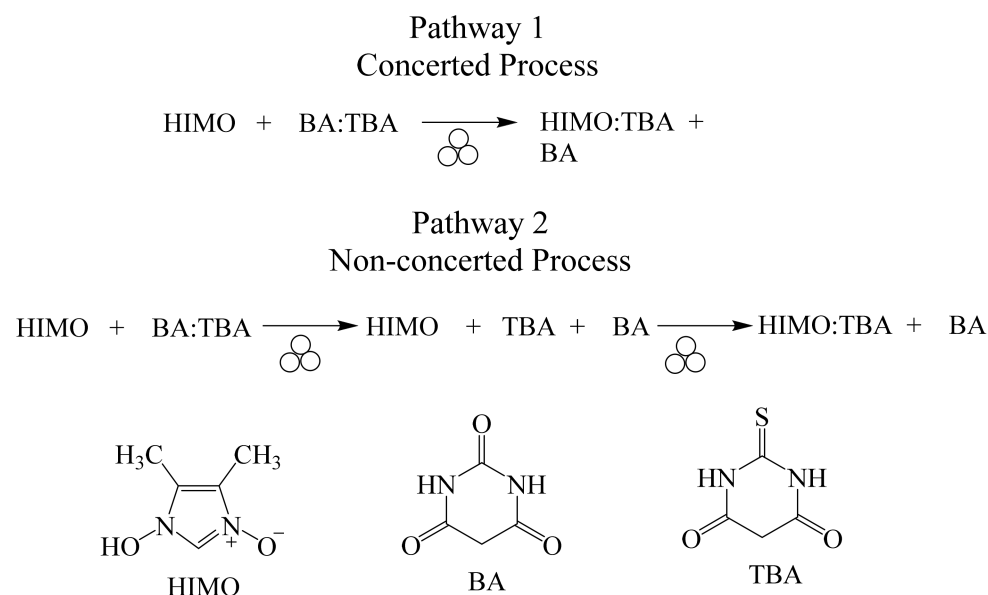


**Figure 10.** Schematic representation of the two proposed mechanisms behind the formation of HIMO:TBA.

According to the ssNMR experiments and theoretical calculations, this mechanochemical reaction leading to the formation of HIMO:TBA follows a non-concerted mechanism. It is important to remark that authors indicate that both pathways are equivalent to the mechanisms observed in organic chemistry ( $S_N1$  and  $S_N2$  reactions).

### 3. Cocrystal

#### 3.1. Cocrystal Definition

For many years, there has been an intense debate in the attempt to propose a formal definition of what a cocrystal is [18]. Thus, several variations and modifications in the definition have been made in the last years [48]. The difficulty to have a proper definition of a cocrystal is due to the diversity observed in the scale range-order periodicity and composition amongst the different multicomponent solid forms of an API, Figure 1 [15,247]. Apparently, before the contributions of Aitipamula et al. [18] and Groethe [56], it was somewhat difficult to delimitate the cut-off amongst polymorphs, solvates, hydrates, molecular salts, polymorphs of cocrystals, etc. However, it seems that Aitipamula and

Groethe's approaches have had a great impact in the development of a simplistic way to classify and differentiate all of this.

By itself, the term cocrystal is referred as a crystalline molecular complex, in which the components are neutral species forming an adduct, otherwise it should be considered a multicomponent salt (charged anions and cations) [248]. Thus, in a binary system (A: acid; B: base), a salt is formed when a proton transfer exists establishing the molecular specie ( $A^-B^+ - H$ ) [60]. Thus, from the Crystal Engineering context, the formation of multicomponent salts comes from the combination of acids and bases, and cocrystals are not necessarily made up from these species, Figure 11 [248]. Thus, it is noteworthy to mention three important considerations described by Aakeröy et al., to define a cocrystal [249].

1. "Only compounds constructed from discrete neutral molecular species will be considered cocrystals. Consequently, all solids containing ions, including complex transition-metal ions, are excluded".
2. "Only cocrystals made from reactants that are solids at ambient conditions will be included. Therefore, all hydrates and other solvates are excluded which, in principle, eliminates compounds that are typically classified as clathrates or inclusion compounds (where the guest is a solvent or a gas molecule)".
3. "A cocrystal is a structurally homogeneous crystalline material that contains two or more neutral building blocks that are present in definite stoichiometric amounts".

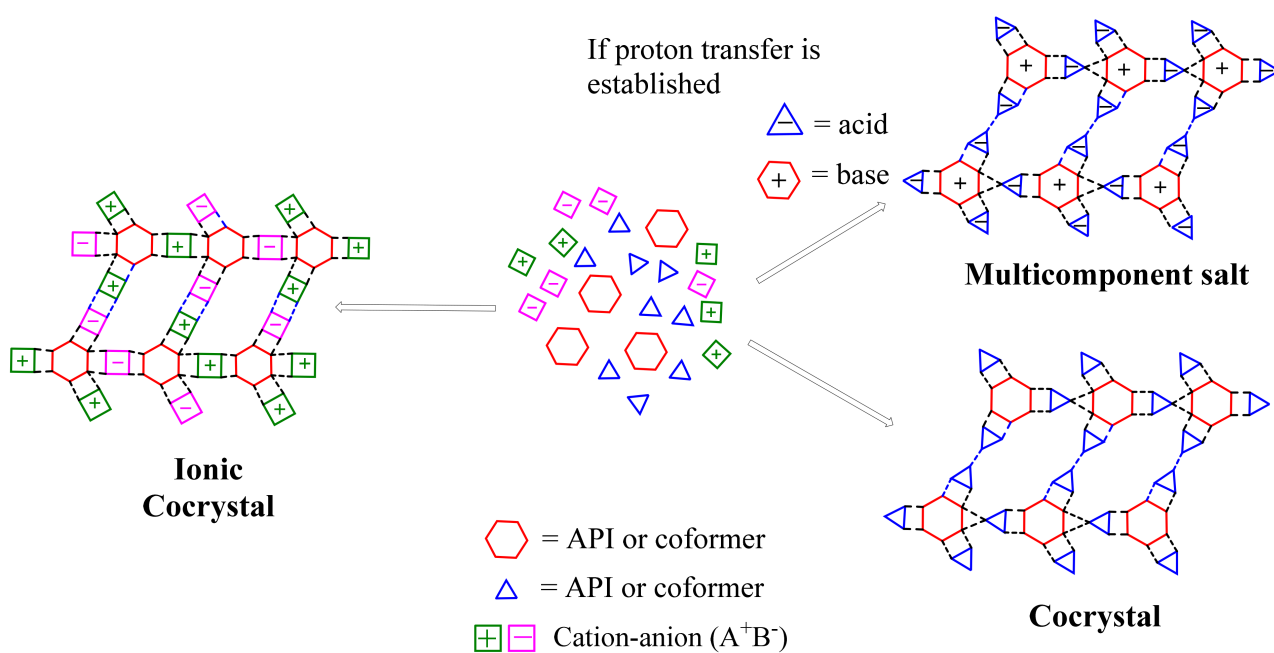


**Figure 11.** Schematic representation of the formation of multicomponent salt or cocrystal or ionic cocrystal.

In addition, some authors have mentioned that the prediction of whether a cocrystal or salt will be formed can be on basis of the  $\Delta pK_a$  rule [250,251]. This empirical consideration refers that a salt is expected to be formed when a  $\Delta pK_a$  value between the acid and the base is greater than 3 ( $\Delta pK_a > 3$ ), thus observing a proton transfer ( $A^-:B^+ - H$ ) [13,61,252]. Further, when the value is  $\Delta pK_a < 0$ , the product is a neutral cocrystal (proton is retained on the acid). However, many cocrystallization attempts may fall in the range of  $0 < \Delta pK_a < 3$ , which will form mixed ionization states between components (proton is in-between the acid and the base) [253]. These multicomponent forms found in this situation are denominated salt-cocrystal continuum [48,61,254].

From these borderline concepts, apparently, the distinction between cocrystal vs. multicomponent salt is well defined. However, difficulties have emerged when the ionization state of the charged species can change upon variations in temperature [255]. Additionally,

few papers have reported binary systems where some multicomponent pharmaceutical solid forms crystallize concomitantly as cocrystals and salts in the same stoichiometric proportions [256,257]. In fact, recently, Boldyreva et al., reported that the formation of a cocrystal or a salt is dependent of the synthetic method used [258]. Boldyreva et al., specifically mentioned that the binary system  $\beta$ -alanine ( $\beta$ -ala) and DL-tartaric acid (DL-ta) in 1:1 stoichiometry is an interesting case of study since by ball-milling under liquid assisted conditions and/or by slow evaporation crystallization, the cocrystal form can be produced (CSD refcode: VELBIA; P2<sub>1</sub>/c). However, by ball-milling under dry conditions, the multicomponent salt is formed (CSD refcode: VELBIA01; P1), Figure 12.

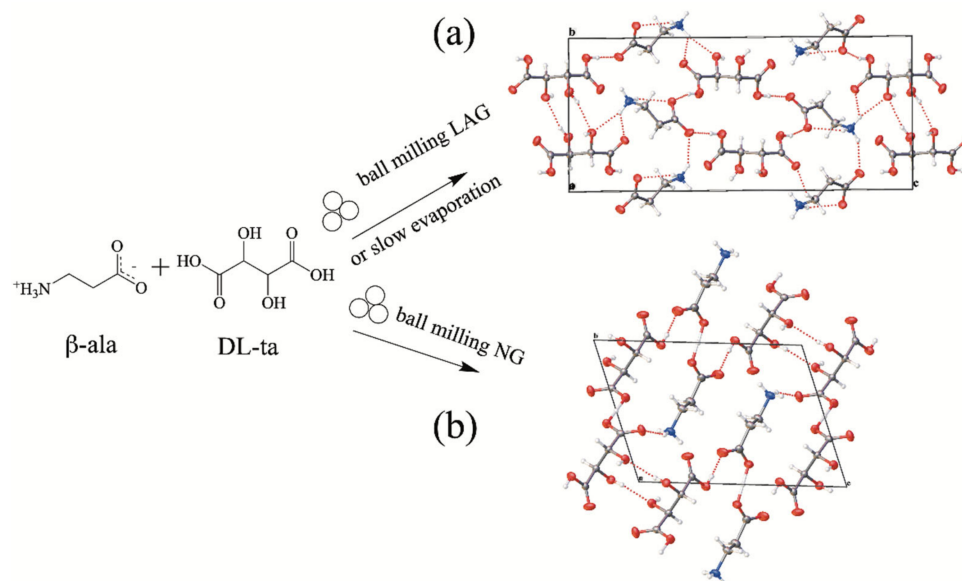


**Figure 12.** Formation of different multicomponent solid forms ( $\beta$ -ala + DL-ta; 1:1) depending on the synthetic method used: (a) cocrystal (plane  $bc$ ; CSD refcode: VELBIA) and (b) multicomponent salt (plane  $bc$ ; CSD refcode: VELBIA01).

Aitipamula et al., indicate that the FDA definition of a cocrystal is ambiguous: “solids that are crystalline materials composed of two or more molecules in the same crystal lattice” [18]. Therefore, they proposed a more ample and broader definition: “cocrystals are solids that are crystalline single-phase materials composed of two or more different molecular and/or ionic compounds generally in a stoichiometric ratio” [18]. Recently, Zhang et al., redefined the term cocrystal in an attempt to achieve a more uniform definition: “a cocrystal is a single-phase crystalline solid composed of two or multiple components in a stoichiometric ratio, and the components of a cocrystal can be atoms, molecules, anions, and cations in pairs, and/or metallic cations with free electrons shared [259].” According to this definition, cocrystals can be subdivided in five groups depending of the type of the components and their interactions in the crystal entity: atomic cocrystal, molecular cocrystal, ionic cocrystal, metallic cocrystal, and mixed-type cocrystal [259]. It should be noted that typically, ionic cocrystals are defined as multicomponent materials composed from a salt (or an ionic compound) and a neutral organic molecule [57,58,260]. Ionic cocrystals are defined in general as  $A^+B^-N$  where  $A^+$  is a cation,  $B^-$  is an anion, and  $N$  is a neutral molecule, Figure 11.

Thus, a straightforward form to view a pharmaceutical cocrystal is a *crystalline single phase where in the crystal lattice of an API is incorporated another neutral component denominated coformer (cocrystallizer agent or cocrystal former) in a specific stoichiometric ratio* [55,58]. In this context, the incorporation of a coformer alters the physicochemical and biological properties of the parental API (e.g., solubility, thermal stability, dissolution rate, bioavailability) without any covalent modification [57]. Both API/coformer are held together by non-covalent interactions (van der Waals contact forces,  $\pi$ - $\pi$  interactions, and/or hydrogen

bond). The cofomer to be incorporated in the crystal lattice of an API must be selected as a pharmaceutical molecule accepted, Generally Recognized as Safe (GRAS) [57,261]. On the other hand, agglutination of two or more APIs into one unit dose yields the formation of a drug–drug cocrystal also known as multidrug cocrystal [227]. Recently, the preparation of drug–drug cocrystals has gained a lot of interest in combination therapy [57,262]. The importance of these multidrug materials lies mainly in their potential activity in the treatment of complex diseases which require the simultaneously administration of two drugs [64,263,264]. Despite the potential therapeutic properties that may show drug–drug cocrystals, few examples are found marketed (Entresto™: Valsartan sodium–sacubitril sodium) and some are encountered in clinical trials (Esteve™: tramadol hydrochloride–celecoxib) [20,265].

Another important point to highlight is that from the legal and regulatory perspective, pharmaceutical cocrystals are a patentable product [266,267].

### 3.2. Design of Pharmaceutical Cocrystals: Selection of Appropriate API/Cofomer

The ability of an API to cocrystallize in the presence of a cofomer depends on diverse parameters: stoichiometry ratio (API/cofomer), solvent(s) employed, temperature, and crystallization technique used. Usually an API is more apt to cocrystallize when possessing donor and acceptor sites able to form reliable hydrogen bonding (supramolecular synthons [268]) with the cofomer [14,269]. The selection of an appropriate cofomer is mainly on basis of hydrogen bond propensities, molecular recognition, and innocuousness (GRAS), nevertheless these considerations do not guarantee the formation of the cocrystal [12,270]. For the design of pharmaceutical cocrystals, there are two approaches: (1) identification of complementary sites of the API and the cofomer to form reliable hydrogen bonds, and (2) the preparation of cocrystals based on high throughput screening crystallization [5,263]. The first approach is mainly based on the precepts of the graph set theory (Etter's rules) [271]. The second approach may result time-consuming and expensive. In addition, the help of computational and informatics approaches are recurrently used as tools in the prediction and selection of suitable API/cofomer candidates [272–274]. Recently, Aakeröy et al., reported a systematic process to find a proper selection of cofomers based on hydrogen-bond propensities using the CSD database [275].

### 3.3. Characterization of Pharmaceutical Cocrystals

Single crystal X-ray diffraction (SCXRD) is by far the most preferable technique to gain information on molecular recognition, hydrogen bonding patterns, assembly and packing of pharmaceutical cocrystals [276,277]. SCXRD is an excellent technique to make distinction between the formation of cocrystal vs. multicomponent salts [278,279], and salt-cocrystal continuum forms [61]. Unfortunately, in most of the cases obtaining suitable single crystals for X-ray diffraction is not easy, and other analytical methods must be used to gain knowledge about the formation of cocrystals.

Among these other techniques for the characterization of cocrystals, we found PXRD. This diffraction analysis technique is extensively used for the characterization of different multicomponent solid forms: cocrystals/salts [276,277], eutectics solid mixtures [63], coamorphous [52], allowing to understand the structural properties of these materials. In some cases, simulated molecular structures can be predicted from PXRD data [14]. The employment of software programs as DIFFRAC.TOPAS (Bruker AXS, Karlsruhe Germany) [280] or DASH [281] help in the structural determination of molecular structures based on Rietveld analysis.

Thermal analysis methods are of high importance in the structural characterization of cocrystals; for instance, DSC, differential thermal analysis (DTA), and thermogravimetric analysis (TGA) [14,276,277]. These analytical methods help to determine the formation of new solid phases; to determine percentages of crystallinity and percentages of weight loss, providing quantitative measurement of the associated enthalpy change, observation of thermal transitions, and detection of polymorphism, etc. DSC can prove the formation

of cocrystals, since the melting point determined is usually observed between the melting temperatures of the pure components. However, some DSC cocrystal thermograms exhibit consecutive multiple peaks. When DSC thermograms show two peaks, the first is due to the eutectic melting and the second corresponds to the cocrystal melting. In some cases, DSC scans may show three peaks, the first again corresponding to the eutectic melting, the second endotherm indicates the melting of the excess of one of the components (API or conformer) and the third corresponds to the cocrystal melting. Additionally, the appearance of multiple peaks in DSC scans could be associated with a polymorphic transformation of cocrystals [48].

Currently, the construction of binary phase diagrams (components A + B) based on DSC data is fundamental to distinguish among different solid forms: eutectic mixtures, cocrystals, solid solutions, physical mixtures, etc., Figure 13 [13,48].

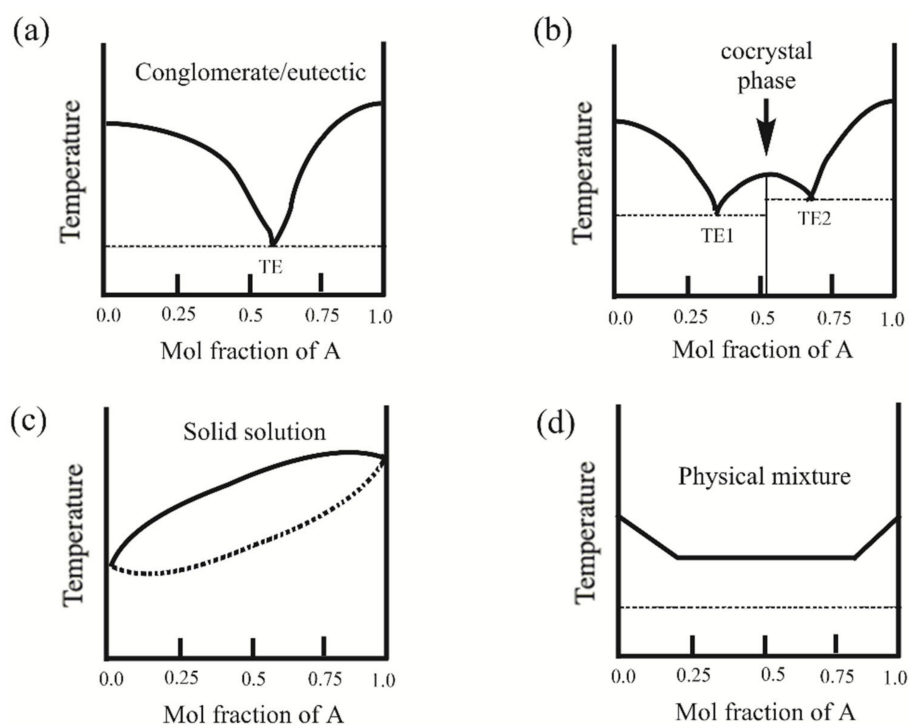


**Figure 13.** Schematic representation of binary phase diagrams (components A + B). (a) Solid eutectic mixture; TE: eutectic temperature. (b) Cocrystal formation; TE1 and TE2: eutectic temperatures 1 and 2. (c) Solid solution formation. (d) Physical mixture. Adapted with permission from [48], MDPI, 2018.

The construction of binary phase diagrams are made from data obtained from DSC scans at different compositions [282]. The formation of a binary eutectic mixture can be proved by the observation of the characteristic V-shaped diagram (depression in the melting point, TE: eutectic temperature, Figure 13a).

On the other hand, a pharmaceutical cocrystal has a W-shaped graph (Figure 13b). A W-shaped diagram exhibits at least two or more eutectic points (TE1 and TE2) and among them is found the cocrystal phase, Figure 13b [283]. Thus, the screening and detection of pharmaceutical cocrystals [284,285], solid eutectic mixtures [286,287], solid solutions [288], and physical mixtures (in binary systems two endotherms are observed in DSC thermograms corresponding of each component) [289] can be carried out by DSC analysis.

Additionally, ternary phase diagrams (component A + component B + solvent) help in the determination of the suitable stoichiometric ratio for the formation of a cocrystal. These types of diagrams are employed when cocrystals are not formed in a particular solvent due to the fact that both components exhibit incongruent solubility during solution crystallization [48,117].

Spectroscopic analysis is also widely used in the cocrystal characterization. According with Pindelska et al., there are two types of spectroscopic characterization methods: vibrational and nuclear magnetic resonance (NMR) [276]. Vibrational methods span from Fourier transform infrared spectroscopy (FT-IR), Raman scattering and Terahertz spectroscopy.

Specifically, a FT-IR spectrum shows the frequency, shape, position, and intensity of a peak related with the absorption of a vibrational mode associated with a functional group. Raman spectroscopy on the other hand, exhibits vibrational and rotational modes at low frequencies, mainly nonpolar functional groups that FT-IR cannot detect. Terahertz time-domain spectroscopy on the other hand, records frequencies in the interval (0.1–10 THz, which is 3.3–333.6  $\text{cm}^{-1}$ ), where bands correspond to vibrations associated with intermolecular interactions (hydrogen bonds, van der Waals, etc.) [276].

Another spectroscopic technique gaining relevance lately is X-ray photoelectron spectroscopy (XPS). This technique is capable of exhibiting the changes involved in the chemical environment of a substance as a result of the supply of different amounts of energy (binding energy), required to emit an electron from the nucleus at the atomic level. Fundamentally, XPS records the binding energy (kinetic energy) of photoelectrons emitted from a sample after being irradiated with X-rays [290,291]. XPS can distinguish between the formation of a cocrystal or a multicomponent salt. However, although Tothadi et al., indicated that the reliability of XPS in the distinction between a cocrystal and a multicomponent salt is robust, the determination of a salt-cocrystal continuum is difficult to distinguish [253].

Solid-state NMR (ssNMR) is another important technique to gain more valuable insights in the cocrystal characterization [248,276,277]. Recently, a new approach denominated NMR crystallography has been developed [276]. This approach combines the long-order data provided by PXRD and short-order data obtained by ssNMR (e.g., local symmetry, number of molecules contained in the unit cell, orientations, and non-covalent distances of the molecules). NMR crystallography provides a complete characterization using molecular modeling and quantum chemical to offer a prediction of the crystal structure when structures cannot be determined by SCXRD [292].

### 3.4. Diverse Preparation Methods of Pharmaceutical Cocrystals

The preparation of cocrystals comprises diverse strategies: refs. [48,227,293] dissolutive cocrystallization methods, antisolvent addition, slurry conversion, sublimation, vapor digestion, hot-stage microscopy melt interface, supercritical fluids, sonic slurrying, melt extrusion, wet compression, dry compression, microwave synthesis, and various solid-state synthetic methods, including NG, LAG, POLAG [293], TSE [48,182,183,294,295], resonant acoustic mixing (RAM) [296–299], ultrasound methods, etc.

TSE offers a unique opportunity not found in grinding or milling approaches because they are difficult to scale up to manufacture large amounts of the desired cocrystal [298]. In fact, one of the benefits of TSE is that the process of crystallization can be carried out under solventless conditions [181]. Alvarez-Núñez et al., demonstrated that TSE can be an important method of preparation of cocrystals at the large scale by studying four different cocrystal systems [182]. The authors emphasize that temperature and extent of mixing are the main parameters for a successful conversion in the process. TSE equipment consists basically of two co-/counter-rotating screws in a single barrel. By mechanical action of screwing, the components are mixed along the length of the barrel forming cocrystals [227].

RAM is another technique that deserves to be described in this review, since within the branches of mechanochemistry, sonochemistry considers chemical transformations produced by the action of sound, Figure 3 [80]. RAM was born as an alternative to mechanochemical synthesis, because the considerable amount of mechanical energy transferred from milling bodies to the sample may cause damage to particles, or large numbers of defects into the crystalline lattice or complete amorphization. Mainly, RAM is an alternative for the preparation of highly sensitive-explosive materials and propellants. Furthermore, RAM is recommended when the desired outcome is required to have high crystallinity. Be-

sides, another benefit found in the use of RAM is the scale-up possibility for the formation of a given cocrystal [298,299].

Basically, RAM is a technique where the components are mixed intimately at high frequency, promoting the formation of cocrystals. The acoustic energy is generated by the action of the oscillation of springs, which induce mechanical resonance, frequency directly transferred to the sample vessel originating local mixing zones [296].

An interesting case of the scale-up benefits of RAM in cocrystal production is reported by Nagapudi et al. [299]. The authors carried out high throughput screening to 16 cocrystal systems previously reported. A 96-well plate was adapted to screen the 16 cocrystal systems using RAM. The screening experiments at each well were carried out at different conditions: (i) components with no zirconia beads, (ii) components with water, (iii) components with zirconia beads and water, (iv) components with ethanol, (v) components with zirconia beads and ethanol.

According with the number of hits obtained after the screening of the 16 cocrystal systems, the best conditions found were when solvent was added (13 out of 16). Further, the worst conditions (3 out of 16) were when no solvent or beads were added. Under conditions of adding beads without solvent, moderate hits were obtained (5 out of 16). Then, Nagapudi et al., reported that solvents played a crucial role in the screening. The use of beads and solvent showed similar results as those observed in the hits with just the use of solvents. The liquid assisted high-throughput screening using RAM is an effective technique to produce cocrystals. In addition, the cases where the screening were unsuccessful could be due two factors: (i) wrong choice of solvent or (ii) no proper selection of energy-input.

In a second experiment, the theophylline-citric acid (thp:ca) system was used as a model. The cocrystal system thp:ca can be prepared by NG or LAG [212]. The cocrystallization outcome is dependent of the conditions used. If one of the initial components is hydrated or water is added during the grinding, the cocrystal hydrated form is obtained. Otherwise, if both components are anhydrous or the solvent used is not water, then the anhydrous cocrystal form is yielded. In this case, Nagapudi et al., reproduced all the above-mentioned experiments using RAM. The experiments were carried out with 50  $\mu$ L of either ethanol or water. In addition, essays were conducted with and without beads. From these results, it was observed that both forms can be obtained by RAM (anhydrous and hydrated). Experiments using simultaneously beads and solvent exhibited complete conversion of the reaction. However, essays only employing solvent, presented unreacted amounts of thp. It was observed that addition of beads accelerates the kinetics of the conversion.

Another set of experiments were carried out evaluating  $\eta$  at different values (0.0, 0.25, 0.5, 1.0, and 2.0, using water). The cocrystal system used was thp and oxalic acid (ox) in a 2:1 stoichiometry. The results obtained from  $\eta = 0.0$  to 1.0 showed that the reactions almost completely led to the formation of the cocrystal thp:ox. However, when  $\eta = 2.0$  exhibited unreacted thp. It should be noted that solubility in water of thp is  $\sim 8.3$  mg/mL whilst ox is  $\sim 143$  mg/mL. Under  $\eta = 2.0$ , probably ox is completely solubilized and thp not. It is important to note that at  $\eta = 2.0$ , a significant conversion to the cocrystal thp:ox is observed, but due to the lower solubility of thp compared to ox, this hampers the completeness of reaction.

Besides, scale-up experiments were carried out using the cocrystal system thp:ox. For the scale up entry at 80 g, it was observed that the successful formation of the cocrystal depends at least on two parameters, acceleration and mixing time. For instance, the first 30 min of mixing at 60 g the conversion to the cocrystal reaches 97–98%. No perceptible changes in conversion were detected increasing from 30 min to 6 h. In addition, increasing to 10 h of mixing led to a similar conversion percentage as that observed at 30 min. However, according to PXRD data, it is possible that the thp experiences polymorphism. According to these results, an excellent balance between acceleration and mixing time is important for the formation of the cocrystal.

In general, Nagapudi et al., indicated that TSE and RAM are important techniques for the scaling up of cocrystals. TSE seems not to be effective for the cocrystal screening but provides higher shear and access to a greater temperature range than RAM. When cocrystal formation occurred by an eutectic intermediate, TSE is more appropriate than RAM. In scale up proportions, RAM is suitable to produce hundreds of grams to 1 kg of the desired cocrystal while TSE is appropriate for larger manufacturing scales (various kilograms).

Michalchuk et al., reported the first in situ real-time study of cocrystal formation by RAM using synchrotron X-ray radiation and a Resodyn LabRAM instrument [296]. The cocrystal system used as the model was carbamazepine:nicotinamide (cbz:nic 1:1; CSD refcode: UNEZES;  $P2_1/n$ ) [300] starting from cbz Form III + nic Form I, Figure 14. Previously, it has been reported the cocrystallization of cbz:nic 1:1 using RAM [298].

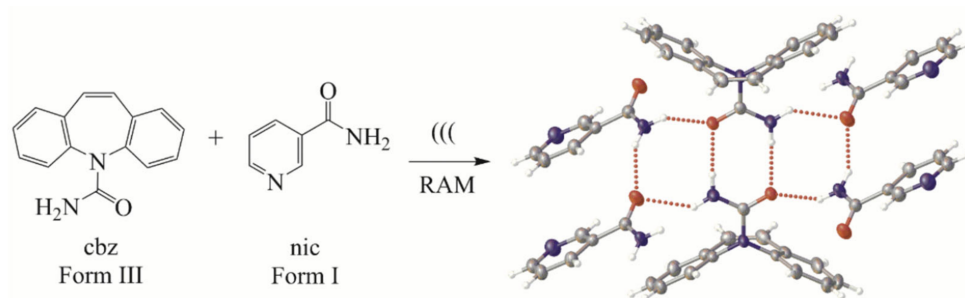


**Figure 14.** Cocrystal formation of cbz:nic 1:1 (CSD refcode: UNEZES;  $P2_1/n$ ) using RAM.

RAM experiments under dry conditions did not produce the cocrystallization product between cbz and nic. Nevertheless, the reaction proceeded after addition of one drop of water (ca. 20  $\mu\text{L}$ ). The experimental conditions of the Resodyn LabRAM instrument were kept fixed with respect to the magnetic resonance frequency approximately 61 Hz, however, the amplitude of the oscillation was adjusted to two acceleration values 50 and 100 G.

After 90 s of mixing of both components under 50 G using RAM, Rietveld refinement of the in situ PXRD data indicated that the major product detected was the dihydrated form of cbz ( $\text{cbz}\cdot 2\text{H}_2\text{O}$ ). The formation of  $\text{cbz}\cdot 2\text{H}_2\text{O}$  implies that this is the kinetically controlled product. Additionally, according with the Rietveld refinement, after 90 s of reaction, only 10 mol% of the cocrystal cbz:nic 1:1 is formed.

Substantial acceleration in the cocrystal formation of cbz:nic 1:1 was observed under 100 G. During the first 30 s of mixing, it was detected only traces of the initial components and the cocrystallization occurred rapidly. Contrary to the Rietveld refinement observed at 50 G, suggesting the formation of the product  $\text{cbz}\cdot 2\text{H}_2\text{O}$ , at 100 G, the dominant phase was the cocrystal cbz:nic 1:1.

Therefore, the authors suggested that higher accelerations conditions led to a more rapid mixing of the components. Higher accelerations promote more reaction zones (comminution, particle–particle interfaces, surface regeneration, etc.) favoring the intimate mixing, while at lower accelerations particles tend to be agglomerated inhibiting this process. According to the authors, temperatures reached in situ in the sample jar at different acceleration conditions vary slightly (ca. 40  $^\circ\text{C}$ ).

Cocrystal formation by sonochemistry is another technique that is worth mentioning [124]. Sonochemistry is based on the formation of acoustic cavitation (formation, growth, and implosive collapse of bubbles in liquids) caused by the action of mechanical effects of sound. Application of ultrasound generates interruption and breaking of attractive forces between the molecules of the liquid medium, causing a considerable drop in the internal pressure forming bubbles. Bubble collapse or collision creates unique conditions: temperatures above 5000 K, pressures exceeding 1000 atmospheres, and heating and cooling rates in excess of  $10^{10} \text{ K}\cdot\text{s}^{-1}$  providing mechanical energy [80].

Some examples using sonochemistry for the preparation of cocrystals have been reported [206,301]. It should be noted that sonochemistry processes typically proceed, adding

a drop of solvent or under slurry conditions. Usually, all the papers reporting sonochemical reactions mentioned were conducted under ultrasonic cavitation of a liquid phase (formation of microbubbles). However, recently, Roy et al., published that preparation of cocrystals by this method can be performed under dry conditions employing an ultrasonic cleaning bath [124]. Specifically, the report of the formation of two cocrystal systems; first, paracetamol in the presence of caf; 4,4'-bipy or 5-nitroisophthalic acid (5-nip) each in a 1:1 ratio. Additionally, the other cocrystalline form is meloxicam:aspirin (1:1) reported previously by Zaworotko et al. [302].

Initially, for the systems using paracetamol, each pair of solids were sonicated for 60 min in a glass vial sealed and suspended in an ultrasonic cleaning bath under dry conditions. Analysis by PXRD of the solid forms paracetamol:caf and paracetamol:4,4'-bipy exhibited the successful formation of the cocrystals. However, the system paracetamol:5-nip only showed the unreacted starting components by PXRD. Another set of time-dependent experiments were carried out to determine how the percentage of conversion towards the cocrystal was affected. Samples of paracetamol:caf and paracetamol:4,4'-bipy were sonicated for 15, 30, 45, and 60 min. The full conversion for the cocrystalline product in both systems was observed only at 60 min. For the cocrystal formation of paracetamol:5-nip, it was necessary to micronize the powders in particle size of <500 or <150  $\mu\text{m}$ . Decreasing particle size enhances the rate of reaction since the surface area was increased. Sonication experiments using micronized powders were unsuccessful in the transformation to the cocrystal phase. Thus, liquid assisted sonochemical irradiation (LASI, analogous to LAG) was applied. The successful conversion into the cocrystal form paracetamol:5-nip was observed, sonicating the powders by 60 min using methanol (1.0 mol·eq). Additionally, experiments at different times of sonication (15, 30, and 45 min) and employing different LASI conditions (0.25, 0.5, and 0.75 mol·eq) were carried out. The reaction at 15 min and in the presence of 0.25 mol·eq of methanol was quantitative. Therefore, the authors concluded that adding solvent in catalytic amounts dramatically accelerates the reaction. Additionally, they suggested that despite the melting points of the starting materials being high, formation of a melt as an intermediate during the reaction is not discarded.

Regarding the cocrystal system meloxicam:aspirin, produced by sonication of both components in complete dry conditions, analysis by PXRD exhibited the formation of the desired solid form. However, traces of the starting constituents were observed. Additionally, the starting powders were micronized and sonicated by 60 min. The resulting PXRD patterns indicated that the reaction occurred, however the crystallinity of the product was very low. With these results, it could not be categorically concluded the formation of the desired cocrystal. Thus, in an attempt to optimize the reaction LASI was carried out using  $\text{CHCl}_3$  (10.0 mol·eq) sonicating by 60 min. Being these conditions enough for the complete formation of the desired cocrystal. Thus, globally, this work demonstrated that ultrasonic cavitation of the liquid phase (formation of microbubbles) is not necessary, since some reactions were carried out in the absence of solvent.

### 3.5. Benefits of Pharmaceutical Cocrystals

Cocrystallization methods have emerged as a Crystal Engineering approach in an attempt to modify the solid-state properties of an API without affecting its intrinsic properties [303]. The implications of these solid-state modifications by cocrystallization procedures rely mainly in the improvement of properties as: solubility [47–49,304], dissolution rate [45,46], bioavailability [55,304,305], permeability [304], tablet ability [306,307], and thermal stability [308], or taste masking [55].

### 3.6. Chronological Survey of Papers Mentioning Mechanochemical Synthesis of Pharmaceutical Cocrystals

Various scientific reports are available in the literature describing the formation of diverse pharmaceutical cocrystals by mechanochemical methods. These mechanochemical methods span from grinding/milling under dry or liquid assisted conditions, TSE, RAM, impact/shear/vibratory treatment, POLAG, ILAG, etc. In this regard, Table 1 shows a

chronological summary of the most representative publications associated with these procedures. Table 1 is related with the formation of pharmaceutical cocrystal or multicomponent salts (and all their different solid forms described in Figure 1 and Section 3.1) of the type API + coformer or API + API forms (multidrug). In this survey, also were included natural products (NP hereafter) instead an API. NP should exhibit pharmaceutical activity. The survey was made using Scifinder® (Columbus, OH, USA) under the restriction search “Liquid assisted grinding cocrystals or neat grinding cocrystals or milling cocrystals or grinding cocrystals or grinding salt-cocrystal continuum”. The survey was made for the period of 16 November 2020 to 5 February 2021. Patents were not included in this survey.

**Table 1.** Chronological summary of the most representative publications related with the formation of pharmaceutical cocrystals or multicomponent salts by mechanochemical procedures.

API or NP + Coformer or API + API	Year of the Paper	Type of Grinding or Method of Synthesis and Characterization	Type of Multicomponent Form	Reference
Adenine + Thymine	1993	NG/slow evaporation	Cocrystal	[309]
Sulfadimidine + 8 diverse Carboxylic acids coformers	1995	NG	Cocrystal	[310]
Caffeine + Glutaric acid	2004	SDG	Cocrystal	[155]
Caffeine or Theophylline + chiral or racemic forms D,L-tartaric acid	2006	LAG	Cocrystal	[311]
Ternary system Caffeine + Succinic acid + diverse solvent guest	2006	NG/LAG/slow evaporation	Cocrystal solvent	[312]
Caffeine or Theophylline + citric acid	2007	NG/LAG	Cocrystal	[212]
Theophylline + 1,7-Heptanediamine	2007	NG	Salt-Cocrystal Continuum	[61]
Nicotinamide + Mandelic acid or Ibuprofen	2007	NG/LAG	Cocrystal	[313]
Carbamazepine + diverse coformers	2009	SDG/slow evaporation	Cocrystal	[149]
Theophylline or Caffeine + L-Malic or L-Tartaric acid	2009	LAG/sonochemical reactions	Cocrystal	[206]
Meloxicam + Succinic acid or Maleic acid	2009	SDG	Cocrystal	[314]
Nicotinamide + 10 diverse dicarboxylic acids coformers	2009	Melt/NG/LAG/slow evaporation	Cocrystal	[241]
Paracetamol + 13 diverse coformers	2009	NG/LAG	Cocrystal	[306]
2-Chloro-4-nitrobenzoic acid + Nicotinamide	2010	LAG/slow evaporation	Cocrystal	[315]
Indomethacin + 30 diverse coformers	2011	LAG/Prediction of cocrystal formation employing Hansen solubility parameter	Cocrystal	[316]
Piracetam + Citric acid or Tartaric acid	2011	NG/LAG	Cocrystal	[317]
Nicotinamide + five Fenamic acid derivatives	2011	LAG/liquid assisted sonication/slow evaporation	Cocrystal	[318]
Curcumin + Resorcinol or Pyrogallol	2011	LAG	Cocrystal	[319]
Prulifloxacin + Salicylic acid	2011	Kneading	Cocrystal	[320]
Furosemide + 8 diverse coformers	2012	LAG	Cocrystal	[321]
Acetazolamide + diverse carboxylic acids or amide derivatives coformers	2012	LAG	Cocrystal	[322]

Table 1. Cont.

API or NP + Coformer or API + API	Year of the Paper	Type of Grinding or Method of Synthesis and Characterization	Type of Multicomponent Form	Reference
Indomethacin + Saccharin	2012	LAG	Cocrystal	[323]
Nitrofurantoin + 4-Hydroxybenzoic acid or Nicotinamide or L-Proline or Vanillic acid	2012	LAG	Cocrystal	[324]
Piroxicam + 20 different carboxylic acids	2012	LAG/fast cooling and slow cooling of a hot saturated solution/precipitation with an antisolvent/slow evaporation/melting	Cocrystal/cocrystal hydrate/coamorphous	[325]
Meloxicam + diverse carboxylic acids	2012	SDG	Cocrystal	[326]
DL-Malic acid + L-Tartaric acid and L-Malic acid + DL-Tartaric acid	2012	LAG	Cocrystal	[327]
Andrographolide (NP) + Vanilin or Vanillic acid or Salicylic acid or Guaiacol	2013	LAG	Cocrystal	[328]
$\alpha$ - or $\gamma$ -Glycine + 7 carboxylic acids cofomers	2013	NG/spray drying/fast and slow anti-solvent techniques	Cocrystal/multicomponent salt	[329]
Racemic Praziquantel + diverse aliphatic dicarboxylic acids cofomers	2013	LAG/slurry method	Cocrystal	[330]
Carbamazepine + Saccharin and Nicotinamide + Suberic acid	2013	LAG	Cocrystal	[200]
L-Serine (anhydrous or monohydrate) + Oxalic acid (anhydrous or dihydrate)	2014	NG/LAG/slow evaporation/precipitation on antisolvent crystallization	Multicomponent salt/multicomponent salt hydrate/multicomponent salt polymorph	[331]
Trospium chloride + diverse carboxylic acid cofomers	2014	NG/LAG/slurry method/slow evaporation	Cocrystal	[332]
AMG 517 + Sorbic acid	2014	Ball-milling/TSE	Cocrystal	[294]
Caffeine + Anthranilic acid	2014	LAG	Cocrystal polymorph	[68]
Lenalidomide + urea or 3,5-Dihydroxybenzoic acid (1:1 and 1:2:1 monohydrate)	2014	LAG	Cocrystal	[333]
Ezetimibe + Methyl paraben	2014	LAG/slow evaporation	Cocrystal	[334]
$\alpha$ -Glycine + $\beta$ -Malonic acid	2014	NG/LAG/Impact treatment/shear treatment/vibratory treatment	Multicomponent salt	[335]
Stanozolol + Malonic acid or D-Phenyllactic acid or 6-Hydroxy-2-Naphthoic Acid	2014	LAG	Cocrystal	[336]
Caffeine + Citric acid or Anthranilic acid and Phenazine + Mesaconic acid	2015	LAG/POLAG	Cocrystal	[211]
Pyrazinamide + <i>p</i> -Nitrobenzoic acid	2015	LAG	Stoichiometric cocrystals	[337]
Theobromine + Oxalic acid	2015	NG/structure solved based on the powder X-ray data/in situ using synchrotron powder X-ray diffraction	Cocrystal	[338]
Theophylline + 4-Aminosalicylic acid or 4-Aminobenzoic acid	2015	LAG/slow evaporation	Cocrystal	[339]

Table 1. Cont.

API or NP + Coformer or API + API	Year of the Paper	Type of Grinding or Method of Synthesis and Characterization	Type of Multicomponent Form	Reference
Pyrimidin-2-amine + Glutaric acid	2015	NG/slow evaporation	Cocrystal/salt-cocrystal continuum	[340]
Theophylline + Benzoic acid	2015	NG/In Situ investigations of milling reactions using combined powder X-ray Diffraction and Raman spectroscopy	Cocrystal	[341]
Anthranilic acid + Carbamazepine or Salicylic acid or Theophylline and Salicylic acid + theobromine	2015	NG/LAG/slurry methods/competitive milling reactions	Cocrystal	[342]
Pentoxifylline + diverse carboxylic acid derivatives or Furosemide or L-Ascorbic acid	2015	NG/LAG/ <i>In Silico</i> screening	Cocrystal	[343]
Triamterene + DL-Mandelic acid or Saccharin	2015	LAG/slurry method	Cocrystal	[344]
Theophylline + <i>o</i> -Aminobenzoic acid or <i>m</i> -Aminobenzoic acid or <i>p</i> -Aminobenzoic acid	2015	LAG/slow evaporation	Cocrystal	[345]
Adefovir Dipivoxil + Glutaric acid	2015	LAG	Cocrystal	[346]
Resveratrol + 4-Aminobenzamide or Isoniazid	2016	LAG/rapid solvent removal	Cocrystal	[307]
Ethionamide + Oxalic acid or Glutaric acid or Adipic acid or Sebacic acid or Fumaric acid	2016	LAG	Cocrystal/multicomponent salt	[347]
Piroxicam + Saccharin	2016	NG/LAG/slow evaporation	Cocrystal	[348]
Theophylline + Benzamide	2016	LAG/solvent screening/in situ synchrotron powder X-ray diffraction	Cocrystal/Cocrystal polymorph	[349]
Glicazide + Malic acid or Succinic acid	2016	LAG	Cocrystal	[350]
Ibuprofen + Nicotinamide	2016	NG/in situ Raman spectroscopy	Cocrystal	[351]
Simvastatin + Malic acid	2016	LAG	Cocrystal	[352]
Theophylline + Benzamide	2016	NG/synchrotron X-ray powder diffraction data	Cocrystal	[353]
Meloxicam + Acetylendicarboxylic acid	2016	LAG/slow evaporation	Cocrystal	[354]
Theophylline + Benzamide or Benzoic acid or Isonicotinamide	2016	NG/Competitive Cocrystal Reactions/in situ powder X-ray diffraction	Cocrystal	[355]
Pyrazinamide + Oxalic acid	2016	NG/LAG/in situ using combined synchrotron Powder X-ray Diffraction and Raman	Cocrystal	[356]
5-Fluorouracil + 3-Hydroxybenzoic acid or 4-Aminobenzoic acid or Cinnamic acid	2016	LAG/slurry method	Cocrystal	[357]
Lamotrigine + 4,4'-Bipyridine or 2,2'-Bipyridine	2017	LAG	Cocrystal	[358]
Aripiprazole + Orcinol	2017	LAG	Cocrystal	[359]

Table 1. Cont.

API or NP + Coformer or API + API	Year of the Paper	Type of Grinding or Method of Synthesis and Characterization	Type of Multicomponent Form	Reference
Hydrochlorothiazide + Piperazine or Tetramethylpyrazine or Picolinamide or Isoniazid or Malonamide or Isonicotinic acid	2017	NG/LAG	Cocrystal	[360]
Glicazide + Sebacic acid or $\alpha$ -Hydroxyacetic acid	2017	LAG	Cocrystal	[361]
Praziquantel + Citric acid or Malic acid or Salicylic acid or Tartaric acid	2017	NG/LAG	Cocrystal	[362]
$\gamma$ -Glycine + Oxalic acid dihydrate	2017	NG/Real-time in situ X-ray powder diffraction	Multicomponent salt	[363]
Mycophenolic acid + Isonicotinamide or Minoxidil or 2,2'-Dipyridylamine	2017	LAG/slow evaporation	Cocrystal	[364]
Gliclazide + Catechol or Resorcinol or <i>p</i> -Toluene sulfonic acid or Piperazine	2017	LAG/slow evaporation	Cocrystal/ multicomponent salt	[365]
Pyrazinamide + Malonic acid	2017	NG/LAG/slurry methods/In situ Powder X-ray Diffraction	Cocrystal polymorph	[366]
Carbamazepine + <i>p</i> -Aminosalicylic acid	2017	LAG/slurry methods/ slow evaporation	Cocrystal	[367]
Theobromine + Oxalic acid and Pyrazinamide + Oxalic acid	2017	NG/LAG/in situ Raman experiments	Cocrystal	[368]
Felodipine + Imidazole	2017	LAG/in situ Raman experiments	Cocrystal	[369]
Metformin hydrochloride + Dehydrated disodium succinate	2017	NG/melting/slow evaporation	Multicomponent salt	[370]
Chlorothiazide + 13 diverse coformers	2017	LAG/slow evaporation	Cocrystal/ multicomponent salt	[371]
11-Azaartemisinin + 13 diverse carboxylic acids coformers	2018	LAG	Cocrystal	[372]
Fluoxetine·HCl + Fumaric acid or Benzoic acid or Succinic acid	2018	NG/LAG/solvothermal synthesis/slow evaporation	Cocrystal	[373]
11-Azaartemisinin + <i>trans</i> -Cinnamic or Maleic acid (1:1 and 2:1) or Fumaric acid	2018	LAG	Cocrystal	[374]
Seselin (NP) + Thiourea	2018	LAG/slow evaporation	Cocrystal	[375]
$\beta$ -Alanine + DL-Tartaric acid	2018	NG/LAG	Cocrystal/ multicomponent salt	[258]
Naproxen + Proline	2018	LAG	Cocrystal polymorph/cocrystal hydrate/cocrystal solvate	[376]
Caffeine + Dapsone	2018	Slow evaporation/LAG/ spray drying	Cocrystal	[377]
Theophylline + Aspirin	2018	NG/LAG/slurry method/ternary phase diagram	Multidrug cocrystal	[378]
Caffeine + Citric acid or Glutaric acid	2018	ILAG	Cocrystal polymorph	[217]
Glipizide + Glycolic acid	2018	NG/LAG/slurry method/ slow evaporation	Cocrystal	[379]
Theophylline + Benzamide	2018	LAG	Cocrystal polymorph	[380]

Table 1. Cont.

API or NP + Coformer or API + API	Year of the Paper	Type of Grinding or Method of Synthesis and Characterization	Type of Multicomponent Form	Reference
Diclofenac acid + L-Proline	2018	NG/LAG	Cocrystal	[381]
Pefloxacin + 10 diverse dicarboxylic acids	2018	LAG/solvent evaporation	Multicomponent salt/multicomponent salt hydrate/salt cocrystal	[382]
Tofogliflozin + Sodium acetate or Potassium acetate	2018	LAG	Salt cocrystal	[383]
Flurbiprofen + Proline	2018	LAG/in situ Variable Temperature Synchrotron X-ray Diffraction	Chiral cocrystal/cocrystal solvate/stoichiometric cocrystal/cocrystal polymorph	[384]
Piroxicam + Succinic acid or Methylparaben or Resorcinol	2019	LAG	Cocrystal	[385]
Lamotrigine + Phthalimide or Succinimide	2019	LAG/slow evaporation/Ternary phase diagram	Cocrystal/Cocrystal hydrate	[386]
Pyrazinamide + Pimelic acid	2019	NG/LAG/Time Resolved In situ Powder X-ray Diffraction	Cocrystal polymorph	[231]
Nevirapine + <i>p</i> -Aminobenzoic acid	2019	NG/LAG	Cocrystal	[387]
Luteolin (NP) + Isoniazid or Caffeine	2019	LAG/Rapid solvent removal	Cocrystal	[388]
Meloxicam + Salicylic acid or Fumaric acid or Malic acid	2019	LAG	Cocrystal	[389]
Oxcarbazepine + Oxalic acid or 2,5-Dihydroxybenzoic acid or Salicylic acid	2019	LAG/slow evaporation	Cocrystal	[390]
$\alpha$ -D-Glucose + NaCl or NaBr or NaI	2019	NG/LAG	Ionic cocrystal	[391]
Carbamazepine + DL-Mandelic acid or DL-Tartaric acid	2019	LAG/computational prediction	Cocrystal/cocrystal polymorph	[392]
2-Pyridine-carboxaldehyde benzoylhydrazone (hydrazone) + Malonic acid + Succinic acid + Glutaric acid + Mesaconic acid	2019	NG/LAG/slow evaporation	Cocrystal/cocrystal solvate/multicomponent salt	[393]
Betulin + Adipic acid or Succinic acid or Suberic acid	2019	LAG	Cocrystal	[394]
Ciprofloxacin + Salicylic acid	2019	LAG/in situ Raman spectroscopy experiments	Multicomponent salt/multicomponent salt hydrate and solvate/salt-cocrystal	[395]
Pyrazinamide + Glutaric acid + Isonicotinamide and Pyrazin-2-carboxylic acid + Glutaric acid + Isonicotinamide	2019	LAG/In situ Powder X-ray Diffraction	Ternary cocrystal	[396]
Pirfenidone + Fumaric acid or Trimesic acid	2019	LAG/slow evaporation	Cocrystal	[397]
Glipizide + Glutaric acid	2019	NG/LAG/slow evaporation/slurry method	Cocrystal	[398]
Gemfibrozil + Isonicotinamide	2019	Milling	Cocrystal	[399]
Salicylic acid + diverse Imidazole coformers	2019	NG/structures were solved by powder X-ray diffraction	Multicomponent salt	[400]
Caffeine + Glutaric acid	2020	NG/LAG/POLAG	Cocrystal	[214]

Table 1. Cont.

API or NP + Coformer or API + API	Year of the Paper	Type of Grinding or Method of Synthesis and Characterization	Type of Multicomponent Form	Reference
Oxyresveratrol + Nicotinamide or Proline	2020	LAG/employing principal component analysis	Cocrystal	[401]
Itraconazole + Terephthalic acid	2020	LAG	Cocrystal	[402]
Ciprofloxacin + Nicotinic acid or Isonicotinic acid	2020	LAG	Cocrystal	[403]
Nicotinamide + Adipic acid	2020	Ball-milling LAG/Demonstration of reversible mechanochemical cocrystal polymorph interconversion (stable → metastable phase transformation). This process can be controlled by the choice of milling assembly/Real-time X-ray powder diffraction	Cocrystal polymorph	[229]
Betulin + Terephthalic acid	2020	LAG	Cocrystal	[404]
Ciprofloxacin + Carvacrol or Thymol	2020	NG/ball-milling LAG/slow evaporation/slurry method	Cocrystal	[405]
5-Fluorouracil + Kaempferol	2020	LAG/slurry method/slow evaporation/ternary phase diagram	Multidrug cocrystal	[406]
Chromotropic acid + 1,10-Phenanthroline	2020	LAG/solvent evaporation	Cocrystal salt hydrate	[407]
Ibuprofen + Nicotinamide	2020	Ball-milling NG/melting/slow evaporation. Detection of cocrystal polymorphism (2 forms). Formation of one or another polymorph depend on the synthetic method used.	Cocrystal polymorph	[243]
Thiobarbituric acid or Barbituric acid + 1-Hydroxy-4,5-Dimethyl-Imidazole 3-Oxide	2020	LAG/solvent evaporation	Cocrystal	[408]
Telmisartan + Hydrochlorothiazide	2020	LAG/slow evaporation	Multidrug cocrystal	[409]
Chlorothiazide + 13 diverse coformers	2020	Ball-milling LAG/Study of the effect of grinding on 11 cocrystals an one salt in the presence of the excipients polyvinylpyrrolidone and microcrystalline cellulose	Cocrystal/ multicomponent drug	[410]
Nebivolol hydrochloride + 4-Hydroxybenzoic acid or Nicotinamide	2020	LAG	Cocrystal	[411]
9-Ethyladenine + Malonic acid or Succinic acid or Fumaric acid or Glutaric acid or Adipic acid	2020	LAG/slow evaporation	Cocrystal/ multicomponent salt	[412]
Carbamazepine + DL-Tartaric acid	2020	LAG	Cocrystal	[413]
Emtricitabine + 1,2-Bis(4-pyridyl)ethane or 1,2-Bis(4-pyridyl)ethylene or 4,4'-Azopyridine or 4,4'-Bipyridine	2020	LAG	Cocrystal	[414]
Caffeine + Glutaric acid	2020	NG/LAG/POLAG/in situ X-ray powder diffraction	Cocrystal	[214]

Table 1. Cont.

API or NP + Coformer or API + API	Year of the Paper	Type of Grinding or Method of Synthesis and Characterization	Type of Multicomponent Form	Reference
Cocrystal (Barbituric acid/Thiobarbituric acid) BA <sub>0.5</sub> TBA <sub>0.5</sub> + 1-Hydroxy-4,5-dimethyl-imidazole 3-oxide	2020	Ball-milling LAG/Preparation of ternary cocrystal system beginning from binary cocrystal system. Evaluation of the possible pathways involved, the evidence suggests a non-concerted process.	Binary and ternary cocrystal	[245]
Tinidazol + <i>p</i> -Aminobenzoic acid or Citric acid or Salicylic acid	2020	NG/LAG	Cocrystal	[415]
Ciprofloxacin + Pyrazinoic acid or <i>p</i> -Aminobenzoic acid	2020	NG/LAG	Cocrystal	[416]
Zaltoprofen + Nicotinamide (1:1 or 1:2)	2020	LAG	Cocrystal	[417]
Metronidazole + 3,5-Dihydroxybenzoic or 3,4,5-Trihydroxybenzoic acid	2020	LAG/melt/slow evaporation	Cocrystal	[418]
Exemestane + 9-Hydroxyphenanthrene and 1-Hydroxypyrene	2020	LAG	Cocrystal	[419]
Penciclovir + 3,5-Dihydroxybenzoic acid or Gallic acid (1:1 or 1:1:1 hydrate) or 4-Hydroxycinnamic acid (1:1 or 1:1:1 hydrate)	2020	LAG	Cocrystal/cocrystal hydrate	[420]
Berberine chloride + Pyromellitic dianhydride	2020	LAG	Diverse multicomponent stoichiomorphs: multicomponent salt/multicomponent salt polymorph/ionic cocrystal hydrate	[421]
Allopurinol + Isonicotinamide or Piperazine or 2,4-Dihydroxybenzoic acid	2020	LAG/slurry methods/slow evaporation	Cocrystal	[422]
Trimethoprim + Flufenamic acid or Tolfenamic acid or Mefenamic acid and Sulfamethazine + Flufenamic acid or Niflumic acid	2020	LAG/slow evaporation	Multicomponent salt hydrate/multidrug cocrystal	[423]
Ciprofloxacin + 4-Hydroxybenzoic acid or 4-Aminobenzoic acid or Gallic acid	2020	LAG	Multicomponent salt hydrate	[424]
Regorafenib + Malonic acid or Glutaric acid or Pimelic acid	2021	LAG/slurry methods	Cocrystal	[425]
Theobromine + Trimesic acid or Hemimellitic acid and Caffeine + Trimesic acid or Hemimellitic acid	2021	NG/LAG/slow evaporation	Cocrystal/multicomponent salt/cocrystal hydrate	[426]
Temozolomide + Hesperetin	2021	LAG/slurry methods/slow evaporation	Multidrug cocrystal	[427]

#### 4. Conclusions

In conclusion, we have highlighted most of the benefits found in the field of the mechanochemistry particularly in the formation of pharmaceutical cocrystals. Mechanochemistry offers unique opportunities in a green approach, eliminating or minimizing

almost entirely the use of solvents. It must be noted, that mechanochemistry has an extensive set of advantages compared with classical solution synthesis. For instance, the selective formation of solid or polymorphic forms that would not otherwise be obtained by solution-based synthesis. Additionally, the decrease in energy consumption, reduction in the generation of residual solvents, etcetera.

Despite the benefits mentioned above, the emerging understanding of mechanistic factors leading to the formation of pharmaceutical cocrystals through mechanochemistry, has limited the use of these methods, because of the significant differences often found between reaction outcomes compared to classical solution methods. This must trigger further studies of these procedures with the aim of prioritizing these ecofriendly reactions. Besides, this review makes a chronological recount of the most relevant publications dealing with relevant studies related to mechanochemical synthesis of pharmaceutical cocrystals.

In this sense, mechanochemistry can be seen as an attractive prospective green tool, not only for the preparation of cocrystals, but also finding many applications in other fields (e.g., physics, chemistry, materials science).

**Author Contributions:** Conceptualization, D.M.-M. and J.M.G.-A.; writing—original draft preparation, D.M.-M.; J.M.G.-A.; M.S.-B.; G.C.-D.; J.C.P.-F.; M.R.Z.-O.; C.M.d.l.O.C.; D.C.-G.; A.A.-S.; writing—review and editing, D.M.-M. and J.M.G.-A. All authors have read and agreed to the published version of the manuscript.

**Funding:** This research was funded by PAPIIT-DGAPA IT200920 from the National Autonomous University of México. D.M.-M. would like to thank PAPIIT-DGAPA-UNAM (PAPIIT IN210520) and CONACYT A1-S-33933 and FORDECYT-PRONACES FON.INST 22/2020 (FOINS 307152) for generous financial support.

**Institutional Review Board Statement:** Not applicable.

**Informed Consent Statement:** Not applicable.

**Data Availability Statement:** No new data were created or analyzed in this study. Data sharing is not applicable to this article.

**Acknowledgments:** We would like to thank Lizbeth Triana Cruz, Ma. De las Nieves Zavala Segovia, Alejandra Núñez Pineda, Adriana Tejeda Cruz, Eriseth Reyes Morales and Powder X-ray Diffraction Laboratory CCIQS-UNAM (Uvaldo Hernández B.). The authors would like to thank to programa de muestras externas no remuneradas para su análisis del CCIQS, for the Project DMM-2016-1 "Preparación y caracterización de fases sólidas fármaco:fármaco conteniendo agentes para el tratamiento de la diabetes tipo 2 y sus factores de riesgo asociados".

**Conflicts of Interest:** The authors declare no conflict of interest.

## Abbreviations

adi	Adipic acid
ana	Anthranilic Acid
API	Active Pharmaceutical Ingredient
$\alpha$ -alanine	$\alpha$ -ala
BA	Barbituric acid
BSC	Biopharmaceutics classification system
4,4'-bipy	4,4'-Bipyridine
ca	Citric Acid
caf	Caffeine
cbz	Carbamazepine
CSD	Cambridge structural database
CTA	Cyclohexane-1,3-cis-5-cis-tricarboxylic Acid
$\delta$	$\delta$ parameter
dabco	1,4-diazabicyclo [2.2.2]octane
DL-ta	DL-tartaric acid

DSC	Differential Scanning Calorimetry
DTA	Differential thermal analysis
FDA	Food and drug administration
FT-IR	Fourier Transform Infrared Spectroscopy
GRAS	Generally recognized as safe
Glu	Glutaric acid
HIMO	4,5-dimethyl-imidazole-3-oxide
IL	Imidazolium based ionic liquids
ILAG	Ion liquid-assisted grinding
IUPAC	International Union of Pure and Applied Chemistry
LAG	Liquid-Assisted Grinding
LASI	Liquid-assisted sonochemical irradiation
ma	Mesaconic Acid
MeNO <sub>3</sub>	Methyl nitrate
MOF	Metal-organic framework
<i>m</i>	weights of cocrystal components
NP	Natural product
NG	Neat Grinding
Nicotinamide	nic
5-nip	5-Nitroisophtalic acid
η	η parameter
ox	Oxalic Acid
PEG	Polyethylene Glycol
phe	Phenazide
4,7-phen	4,7-phenanthroline
POLAG	Polymer-Assisted Grinding
PMMA	Poly(methyl methacrylate)
PXRD	Powder X-ray Diffraction
RAM	Resonant acoustic mixing
RS-ibp	RS-ibuprofen
sa	Salicylic Acid
SCXRD	Single Crystal X-ray Diffraction
SDG	Solvent Drop Grinding
S-ibp	S-ibuprofen
ssNMR	solid-state Nuclear Magnetic Resonance
ta	Terephthalate
thp	Theophylline
TBA	Thiobarbituric acid
TGA	Thermogravimetric Analysis
TSE	Twin-screw extrusion
tp	Theophylline
<i>V</i>	volume
VALAG	Variable amount liquid-assisted grinding
VATEG	Variable temperature grinding
XPS	X-ray photoelectron spectroscopy

## References

1. Datta, S.; Grant, D.J.W. Crystal Structures of Drugs: Advances in Determination, Prediction and Engineering. *Nat. Rev. Drug Discov.* **2004**, *3*, 42–57. [[CrossRef](#)]
2. Shekunov, B.Y.; York, P. Crystallization Processes in Pharmaceutical Technology and Drug Delivery Design. *J. Cryst. Growth* **2000**, *211*, 122–136. [[CrossRef](#)]
3. Grunenberg, A.; Henck, J.O.; Siesler, H.W. Theoretical Derivation and Practical Application of Energy/Temperature Diagrams as an Instrument in Preformulation Studies of Polymorphic Drug Substances. *Int. J. Pharm.* **1996**, *129*, 147–158. [[CrossRef](#)]
4. Morissette, S.L.; Soukasene, S.; Levinson, D.; Cima, M.J.; Almarsson, O. Elucidation of Crystal Form Diversity of the HIV Protease Inhibitor Ritonavir by High-throughput Crystallization. *Proc. Natl. Acad. Sci. USA* **2003**, *100*, 2180–2184. [[CrossRef](#)]
5. Morissette, S.L.; Almarsson, Ö.; Peterson, M.L.; Remenar, J.F.; Read, M.J.; Lemmo, A.V.; Ellis, S.; Cima, M.J.; Gardner, C.R. High-throughput Crystallization: Polymorphs, Salts, Co-crystals and Solvates of Pharmaceutical Solids. *Adv. Drug Deliv. Rev.* **2004**, *56*, 275–300. [[CrossRef](#)]

6. Tiekink, E.R.T.; Vittal, J.; Zaworotko, M. *Organic Crystal Engineering: Frontiers in Crystal Engineering*; Tiekink, E.R.T., Vittal, J.J., Zaworotko, M.J., Eds.; John Wiley & Sons: New York, NY, USA, 2010; ISBN 9780470319901.
7. Lee, E.H. A Practical Guide to Pharmaceutical Polymorph Screening & Selection. *Asian J. Pharm. Sci.* **2014**, *9*, 163–175. [[CrossRef](#)]
8. Aaltonen, J.; Allesø, M.; Mirza, S.; Koradia, V.; Gordon, K.C.; Rantanen, J. Solid Form Screening—A Review. *Eur. J. Pharm. Biopharm.* **2009**, *71*, 23–37. [[CrossRef](#)]
9. Tung, H.H. Industrial Perspectives of Pharmaceutical Crystallization. *Org. Process Res. Dev.* **2013**, *17*, 445–454. [[CrossRef](#)]
10. Croker, D.M.; Kelly, D.M.; Horgan, D.E.; Hodnett, B.K.; Lawrence, S.E.; Moynihan, H.A.; Rasmuson, Å.C. Demonstrating the Influence of Solvent Choice and Crystallization Conditions on Phenacetin Crystal Habit and Particle Size Distribution. *Org. Process Res. Dev.* **2015**, *19*, 1826–1836. [[CrossRef](#)]
11. Keraliya, R.A.; Soni, T.G.; Thakkar, V.T.; Gandhi, T.R. Effect of Solvent on Crystal Habit and Dissolution Behavior of Tolbutamide by Initial Solvent Screening. *Dissolution Technol.* **2010**, *17*, 16–21. [[CrossRef](#)]
12. Schultheiss, N.; Newman, A. Pharmaceutical Cocrystals and Their Physicochemical Properties. *Cryst. Growth Des.* **2009**, *9*, 2950–2967. [[CrossRef](#)]
13. Berry, D.J.; Steed, J.W. Pharmaceutical Cocrystals, Salts and Multicomponent Systems; Intermolecular Interactions and Property Based Design. *Adv. Drug Deliv. Rev.* **2017**, *117*, 3–24. [[CrossRef](#)]
14. Karagianni, A.; Malamataris, M.; Kachrimanis, K. Pharmaceutical Cocrystals: New Solid Phase Modification Approaches for the Formulation of APIs. *Pharmaceutics* **2018**, *10*, 18. [[CrossRef](#)]
15. Healy, A.M.; Worku, Z.A.; Kumar, D.; Madi, A.M. Pharmaceutical Solvates, Hydrates and Amorphous Forms: A Special Emphasis on Cocrystals. *Adv. Drug Deliv. Rev.* **2017**, *117*, 25–46. [[CrossRef](#)]
16. Myrdal, P.B.; Jozwiakowski, M.J. Alteration of the Solid State of the Drug Substances: Polymorphs, Solvates, and Amorphous Forms. In *Water-Insoluble Drug Formulation*; CRC Press: Boca Raton, FL, USA, 2008; pp. 531–566.
17. Babu, N.J.; Nangia, A. Solubility Advantage of Amorphous Drugs and Pharmaceutical Cocrystals. *Cryst. Growth Des.* **2011**, *11*, 2662–2679. [[CrossRef](#)]
18. Aitipamula, S.; Banerjee, R.; Bansal, A.K.; Biradha, K.; Cheney, M.L.; Choudhury, A.R.; Desiraju, G.R.; Dikundwar, A.G.; Dubey, R.; Duggirala, N.; et al. Polymorphs, Salts, and Cocrystals: What's in a Name? *Cryst. Growth Des.* **2012**, *12*, 2147–2152. [[CrossRef](#)]
19. Kalepu, S.; Nekkanti, V. Insoluble Drug Delivery Strategies: Review of Recent Advances and Business Prospects. *Acta Pharm. Sin. B* **2015**, *5*, 442–453. [[CrossRef](#)]
20. Kavanagh, O.N.; Croker, D.M.; Walker, G.M.; Zaworotko, M.J. Pharmaceutical Cocrystals: From Serendipity to Design to Application. *Drug Discov. Today* **2019**, *24*, 796–804. [[CrossRef](#)]
21. Bučar, D.-K.; Lancaster, R.W.; Bernstein, J. Disappearing Polymorphs Revisited. *Angew. Chem.* **2015**, *54*, 6972–6993. [[CrossRef](#)]
22. Kaushal, A.M.; Gupta, P.; Bansal, A.K. Amorphous Drug Delivery Systems: Molecular Aspects, Design, and Performance. *Crit. Rev. Ther. Drug Carrier Syst.* **2004**, *21*, 133–193. [[CrossRef](#)]
23. Lipinski, C.A.; Lombardo, F.; Dominy, B.W.; Feeney, P.J. Experimental and Computational Approaches to Estimate Solubility and Permeability in Drug Discovery and Development Settings. *Adv. Drug Deliv. Rev.* **1997**, *23*, 3–25. [[CrossRef](#)]
24. Lipinski, C.A.; Lombardo, F.; Dominy, B.W.; Feeney, P.J. Experimental and Computational Approaches to Estimate Solubility and Permeability in Drug Discovery and Development Settings. *Adv. Drug Deliv. Rev.* **2012**, *64*, 4–17. [[CrossRef](#)]
25. Rinaki, E.; Valsami, G.; Macheras, P. Quantitative Biopharmaceutics Classification System: The Central Role of Dose/Solubility Ratio. *Pharm. Res.* **2003**, *20*, 1917–1925. [[CrossRef](#)]
26. Amidon, G.L.; Lennernäs, H.; Shah, V.P.; Crison, J.R. A Theoretical Basis for a Biopharmaceutic Drug Classification: The Correlation of in Vitro Drug Product Dissolution and in vivo Bioavailability. *Pharm. Res. An Off. J. Am. Assoc. Pharm. Sci.* **1995**, *12*, 413–420. [[CrossRef](#)]
27. Amidon, G.L.; Lennernas, H.; Shah, V.P.; Crison, J.R. A Theoretical Basis for a Biopharmaceutic Drug Classification: The Correlation of In Vitro Drug Product Dissolution and In Vivo Bioavailability, *Pharm. Res.* **12**, 413–420, 1995—Backstory of BCS. *AAPS J.* **2014**, *16*, 894–898. [[CrossRef](#)]
28. Fujii, S.; Yokoyama, T.; Ikegaya, K.; Sato, F.; Yokoo, N. Promoting Effect of the New Chymotrypsin Inhibitor FK-448 on the Intestinal Absorption of Insulin in Rats and Dogs. *J. Pharm. Pharmacol.* **1985**, *37*, 545–549. [[CrossRef](#)]
29. Doroshenko, O.; Jetter, A.; Odenthal, K.P.; Fuhr, U. Clinical Pharmacokinetics of Trospium Chloride. *Clin. Pharmacokinet.* **2005**, *44*, 701–720. [[CrossRef](#)]
30. Aungst, B.J. Intestinal Permeation Enhancers. *J. Pharm. Sci.* **2000**, *89*, 429–442. [[CrossRef](#)]
31. Aungst, B.J. Novel Formulation Strategies for Improving Oral Bioavailability of Drugs with Poor Membrane Permeation or Presystemic Metabolism. *J. Pharm. Sci.* **1993**, *82*, 979–987. [[CrossRef](#)]
32. Fleisher, D.; Bong, R.; Stewart, B.H. Improved Oral Drug Delivery: Solubility Limitations Overcome by the Use of Prodrugs. *Adv. Drug Deliv. Rev.* **1996**, *19*, 115–130. [[CrossRef](#)]
33. Morris, K.R.; Fakes, M.G.; Thakur, A.B.; Newman, A.W.; Singh, A.K.; Venit, J.J.; Spagnuolo, C.J.; Serajuddin, A.T.M. An Integrated Approach to the Selection of Optimal Salt Form for a New Drug Candidate. *Int. J. Pharm.* **1994**, *105*, 209–217. [[CrossRef](#)]
34. Huang, Y.; Dai, W.-G. Fundamental Aspects of Solid Dispersion Technology for Poorly Soluble Drugs. *Acta Pharm. Sin. B* **2014**, *4*, 18–25. [[CrossRef](#)] [[PubMed](#)]
35. Kumar, A. Solid Dispersion- Strategy To Enhance Solubility and Dissolution of Poorly Water Soluble Drugs. *Univers. J. Pharm. Res.* **2017**, *2*, 54–59. [[CrossRef](#)]

36. Jacob, S.; Nair, A.B. Cyclodextrin Complexes: Perspective from Drug Delivery and Formulation. *Drug Dev. Res.* **2018**, *79*, 201–217. [[CrossRef](#)]
37. Shah, S.; Date, A.; Holm, R. Strategies for the Formulation Development of Poorly Soluble Drugs via Oral Route. In *Innovative Dosage Forms: Design and Development at Early Stage*; Bachhav, Y., Ed.; Wiley-VCH Verlag GmbH: Weinheim, Germany, 2019; Chapter 2; pp. 49–89.
38. Tran, P.H.L.; Tran, T.T.D. Dosage Form Designs for the Controlled Drug Release of Solid Dispersions. *Int. J. Pharm.* **2020**, *581*, 119274. [[CrossRef](#)]
39. Jornada, D.H.; dos Santos Fernandes, G.F.; Chiba, D.E.; de Melo, T.R.; dos Santos, J.L.; Chung, M.C. The Prodrug Approach: A Successful Tool for Improving Drug Solubility. *Molecules* **2016**, *21*, 42. [[CrossRef](#)]
40. Berge, S.M.; Bighley, L.D.; Monkhouse, D.C. Pharmaceutical Salts. *J. Pharm. Sci.* **1977**, *66*, 1–19. [[CrossRef](#)]
41. Loftsson, T.; Duchêne, D. Cyclodextrins and Their Pharmaceutical Applications. *Int. J. Pharm.* **2007**, *329*, 1–11. [[CrossRef](#)]
42. Swarnakar, N.K.; Venkatesan, N.; Betageri, G. Critical In Vitro Characterization Methods of Lipid-Based Formulations for Oral Delivery: A Comprehensive Review. *AAPS PharmSciTech* **2019**, *20*, 16. [[CrossRef](#)]
43. Vo, C.L.-N.; Park, C.; Lee, B.-J. Current Trends and Future Perspectives of Solid Dispersions Containing Poorly Water-soluble Drugs. *Eur. J. Pharm. Biopharm.* **2013**, *85*, 799–813. [[CrossRef](#)]
44. Miroshnyk, I.; Mirza, S.; Sandler, N. Pharmaceutical Co-crystals-An Opportunity for Drug Product Enhancement. *Expert Opin. Drug Deliv.* **2009**, *6*, 333–341. [[CrossRef](#)]
45. Yousef, M.A.E.; Vangala, V.R. Pharmaceutical Cocryystals: Molecules, Crystals, Formulations, Medicines. *Cryst. Growth Des.* **2019**, *19*, 7420–7438. [[CrossRef](#)]
46. Shaikh, R.; Singh, R.; Walker, G.M.; Croker, D.M. Pharmaceutical Cocryystal Drug Products: An Outlook on Product Development. *Trends Pharmacol. Sci.* **2018**, *39*, 1033–1048. [[CrossRef](#)]
47. Thakuria, R.; Delori, A.; Jones, W.; Lipert, M.P.; Roy, L.; Rodríguez-Hornedo, N. Pharmaceutical Cocryystals and Poorly Soluble Drugs. *Int. J. Pharm.* **2013**, *453*, 101–125. [[CrossRef](#)]
48. Sathisaran, I.; Dalvi, S.V. Engineering Cocryystals of Poorly Water-Soluble Drugs to Enhance Dissolution in Aqueous Medium. *Pharmaceutics* **2018**, *10*, 108. [[CrossRef](#)]
49. Perlovich, G.L.; Manin, A.N. Design of Pharmaceutical Cocryystals for Drug Solubility Improvement. *Russ. J. Gen. Chem.* **2014**, *84*, 407–414. [[CrossRef](#)]
50. Cherukuvada, S.; Nangia, A. Eutectics as Improved Pharmaceutical Materials: Design, Properties and Characterization. *Chem. Commun.* **2014**, *50*, 906–923. [[CrossRef](#)]
51. Stoler, E.; Warner, J.C. Non-Covalent Derivatives: Cocryystals and Eutectics. *Molecules* **2015**, *20*, 14833–14848. [[CrossRef](#)]
52. Chavan, R.B.; Thipparaboina, R.; Kumar, D.; Shastri, N.R. Co Amorphous Systems: A Product Development Perspective. *Int. J. Pharm.* **2016**, *515*, 403–415. [[CrossRef](#)]
53. Shi, Q.; Moinuddin, S.M.; Cai, T. Advances in Coamorphous Drug Delivery Systems. *Acta Pharm. Sin. B* **2019**, *9*, 19–35. [[CrossRef](#)]
54. Sarma, B.; Chen, J.; Hsi, H.Y.; Myerson, A.S. Solid Forms of Pharmaceuticals: Polymorphs, Salts and Cocryystals. *Korean J. Chem. Eng.* **2011**, *28*, 315–322. [[CrossRef](#)]
55. Sun, C.C. CocrySTALLIZATION for Successful Drug Delivery. *Expert Opin. Drug Deliv.* **2012**, *10*, 201–213. [[CrossRef](#)] [[PubMed](#)]
56. Grothe, E.; Meekes, H.; Vlieg, E.; Ter Horst, J.H.; De Gelder, R. Solvates, Salts, and Cocryystals: A Proposal for a Feasible Classification System. *Cryst. Growth Des.* **2016**, *16*, 3237–3243. [[CrossRef](#)]
57. Nangia, A.; Bolla, G. Pharmaceutical Cocryystals: Walking the Talk. *Chem. Commun.* **2016**, *52*, 8342–8360. [[CrossRef](#)]
58. Duggirala, N.K.; Perry, M.L.; Almarsson, Ö.; Zaworotko, M.J. Pharmaceutical Cocryystals: Along the Path to Improved Medicines. *Chem. Commun.* **2016**, *52*, 640–655. [[CrossRef](#)] [[PubMed](#)]
59. Mohamed, S.; Tocher, D.A.; Vickers, M.; Karamertzanis, P.G.; Price, S.L. Salt or Cocryystal? A New Series of Crystal Structures Formed from Simple Pyridines and Carboxylic Acids. *Cryst. Growth Des.* **2009**, *9*, 2881–2889. [[CrossRef](#)]
60. Aakeröy, C.B.; Fasulo, M.E.; Desper, J. Cocryystal or Salt: Does It Really Matter? *Mol. Pharm.* **2007**, *4*, 317–322. [[CrossRef](#)] [[PubMed](#)]
61. Childs, S.L.; Stahly, G.P.; Park, A. The Salt–Cocryystal Continuum: The Influence of Crystal Structure on Ionization Stat. *Mol. Pharm.* **2007**, *4*, 323–338. [[CrossRef](#)]
62. Stevens, J.S.; Byard, S.J.; Seaton, C.C.; Sadiq, G.; Davey, R.J.; Schroeder, S.L.M. Proton Transfer and Hydrogen Bonding in the Organic Solid State: A Combined XRD/XPS/ssNMR Study of 17 Organic Acid-base Complexes. *Phys. Chem. Chem. Phys.* **2014**, *16*, 1150–1160. [[CrossRef](#)]
63. Carolina Bazzo, G.; Ramos Pezzini, B.; Karine Stulzer, H. Eutectic Mixtures as an Approach to Enhance Solubility, Dissolution Rate and Oral Bioavailability of Poorly Water-soluble Drugs. *Int. J. Pharm.* **2020**, *588*, 119741. [[CrossRef](#)]
64. Chavan, R.B.; Yadav, B.; Lodagekar, A.; Shastri, N.R. Multicomponent Solid Forms: A New Boost to Pharmaceuticals. In *Multifunctional Nanocarriers for Contemporary Healthcare Applications*; Barkat, A., Harshita, A.B., Sarwar, B., Farhan, J.A., Eds.; IGI Global: Hershey, PA, USA, 2018; pp. 273–300. ISBN 9781522547822.
65. Laitinen, R.; Löbmann, K.; Grohgan, H.; Priemel, P.; Strachan, C.J.; Rades, T. Supersaturating Drug Delivery Systems: The Potential of Co-amorphous Drug Formulations. *Int. J. Pharm.* **2017**, *532*, 1–12. [[CrossRef](#)]
66. Newman, A.; Zograf, G. An Examination of Water Vapor Sorption by Multicomponent Crystalline and Amorphous Solids and Its Effects on Their Solid-State Properties. *J. Pharm. Sci.* **2019**, *108*, 1061–1080. [[CrossRef](#)]

67. Dengale, S.J.; Grohgan, H.; Rades, T.; Löbmann, K. Recent Advances in Co-amorphous Drug Formulations. *Adv. Drug Deliv. Rev.* **2016**, *100*, 116–125. [[CrossRef](#)]
68. Fischer, F.; Scholz, G.; Benemann, S.; Rademann, K.; Emmerling, F. Evaluation of the Formation Pathways of Cocrystal Polymorphs in Liquid-assisted Syntheses. *CrystEngComm* **2014**, *16*, 8272–8278. [[CrossRef](#)]
69. Madusanka, N.; Eddleston, M.D.; Arhangel'skis, M.; Jones, W. Polymorphs, Hydrates and Solvates of a Co-crystal of Caffeine with Anthranilic Acid. *Acta Crystallogr. Sect. B Struct. Sci. Cryst. Eng. Mater.* **2014**, *70*, 72–80. [[CrossRef](#)]
70. Prohens, R.; Barbas, R.; Portell, A.; Font-Bardia, M.; Alcobé, X.; Puigjaner, C. Polymorphism of Cocrystals: The Promiscuous Behavior of Agomelatine. *Cryst. Growth Des.* **2016**, *16*, 1063–1070. [[CrossRef](#)]
71. Bevill, M.J.; Vlahova, P.I.; Smit, J.P. Polymorphic Cocrystals of Nutraceutical Compound p-Coumaric Acid with Nicotinamide: Characterization, Relative Solid-State Stability, and Conversion to Alternate Stoichiometries. *Cryst. Growth Des.* **2014**, *14*, 1438–1448. [[CrossRef](#)]
72. Eddleston, M.D.; Patel, B.; Day, G.M.; Jones, W. Cocrystallization by Freeze-drying: Preparation of Novel Multicomponent Crystal Forms. *Cryst. Growth Des.* **2013**, *13*, 4599–4606. [[CrossRef](#)]
73. Schultheiss, N.; Roe, M.; Boerrigter, S.X.M. Cocrystals of Nutraceutical P-coumaric Acid with Caffeine and Theophylline: Polymorphism and Solid-state Stability Explored in Detail Using Their Crystal Graphs. *CrystEngComm* **2011**, *13*, 611–619. [[CrossRef](#)]
74. Mnguni, M.J.; Michael, J.P.; Lemmerer, A. Binary Polymorphic Cocrystals: An Update on the Available Literature in the Cambridge Structural Database, Including a New Polymorph of the Pharmaceutical 1:1 Cocrystal Theophylline–3,4-dihydroxybenzoic Acid. *Acta Crystallogr. Sect. C Struct. Chem.* **2018**, *74*, 715–720. [[CrossRef](#)]
75. Aitipamula, S.; Chow, P.S.; Tan, R.B.H. Polymorphism in cocrystals: A review and assessment of its significance. *CrystEngComm* **2014**, *16*, 3451–3465. [[CrossRef](#)]
76. Douroumis, D.; Ross, S.A.; Nokhodchi, A. Advanced Methodologies for Cocrystal Synthesis. *Adv. Drug Deliv. Rev.* **2017**, *117*, 178–195. [[CrossRef](#)] [[PubMed](#)]
77. Steed, J.W. The Role of Co-crystals in Pharmaceutical Design. *Trends Pharmacol. Sci.* **2013**, *34*, 185–193. [[CrossRef](#)] [[PubMed](#)]
78. Hoang Pham, U.G. Pharmaceutical Applications of Eutectic Mixtures. *J. Dev. Drugs* **2014**, *2*, 2–3. [[CrossRef](#)]
79. Kaupp, G. Mechanochemistry: The Varied Applications of Mechanical Bond-breaking. *CrystEngComm* **2009**, *11*, 388–403. [[CrossRef](#)]
80. Suslick, K.S. Mechanochemistry and Sonochemistry: Concluding Remarks. *Faraday Discuss.* **2014**, *170*, 411–422. [[CrossRef](#)]
81. Friščić, T. New Opportunities for Materials Synthesis Using Mechanochemistry. *J. Mater. Chem.* **2010**, *20*, 7599–7605. [[CrossRef](#)]
82. Friščić, T.; Mottillo, C.; Titi, H.M. Mechanochemistry for Synthesis. *Angew. Chem.* **2020**, *59*, 1018–1029. [[CrossRef](#)]
83. Achar, T.K.; Bose, A.; Mal, P. Mechanochemical Synthesis of Small Organic Molecules. *Beilstein J. Org. Chem.* **2017**, *13*, 1907–1931. [[CrossRef](#)]
84. Do, J.-L.; Friščić, T. Mechanochemistry: A Force of Synthesis. *ACS Cent. Sci.* **2017**, *3*, 13–19. [[CrossRef](#)]
85. Bruckmann, A.; Krebs, A.; Bolm, C. Organocatalytic Reactions: Effects of Ball Milling, Microwave and Ultrasound Irradiation. *Green Chem.* **2008**, *10*, 1131. [[CrossRef](#)]
86. Pickhardt, W.; Grätz, S.; Borchardt, L. Direct Mechanocatalysis: Using Milling Balls as Catalysts. *Chem. Eur. J.* **2020**, *26*, 12903–12911. [[CrossRef](#)]
87. Hernández, J.G.; Macdonald, N.A.J.; Mottillo, C.; Butler, I.S.; Friščić, T. A Mechanochemical Strategy for Oxidative Addition: Remarkable Yields and Stereoselectivity in the Halogenation of Organometallic Re(I) Complexes. *Green Chem.* **2014**, *16*, 1087–1092. [[CrossRef](#)]
88. Chikunov, I.E.; Ranny, G.S.; Astakhov, A.V.; Tafeenko, V.A.; Chernyshev, V.M. Mechanochemical Synthesis of Platinum(IV) Complexes with N-heterocyclic Carbenes. *Russ. Chem. Bull.* **2018**, *67*, 2003–2009. [[CrossRef](#)]
89. Adams, C.J.; Lusi, M.; Mutambi, E.M.; Orpen, A.G. Two-Step Mechanochemical Synthesis of Carbene Complexes of Palladium(II) and Platinum(II). *Cryst. Growth Des.* **2017**, *17*, 3151–3155. [[CrossRef](#)]
90. Allenbaugh, R.J.; Zachary, J.R.; Underwood, A.N.; Bryson, J.D.; Williams, J.R.; Shaw, A. Kinetic Analysis of the Complete Mechanochemical Synthesis of a Palladium(II) Carbene Complex. *Inorg. Chem. Commun.* **2020**, *111*, 107622. [[CrossRef](#)]
91. Rightmire, N.R.; Hanusa, T.P. Advances in Organometallic Synthesis with Mechanochemical Methods. *Dalt. Trans.* **2016**, *45*, 2352–2362. [[CrossRef](#)]
92. Baig, R.B.N.; Varma, R.S. Alternative Energy Input: Mechanochemical, Microwave and Ultrasound-assisted Organic Synthesis. *Chem. Soc. Rev.* **2012**, *41*, 1559–1584. [[CrossRef](#)]
93. Andersen, J.; Mack, J. Mechanochemistry and Organic Synthesis: From Mystical to Practical. *Green Chem.* **2018**, *20*, 1435–1443. [[CrossRef](#)]
94. Leonardi, M.; Villacampa, M.; Menéndez, J.C. Multicomponent Mechanochemical Synthesis. *Chem. Sci.* **2018**, *9*, 2042–2064. [[CrossRef](#)]
95. Stolle, A.; Szuppa, T.; Leonhardt, S.E.S.; Ondruschka, B. Ball Milling in Organic Synthesis: Solutions and Challenges. *Chem. Soc. Rev.* **2011**, *40*, 2317–2329. [[CrossRef](#)]
96. Margetić, D.; Štrukil, V. Practical Considerations. In *Mechanochemical Organic Synthesis*; Margetić, D., Štrukil, V.B.T.-M.O.S., Eds.; Elsevier: Boston, MA, USA, 2016; Chapter 1; pp. 1–54. ISBN 978-0-12-802184-2.
97. Wang, G.-W. Mechanochemical Organic Synthesis. *Chem. Soc. Rev.* **2013**, *42*, 7668–7700. [[CrossRef](#)]
98. Beillard, A.; Métro, T.X.; Bantreil, X.; Martinez, J.; Lamaty, F. Cu(0), O<sub>2</sub> and Mechanical Forces: A Saving Combination for Efficient Production of Cu-NHC Complexes. *Chem. Sci.* **2017**, *8*, 1086–1089. [[CrossRef](#)]

99. Friščić, T.; Halasz, I.; Štrukil, V.; Eckert-Maksić, M.; Dinnebier, R.E. Clean and Efficient Synthesis Using Mechanochemistry: Coordination Polymers, Metal-organic Frameworks and Metallodrugs. *Croat. Chem. Acta* **2012**, *85*, 367–378. [[CrossRef](#)]
100. Garay, A.L.; Pichon, A.; James, S.L. Solvent-free Synthesis of Metal Complexes. *Chem. Soc. Rev.* **2007**, *36*, 846. [[CrossRef](#)] [[PubMed](#)]
101. Tan, D.; García, F. Main Group Mechanochemistry: From Curiosity to Established Protocols. *Chem. Soc. Rev.* **2019**, *48*, 2274–2292. [[CrossRef](#)]
102. Gečiauskaitė, A.A.; García, F. Main Group Mechanochemistry. *Beilstein J. Org. Chem.* **2017**, *13*, 2068–2077. [[CrossRef](#)]
103. Chen, D.; Zhao, J.; Zhang, P.; Dai, S. Mechanochemical Synthesis of Metal-organic Frameworks. *Polyhedron* **2019**, *162*, 59–64. [[CrossRef](#)]
104. Klimakow, M.; Klobes, P.; Thünemann, A.F.; Rademann, K.; Emmerling, F. Mechanochemical Synthesis of Metal-organic Frameworks: A Fast and Facile Approach toward Quantitative Yields and High Specific Surface Areas. *Chem. Mater.* **2010**, *22*, 5216–5221. [[CrossRef](#)]
105. James, S.L.; Adams, C.J.; Bolm, C.; Braga, D.; Collier, P.; Friščić, T.; Grepioni, F.; Harris, K.D.M.; Hyett, G.; Jones, W.; et al. Mechanochemistry: Opportunities for New and Cleaner Synthesis. *Chem. Soc. Rev.* **2012**, *41*, 413–447. [[CrossRef](#)]
106. Stolar, T.; Užarević, K. Mechanochemistry: An Efficient and Versatile Toolbox for Synthesis, Transformation, and Functionalization of Porous Metal-organic Frameworks. *CrystEngComm* **2020**, *22*, 4511–4525. [[CrossRef](#)]
107. Mottillo, C.; Friščić, T. Advances in Solid-state Transformations of Coordination Bonds: From the Ball Mill to the Aging Chamber. *Molecules* **2017**, *22*, 144. [[CrossRef](#)]
108. Willis-Fox, N.; Rognin, E.; Aljohani, T.A.; Daly, R. Polymer Mechanochemistry: Manufacturing Is Now a Force to Be Reckoned With. *Chem* **2018**, *4*, 2499–2537. [[CrossRef](#)]
109. Akbulatov, S.; Boulatov, R. Experimental Polymer Mechanochemistry and Its Interpretational Frameworks. *ChemPhysChem* **2017**, *18*, 1422–1450. [[CrossRef](#)]
110. May, P.A.; Moore, J.S. Polymer Mechanochemistry: Techniques to Generate Molecular Force via Elongational Flows. *Chem. Soc. Rev.* **2013**, *42*, 7497–7506. [[CrossRef](#)]
111. Zhu, S.-E.; Li, F.; Wang, G.-W. Mechanochemistry of Fullerenes and Related Materials. *Chem. Soc. Rev.* **2013**, *42*, 7535–7570. [[CrossRef](#)]
112. Braga, D.; Maini, L.; Grepioni, F. Mechanochemical Preparation of Co-crystals. *Chem. Soc. Rev.* **2013**, *42*, 7638–7648. [[CrossRef](#)]
113. Delori, A.; Friscic, T.; Jones, W.; Friščić, T.; Jones, W. The Role of Mechanochemistry and Supramolecular Design in the Development of Pharmaceutical Materials. *CrystEngComm* **2012**, *14*, 2350–2362. [[CrossRef](#)]
114. Tan, D.; Loots, L.; Friščić, T. Towards Medicinal Mechanochemistry: Evolution of Milling from Pharmaceutical Solid Form Screening to the Synthesis of Active Pharmaceutical Ingredients (APIs). *Chem. Commun.* **2016**, *52*, 7760–7781. [[CrossRef](#)]
115. Friščić, T. Supramolecular Concepts and New Techniques in Mechanochemistry: Cocrystals, Cages, Rotaxanes, Open Metal-organic Frameworks. *Chem. Soc. Rev.* **2012**, *41*, 3493. [[CrossRef](#)]
116. Trask, A.V.; Jones, W. Crystal Engineering of Organic Cocrystals by the Solid-state Grinding Approach. *Top. Curr. Chem.* **2005**, *254*, 41–70. [[CrossRef](#)]
117. Friščić, T.; Jones, W. Recent Advances in Understanding the Mechanism of Cocrystal Formation via Grinding. *Cryst. Growth Des.* **2009**, *9*, 1621–1637. [[CrossRef](#)]
118. Ahluwalia, V.K.; Kidwai, M. Organic Synthesis in Solid State. In *New Trends in Green Chemistry*; Springer: Dordrecht, The Netherlands, 2004; pp. 189–231.
119. Varma, R.S. Greener and Sustainable Trends in Synthesis of Organics and Nanomaterials. *ACS Sustain. Chem. Eng.* **2016**, *4*, 5866–5878. [[CrossRef](#)] [[PubMed](#)]
120. Anastas, P.T.; Warner, J.C. *Green Chemistry: Theory and Practice*; Oxford University Press: Oxford, UK, 1998; ISBN 9780198502340.
121. Tang, S.L.Y.; Smith, R.L.; Poliakov, M. Principles of Green Chemistry: PRODUCTIVELY. *Green Chem.* **2005**, *7*, 761–762. [[CrossRef](#)]
122. Loupy, A. *Microwaves in Organic Synthesis*; Loupy, A., Ed.; WILEY-VCH Verlag GmbH & Co. KGaA: Weinheim, Germany, 2006; ISBN 3-527-31452-0.
123. Leonelli, C.; Mason, T.J. Microwave and Ultrasonic Processing: Now a Realistic Option for Industry. *Chem. Eng. Process. Process Intensif.* **2010**, *49*, 885–900. [[CrossRef](#)]
124. Roy, D.; James, S.L.; Crawford, D.E. Solvent-free Sonochemistry as a Route to Pharmaceutical Co-crystals. *Chem. Commun.* **2019**, *55*, 5463–5466. [[CrossRef](#)]
125. Crawford, D.E. Solvent-free Sonochemistry: Sonochemical Organic Synthesis in the Absence of a Liquid Medium. *Beilstein J. Org. Chem.* **2017**, *13*, 1850–1856. [[CrossRef](#)]
126. Cole, J.M.; Irie, M. Solid-state Photochemistry. *CrystEngComm* **2016**, *18*, 7175–7179. [[CrossRef](#)]
127. Cohen, M.D. Solid-state Photochemical Reactions. *Tetrahedron* **1987**, *43*, 1211–1224. [[CrossRef](#)]
128. Guillet, J.E. Photochemistry in the Solid Phase. *Polym. Eng. Sci.* **1974**, *14*, 482–486. [[CrossRef](#)]
129. Kaupp, G. Solid-state Photochemistry: New Approaches Based on New Mechanistic Insights. *Int. J. Photoenergy* **2001**, *3*, 392659. [[CrossRef](#)]
130. Howard, J.L.; Cao, Q.; Browne, D.L. Mechanochemistry as an Emerging Tool for Molecular Synthesis: What Can It Offer? *Chem. Sci.* **2018**, *9*, 3080–3094. [[CrossRef](#)]
131. McNaught, A.D.; Wilkinson, A. Mechano-chemical Reaction. *IUPAC Compend. Chem. Terminol.* **2008**, *889*, 7141. [[CrossRef](#)]

132. Baláž, P.; Achimovičová, M.; Baláž, M.; Billik, P.; Cherkezova-Zheleva, Z.; Criado, J.M.; Delogu, F.; Dutková, E.; Gaffet, E.; Gotor, F.J.; et al. Hallmarks of Mechanochemistry: From Nanoparticles to Technology. *Chem. Soc. Rev.* **2013**, *42*, 7571–7637. [[CrossRef](#)]
133. Ostwald, W. *Handbuch der Allgemeinen Chemie, Band I*; Akademische Verlagsgesellschaft: Leipzig, Germany, 1919.
134. Takacs, L. Mechanochemistry and the Other Branches of Chemistry: Similarities and Differences. *Acta Phys. Pol. A* **2012**, *121*, 711–714. [[CrossRef](#)]
135. Fernández-Bertran, J.F. Mechanochemistry: An Overview. *Pure Appl. Chem.* **1999**, *71*, 581–586. [[CrossRef](#)]
136. Kajdas, C. General Approach to Mechanochemistry and Its Relation to Tribochemistry. In *Tribology in Engineering*; InTechOpen: London, UK, 2013.
137. Martini, A.; Eder, S.J.; Dörr, N. Tribochemistry: A Review of Reactive Molecular Dynamics Simulations. *Lubricants* **2020**, *8*, 44. [[CrossRef](#)]
138. Boldyreva, E. Mechanochemistry of Inorganic and Organic Systems: What is Similar, What is Different? *Chem. Soc. Rev.* **2013**, *42*, 7719–7738. [[CrossRef](#)]
139. Takacs, L. The First Documented Mechanochemical Reaction? *J. Met.* **2000**, *52*, 12–13. [[CrossRef](#)]
140. Beyer, M.K.; Clausen-Schaumann, H. Mechanochemistry: The Mechanical Activation of Covalent Bonds. *Chem. Rev.* **2005**, *105*, 2921–2948. [[CrossRef](#)]
141. Takacs, L.M. Carey Lea, the First Mechanochemist. *J. Mater. Sci.* **2004**, *39*, 4987–4993. [[CrossRef](#)]
142. Takacs, L. The Mechanochemical Reduction of AgCl with Metals: Revisiting an Experiment of M. Faraday. *J. Therm. Anal. Calorim.* **2007**, *90*, 81–84. [[CrossRef](#)]
143. Takacs, L. The Historical Development of Mechanochemistry. *Chem. Soc. Rev.* **2013**, *42*, 7649–7659. [[CrossRef](#)]
144. Takacs, L. What is Unique about Mechanochemical Reactions? *Acta Phys. Pol. A* **2014**, *126*, 1040–1043. [[CrossRef](#)]
145. Takacs, L.M. Carey Lea, the Father of Mechanochemistry. *Bull. Hist. Chem.* **2003**, *28*, 26–34.
146. Etter, M.C. Hydrogen Bonds as Design Elements in Organic Chemistry. *J. Phys. Chem.* **1991**, *95*, 4601–4610. [[CrossRef](#)]
147. Pedireddi, V.R.; Jones, W.; Chorlton, A.P.; Docherty, R. Creation of Crystalline Supramolecular Arrays: A Comparison of Co-crystal Formation from Solution and by Solid-state Grinding. *Chem. Commun.* **1996**, *8*, 987–988. [[CrossRef](#)]
148. Braga, D.; Giaffreda, S.L.; Curzi, M.; Maini, L.; Polito, M.; Grepioni, F. Mechanical Mixing of Molecular Crystals: A Green Route to Co-crystals and Coordination Networks. *J. Therm. Anal. Calorim.* **2007**, *90*, 115–123. [[CrossRef](#)]
149. Weyna, D.R.; Shattock, T.; Vishweshwar, P.; Zaworotko, M.J. Synthesis and Structural Characterization of Cocrystals and Pharmaceutical Cocrystals: Mechanochemistry vs. Slow Evaporation from Solution. *Cryst. Growth Des.* **2009**, *9*, 1106–1123. [[CrossRef](#)]
150. Juribašić, M.; Užarević, K.; Gracin, D.; Ćurić, M. Mechanochemical C–H Bond Activation: Rapid and Regioselective Double Cyclopalladation Monitored by in situ Raman Spectroscopy. *Chem. Commun.* **2014**, *50*, 10287–10290. [[CrossRef](#)]
151. Tan, D.; Mottillo, C.; Katsenis, A.D.; Štrukil, V.; Friščić, T. Development of C–N Coupling Using Mechanochemistry: Catalytic Coupling of Arylsulfonamides and Carbodiimides. *Angew. Chem.* **2014**, *53*, 9321–9324. [[CrossRef](#)]
152. Su, Y.T.; Wang, G.W. FeCl<sub>3</sub>-mediated Cyclization of [60]fullerene with N-benzhydryl Sulfonamides under High-speed Vibration Milling Conditions. *Org. Lett.* **2013**, *15*, 3408–3411. [[CrossRef](#)]
153. Haley, R.A.; Zellner, A.R.; Krause, J.A.; Guan, H.; Mack, J. Nickel Catalysis in a High Speed Ball Mill: A Recyclable Mechanochemical Method for Producing Substituted Cyclooctatetraene Compounds. *ACS Sustain. Chem. Eng.* **2016**, *4*, 2464–2469. [[CrossRef](#)]
154. Bučar, D.K.; Friščić, T. Professor William Jones and His Materials Chemistry Group: Innovations and Advances in the Chemistry of Solids. *Cryst. Growth Des.* **2019**, *19*, 1479–1487. [[CrossRef](#)]
155. Trask, A.V.; Motherwell, W.D.S.; Jones, W. Solvent-Drop Grinding: Green Polymorph Control of Cocrystallisation. *Chem. Commun.* **2004**, 890–891. [[CrossRef](#)]
156. Trask, A.V.; Shan, N.; Motherwell, W.D.S.; Jones, W.; Feng, S.; Tan, R.B.H.; Carpenter, K.J. Selective Polymorph Transformation via Solvent-drop Grinding. *Chem. Commun.* **2005**, 880–882. [[CrossRef](#)]
157. Trask, A.V.; Samuel Motherwell, W.D.; Jones, W. Pharmaceutical Cocrystallization: Engineering a Remedy for Caffeine Hydration. *Cryst. Growth Des.* **2005**, *5*, 1013–1021. [[CrossRef](#)]
158. Adams, C.J.; Colquhoun, H.M.; Crawford, P.C.; Lusi, M.; Orpen, A.G. Solid-state Interconversions of Coordination Networks and Hydrogen-bonded Salts. *Angew. Chem.* **2007**, *46*, 1124–1128. [[CrossRef](#)]
159. Skovsgaard, S.; Bond, A.D. Co-crystallisation of Benzoic Acid Derivatives with N-containing Bases in Solution and by Mechanical Grinding: Stoichiometric Variants, Polymorphism and Twinning. *CrystEngComm* **2009**, *11*, 444–453. [[CrossRef](#)]
160. Zhou, Y.; Guo, F.; Hughes, C.E.; Browne, D.L.; Peskett, T.R.; Harris, K.D.M. Discovery of New Metastable Polymorphs in a Family of Urea Co-crystals by Solid-state Mechanochemistry. *Cryst. Growth Des.* **2015**, *15*, 2901–2907. [[CrossRef](#)]
161. Zbačnik, M.; Nogalo, I.; Cinčić, D.; Kaitner, B. Polymorphism Control in the Mechanochemical and Solution-based Synthesis of a Thermo-chromic Schiff Base. *CrystEngComm* **2015**, *17*, 7870–7877. [[CrossRef](#)]
162. Hasa, D.; Jones, W. Screening for New Pharmaceutical Solid Forms Using Mechanochemistry: A Practical Guide. *Adv. Drug Deliv. Rev.* **2017**, *117*, 147–161. [[CrossRef](#)]
163. Toda, F.; Yagi, M.; Kiyoshige, K. Baeyer-Villiger Reaction in the Solid State. *J. Chem. Soc. Chem. Commun.* **1988**, 958–959. [[CrossRef](#)]
164. Stolle, A.; Schmidt, R.; Jacob, K. Scale-up of Organic Reactions in Ball Mills: Process Intensification with Regard to Energy Efficiency and Economy of Scale. *Faraday Discuss.* **2014**, *170*, 267–286. [[CrossRef](#)]
165. Hernández, J.G. C–H Bond Functionalization by Mechanochemistry. *Chem. Eur. J.* **2017**, *23*, 17157–17165. [[CrossRef](#)]

166. Hermann, G.N.; Becker, P.; Bolm, C. Mechanochemical Iridium(III)-Catalyzed C-H Bond Amidation of Benzamides with Sulfonyl Azides under Solvent-Free Conditions in a Ball Mill. *Angew. Chem.* **2016**, *55*, 3781–3784. [CrossRef]
167. Jörres, M.; Aceña, J.L.; Soloshonok, V.A.; Bolm, C. Asymmetric Carbon-carbon Bond Formation under Solventless Conditions in Ball Mills. *ChemCatChem* **2015**, *7*, 1265–1269. [CrossRef]
168. Hernández, J.G.; Bolm, C. Altering Product Selectivity by Mechanochemistry. *J. Org. Chem.* **2017**, *82*, 4007–4019. [CrossRef] [PubMed]
169. Swinburne, A.N.; Steed, J.W. The Mechanochemical Synthesis of Podand Anion Receptors. *CrystEngComm* **2009**, *11*, 433–438. [CrossRef]
170. Aakeröy, C.B.; Chopade, P.D. Oxime Decorated Cavitands Functionalized through Solvent-assisted Grinding. *Org. Lett.* **2011**, *13*, 1–3. [CrossRef] [PubMed]
171. Schneider, F.; Szuppa, T.; Stolle, A.; Ondruschka, B.; Hopf, H. Energetic Assessment of the Suzuki–Miyaura Reaction: A Curtate Life Cycle Assessment as an Easily Understandable and Applicable Tool for Reaction Optimization. *Green Chem.* **2009**, *11*, 1894–1899. [CrossRef]
172. Ling, A.R.; Baker, J.L. XCVI.—Halogen Derivatives of Quinone. Part III. Derivatives of Quinhydrone. *J. Chem. Soc. Trans.* **1893**, *63*, 1314–1327. [CrossRef]
173. Patil, A.O.; Curtin, D.Y.; Paul, I.C. Solid-State Formation of Quinhydrone from Their Components. Use of Solid-Solid Reactions to Prepare Compounds Not Accessible from Solution. *J. Am. Chem. Soc.* **1984**, *106*, 348–353. [CrossRef]
174. Etter, M.C.; Urbańczyk-Lipkowska, Z.; Zia-Ebrahimi, M.; Panunto, T.W. Hydrogen Bond Directed Cocrystallization and Molecular Recognition Properties of Diarylureas. *J. Am. Chem. Soc.* **1990**, *112*, 8415–8426. [CrossRef]
175. Etter, M.C.; Adson, D.A. The Use of Cocrystallization as a Method of Studying Hydrogen Bond Preferences of 2-aminopyrimidine. *J. Chem. Soc. Chem. Commun.* **1990**, 589–591. [CrossRef]
176. Ribas-Arino, J.; Marx, D. Covalent Mechanochemistry: Theoretical Concepts and Computational Tools with Applications to Molecular Nanomechanics. *Chem. Rev.* **2012**, *112*, 5412–5487. [CrossRef]
177. Boldyrev, V.V. Mechanochemistry of Inorganic Solids. *Proc. Indian Natl. Sci. Acad. Part A* **1986**, *52*, 400–417.
178. Suryanarayana, C. Mechanical Alloying and Milling. *Prog. Mater. Sci.* **2001**, *46*, 1–184. [CrossRef]
179. Takacs, L.; McHenry, J.S. Temperature of the Milling Balls in Shaker and Planetary Mills. *J. Mater. Sci.* **2006**, *41*, 5246–5249. [CrossRef]
180. Burmeister, C.F.; Kwade, A. Process Engineering with Planetary Ball Mills. *Chem. Soc. Rev.* **2013**, *42*, 7660–7667. [CrossRef]
181. Medina, C.; Daurio, D.; Nagapudi, K.; Alvarez-Nunez, F. Manufacture of Pharmaceutical Co-crystals Using Twin Screw Extrusion: A Solvent-less and Scalable Process. *J. Pharm. Sci.* **2010**, *99*, 1693–1696. [CrossRef]
182. Daurio, D.; Medina, C.; Saw, R.; Nagapudi, K.; Alvarez-Núñez, F. Application of Twin Screw Extrusion in the Manufacture of Cocrystals, Part I: Four Case Studies. *Pharmaceutics* **2011**, *3*, 582–600. [CrossRef]
183. Moradiya, H.G.; Islam, M.T.; Scoutaris, N.; Halsey, S.A.; Chowdhry, B.Z.; Douroumis, D. Continuous Manufacturing of High Quality Pharmaceutical Cocrystals Integrated with Process Analytical Tools for In-Line Process Control. *Cryst. Growth Des.* **2016**, *16*, 3425–3434. [CrossRef]
184. Crawford, D.E.; Miskimmin, C.K.G.; Albadarin, A.B.; Walker, G.; James, S.L. Organic Synthesis by Twin Screw Extrusion (TSE): Continuous, Scalable and Solvent-free. *Green Chem.* **2017**, *19*, 1507–1518. [CrossRef]
185. Cao, Q.; Howard, J.L.; Crawford, D.E.; James, S.L.; Browne, D.L. Translating Solid State Organic Synthesis from a Mixer Mill to a Continuous Twin Screw Extruder. *Green Chem.* **2018**, *20*, 4443–4447. [CrossRef]
186. Crawford, D.; Casaban, J.; Haydon, R.; Giri, N.; McNally, T.; James, S.L. Synthesis by Extrusion: Continuous, Large-scale Preparation of MOFs Using Little or no Solvent. *Chem. Sci.* **2015**, *6*, 1645–1649. [CrossRef]
187. Crawford, D.E.; Wright, L.A.; James, S.L.; Abbott, A.P. Efficient Continuous Synthesis of High Purity Deep Eutectic Solvents by Twin Screw Extrusion. *Chem. Commun.* **2016**, *52*, 4215–4218. [CrossRef] [PubMed]
188. Thorwirth, R.; Bernhardt, F.; Stolle, A.; Ondruschka, B.; Asghari, J. Switchable Selectivity during Oxidation of Anilines in a Ball Mill. *Chem. Eur. J.* **2010**, *16*, 13236–13242. [CrossRef] [PubMed]
189. Braga, D.; Grepioni, F. Reactions between or within Molecular Crystals. *Angew. Chem.* **2004**, *43*, 4002–4011. [CrossRef] [PubMed]
190. Braga, D.; D’Addario, D.; Giaffreda, S.L.; Maini, L.; Polito, M.; Grepioni, F. Intra-solid and Inter-solid Reactions of Molecular Crystals: A Green Route to Crystal Engineering. *Top. Curr. Chem.* **2005**, *254*, 71–94. [CrossRef]
191. Schmidt, G.M.J. Photodimerization in the Solid State. *Pure Appl. Chem.* **1971**, *27*, 647–678. [CrossRef]
192. Naumov, P.; Bharadwaj, P.K. Single-crystal-to-single-crystal Transformations. *CrystEngComm* **2015**, *17*, 8775. [CrossRef]
193. Martí-Rujas, J. Thermal Reactivity in Metal Organic Materials (MOMs): From Single-crystal-to-single-crystal Reactions and Beyond. *Materials* **2019**, *12*, 4088. [CrossRef]
194. Rodríguez, B.; Bruckmann, A.; Rantanen, T.; Bolm, C. Solvent-free Carbon-carbon Bond Formations in Ball Mills. *Adv. Synth. Catal.* **2007**, *349*, 2213–2233. [CrossRef]
195. Chen, R.; Gokus, M.K.; Pagola, S. Tetrathiafulvalene: A Gate to the Mechanochemical Mechanisms of Electron Transfer Reactions. *Crystals* **2020**, *10*, 482. [CrossRef]
196. Trukil, V.; Fábíán, L.; Reid, D.G.; Duer, M.J.; Jackson, G.J.; Eckert-Maksić, M.; Frii, T. Towards an Environmentally-friendly Laboratory: Dimensionality and Reactivity in the Mechanochemistry of Metal-organic Compounds. *Chem. Commun.* **2010**, *46*, 9191–9193. [CrossRef]

197. Halasz, I.; Friščić, T.; Kimber, S.A.J.; Užarević, K.; Puškarić, A.; Mottillo, C.; Julien, P.; Štrukil, V.; Honkimäki, V.; Dinnebier, R.E. Quantitative in situ and Real-time Monitoring of Mechanochemical Reactions. *Faraday Discuss.* **2014**, *170*, 203–221. [[CrossRef](#)]
198. Friščić, T.; Halasz, I.; Beldon, P.J.; Belenguer, A.M.; Adams, F.; Kimber, S.A.J.; Honkimäki, V.; Dinnebier, R.E. Real-time and in situ Monitoring of Mechanochemical Milling Reactions. *Nat. Chem.* **2013**, *5*, 66–73. [[CrossRef](#)]
199. Halasz, I.; Kimber, S.A.J.; Beldon, P.J.; Belenguer, A.M.; Adams, F.; Honkimäki, V.; Nightingale, R.C.; Dinnebier, R.E.; Friščić, T. In situ and Real-time Monitoring of Mechanochemical Milling Reactions Using Synchrotron X-ray Diffraction. *Nat. Protoc.* **2013**, *8*, 1718–1729. [[CrossRef](#)]
200. Halasz, I.; Puškarić, A.; Kimber, S.A.J.; Beldon, P.J.; Belenguer, A.M.; Adams, F.; Honkimäki, V.; Dinnebier, R.E.; Patel, B.; Jones, W.; et al. Real-time in situ Powder X-ray Diffraction Monitoring of Mechanochemical Synthesis of Pharmaceutical Cocrystals. *Angew. Chem.* **2013**, *52*, 11538–11541. [[CrossRef](#)]
201. Užarević, K.; Halasz, I.; Friščić, T. Real-Time and in Situ Monitoring of Mechanochemical Reactions: A New Playground for All Chemists. *J. Phys. Chem. Lett.* **2015**, *6*, 4129–4140. [[CrossRef](#)] [[PubMed](#)]
202. Gracin, D.; Štrukil, V.; Friščić, T.; Halasz, I.; Užarević, K. Laboratory Real-time and in situ Monitoring of Mechanochemical Milling Reactions by Raman Spectroscopy. *Angew. Chem.* **2014**, *53*, 6193–6197. [[CrossRef](#)] [[PubMed](#)]
203. Julien, P.A.; Malvestiti, I.; Friščić, T. The Effect of Milling Frequency on a Mechanochemical Organic Reaction Monitored by in situ Raman Spectroscopy. *Beilstein J. Org. Chem.* **2017**, *13*, 2160–2168. [[CrossRef](#)] [[PubMed](#)]
204. Bowmaker, G.A. Solvent-assisted Mechanochemistry. *Chem. Commun.* **2013**, *49*, 334–348. [[CrossRef](#)]
205. Shan, N.; Toda, F.; Jones, W. Mechanochemistry and Co-crystal Formation: Effect of Solvent on Reaction Kinetics. *Chem. Commun.* **2002**, 2372–2373. [[CrossRef](#)]
206. Friščić, T.; Childs, S.L.; Rizvi, S.A.A.; Jones, W. The Role of Solvent in Mechanochemical and Sonochemical Cocrystal Formation: A Solubility-based Approach for Predicting Cocrystallisation Outcome. *CrystEngComm* **2009**, *11*, 418–426. [[CrossRef](#)]
207. Hasa, D.; Miniussi, E.; Jones, W. Mechanochemical Synthesis of Multicomponent Crystals: One Liquid for One Polymorph? A Myth to Dispel. *Cryst. Growth Des.* **2016**, *16*, 4582–4588. [[CrossRef](#)]
208. Pfund, L.Y.; Matzger, A.J. Towards Exhaustive and Automated High-throughput Screening for Crystalline Polymorphs. *ACS Comb. Sci.* **2014**, *16*, 309–313. [[CrossRef](#)]
209. Lopez-Mejías, V.; Knight, J.L.; Brooks, C.L.; Matzger, A.J. On the Mechanism of Crystalline Polymorph Selection by Polymer Heteronuclei. *Langmuir* **2011**, *27*, 7575–7579. [[CrossRef](#)]
210. McClelland, A.A.; López-Mejías, V.; Matzger, A.J.; Chen, Z. Peering at a Buried Polymer-crystal Interface: Probing Heterogeneous Nucleation by Sum Frequency Generation Vibrational Spectroscopy. *Langmuir* **2011**, *27*, 2162–2165. [[CrossRef](#)]
211. Hasa, D.; Schneider Rauber, G.; Voinovich, D.; Jones, W. Cocrystal Formation through Mechanochemistry: From Neat and Liquid-Assisted Grinding to Polymer-Assisted Grinding. *Angew. Chem.* **2015**, *54*, 7371–7375. [[CrossRef](#)]
212. Karki, S.; Friščić, T.; Jones, W.; Motherwell, W.D.S. Screening for Pharmaceutical Cocrystal Hydrates via Neat and Liquid-assisted Grinding. *Mol. Pharm.* **2007**, *4*, 347–354. [[CrossRef](#)]
213. Batchelor, E.; Klinowski, J.; Jones, W. Crystal Engineering Using Co-crystallisation of Phenazine with Dicarboxylic Acids. *J. Mater. Chem.* **2000**, *10*, 839–848. [[CrossRef](#)]
214. Germann, L.S.; Emmerling, S.T.; Wilke, M.; Dinnebier, R.E.; Moneghini, M.; Hasa, D. Monitoring Polymer-assisted Mechanochemical Cocrystallisation through in situ X-ray Powder Diffraction. *Chem. Commun.* **2020**, *56*, 8743–8746. [[CrossRef](#)]
215. Thakuria, R.; Eddleston, M.D.; Chow, E.H.H.; Lloyd, G.O.; Aldous, B.J.; Krzyzaniak, J.F.; Bond, A.D.; Jones, W. Use of in situ Atomic Force Microscopy to Follow Phase Changes at Crystal Surfaces in Real Time. *Angew. Chem.* **2013**, *52*, 10541–10544. [[CrossRef](#)]
216. Friščić, T.; Reid, D.G.; Halasz, I.; Stein, R.S.; Dinnebier, R.E.; Duer, M.J. Ion- and Liquid-assisted Grinding: Improved Mechanochemical Synthesis of Metal-organic Frameworks Reveals Salt Inclusion and Anion Templating. *Angew. Chem.* **2010**, *49*, 712–715. [[CrossRef](#)]
217. Mukherjee, A.; Rogers, R.D.; Myerson, A.S. Cocrystal Formation by Ionic Liquid-assisted Grinding: Case Study with Cocrystals of Caffeine. *CrystEngComm* **2018**, *20*, 3817–3821. [[CrossRef](#)]
218. Smit, J.P.; Hagen, E.J. Polymorphism in Caffeine Citric Acid Cocrystals. *J. Chem. Crystallogr.* **2015**, *45*, 128–133. [[CrossRef](#)]
219. Hasa, D.; Carlino, E.; Jones, W. Polymer-Assisted Grinding, a Versatile Method for Polymorph Control of Cocrystallization. *Cryst. Growth Des.* **2016**, *16*, 1772–1779. [[CrossRef](#)]
220. Von Colbe, J.M.B.; Felderhoff, M.; Bogdanović, B.; Schüth, F.; Weidenthaler, C. One-step Direct Synthesis of a Ti-doped Sodium Alanate Hydrogen Storage Material. *Chem. Commun.* **2005**, 4732–4734. [[CrossRef](#)]
221. Doppiu, S.; Schultz, L.; Gutfleisch, O. In situ Pressure and Temperature Monitoring during the Conversion of Mg into MgH<sub>2</sub> by High-pressure Reactive Ball Milling. *J. Alloys Compd.* **2007**, *427*, 204–208. [[CrossRef](#)]
222. Užarević, K.; Štrukil, V.; Mottillo, C.; Julien, P.A.; Puškarić, A.; Friščić, T.; Halasz, I. Exploring the Effect of Temperature on a Mechanochemical Reaction by in Situ Synchrotron Powder X-ray Diffraction. *Cryst. Growth Des.* **2016**, *16*, 2342–2347. [[CrossRef](#)]
223. Chadwick, K.; Davey, R.; Cross, W. How Does Grinding Produce Co-crystals? Insights from the Case of Benzophenone and Diphenylamine. *CrystEngComm* **2007**, *9*, 732–734. [[CrossRef](#)]
224. Lien Nguyen, K.; Friščić, T.; Day, G.M.; Gladden, L.F.; Jones, W. Terahertz Time-domain Spectroscopy and the Quantitative Monitoring of Mechanochemical Cocrystal Formation. *Nat. Mater.* **2007**, *6*, 206–209. [[CrossRef](#)]

225. Rastogi, R.P.; Bassi, P.S.; Chadha, S.L. Mechanism of the Reaction between Hydrocarbons and Picric Acid in the Solid State. *J. Phys. Chem.* **1963**, *67*, 2569–2573. [[CrossRef](#)]
226. Kaupp, G. Solid-state Molecular Syntheses: Complete Reactions without Auxiliaries Based on the New Solid-state Mechanism. *CrystEngComm* **2003**, *5*, 117–133. [[CrossRef](#)]
227. Karimi-Jafari, M.; Padrela, L.; Walker, G.M.; Croker, D.M. Creating Cocrystals: A Review of Pharmaceutical Cocrystal Preparation Routes and Applications. *Cryst. Growth Des.* **2018**, *18*, 6370–6387. [[CrossRef](#)]
228. Rothenberg, G.; Downie, A.P.; Raston, C.L.; Scott, J.L. Understanding Solid/Solid Organic Reactions. *J. Am. Chem. Soc.* **2001**, *123*, 8701–8708. [[CrossRef](#)]
229. Germann, L.S.; Arhangelskis, M.; Etter, M.; Dinnebier, R.E.; Friščić, T. Challenging the Ostwald Rule of Stages in Mechanochemical Cocrystallisation. *Chem. Sci.* **2020**, *11*, 10092–10100. [[CrossRef](#)]
230. Ma, X.; Yuan, W.; Bell, S.E.J.; James, S.L. Better Understanding of Mechanochemical Reactions: Raman Monitoring Reveals Surprisingly Simple ‘Pseudo-fluid’ Model for a Ball Milling Reaction. *Chem. Commun.* **2014**, *50*, 1585–1587. [[CrossRef](#)]
231. Kulla, H.; Becker, C.; Michalchuk, A.A.L.; Linberg, K.; Paulus, B.; Emmerling, F. Tuning the Apparent Stability of Polymorphic Cocrystals through Mechanochemistry. *Cryst. Growth Des.* **2019**, *19*, 7271–7279. [[CrossRef](#)]
232. Schmidt, R.; Martin Scholze, H.; Stolle, A. Temperature Progression in a Mixer Ball Mill. *Int. J. Ind. Chem.* **2016**, *7*, 181–186. [[CrossRef](#)]
233. Kulla, H.; Fischer, F.; Benemann, S.; Rademann, K.; Emmerling, F. The Effect of the Ball to Reactant Ratio on Mechanochemical Reaction Times Studied by in situ PXRD. *CrystEngComm* **2017**, *19*, 3902. [[CrossRef](#)]
234. Schmidt, R.; Burmeister, C.F.; Baláž, M.; Kwade, A.; Stolle, A. Effect of Reaction Parameters on the Synthesis of 5-arylidene Barbituric Acid Derivatives in Ball Mills. *Org. Process Res. Dev.* **2015**, *19*, 427–436. [[CrossRef](#)]
235. Michalchuk, A.A.L.; Tumanov, I.A.; Boldyreva, E.V. Ball Size or Ball Mass—What Matters in Organic Mechanochemical Synthesis? *CrystEngComm* **2019**, *21*, 2174–2179. [[CrossRef](#)]
236. McKissic, K.S.; Caruso, J.T.; Blair, R.G.; Mack, J. Comparison of Shaking vs. Baking: Further Understanding the Energetics of a Mechanochemical Reaction. *Green Chem.* **2014**, *16*, 1628–1632. [[CrossRef](#)]
237. Tumanov, I.A.; Achkasov, A.F.; Boldyreva, E.V.; Boldyrev, V.V. Following the Products of Mechanochemical Synthesis Step by Step. *CrystEngComm* **2011**, *13*, 2213–2216. [[CrossRef](#)]
238. Urakaev, F.K.; Boldyrev, V.V. Mechanism and Kinetics of Mechanochemical Processes in Comminuting Devices: 1. Theory. *Powder Technol.* **2000**, *107*, 93–107. [[CrossRef](#)]
239. Urakaev, F.K.; Boldyrev, V.V. Mechanism and Kinetics of Mechanochemical Processes in Comminuting Devices: 2. Applications of the Theory. Experiment. *Powder Technol.* **2000**, *107*, 197–206. [[CrossRef](#)]
240. Fox, P.G. Mechanically Initiated Chemical Reactions in Solids. *J. Mater. Sci.* **1975**, *10*, 340–360. [[CrossRef](#)]
241. Karki, S.; Friščić, T.; Jones, W. Control and Interconversion of Cocrystal Stoichiometry in Grinding: Stepwise Mechanism for the Formation of a Hydrogen-bonded Cocrystal. *CrystEngComm* **2009**, *11*, 470–481. [[CrossRef](#)]
242. Burley, J.C.; Duer, M.J.; Stein, R.S.; Vrcelj, R.M. Enforcing Ostwald’s Rule of Stages: Isolation of Paracetamol Forms III and II. *Eur. J. Pharm. Sci.* **2007**, *31*, 271–276. [[CrossRef](#)]
243. Guerin, M.; Guinet, Y.; Correia, N.T.; Paccou, L.; Danède, F.; Hédoux, A. Polymorphism and Stability of Ibuprofen/Nicotinamide Cocrystal: The Effect of the Crystalline Synthesis Method. *Int. J. Pharm.* **2020**, *584*, 119454. [[CrossRef](#)]
244. Berry, D.J.; Seaton, C.C.; Clegg, W.; Harrington, R.W.; Coles, S.J.; Horton, P.N.; Hursthouse, M.B.; Storey, R.; Jones, W.; Friščić, T.; et al. Applying Hot-stage Microscopy to Co-crystal Screening: A Study of Nicotinamide with Seven Active Pharmaceutical Ingredients. *Cryst. Growth Des.* **2008**, *8*, 1697–1712. [[CrossRef](#)]
245. Dudek, M.K.; Śniechowska, J.; Wróblewska, A.; Kaźmierski, S.; Potrzebowski, M.J. Cocrystals “Divorce and Marriage”: When a Binary System Meets an Active Multifunctional Synthone in a Ball Mill. *Chem. Eur. J.* **2020**, *26*, 13264–13273. [[CrossRef](#)]
246. Shemchuk, O.; Braga, D.; Grepioni, F. Alloying Barbituric and Thiobarbituric Acids: From Solid Solutions to a Highly Stable Keto Co-crystal Form. *Chem. Commun.* **2016**, *52*, 11815–11818. [[CrossRef](#)]
247. Almarsson, O.; Zaworotko, M.J. Crystal Engineering of the Composition of Pharmaceutical Phases. Do Pharmaceutical Co-Crystals Represent a New Path to Improved Medicines? *Chem. Commun.* **2004**, 1889–1896. [[CrossRef](#)]
248. Reutzel-Edens, S. Chapter 10—Analytical Techniques and Strategies for Salt/Co-crystal Characterization. In *Pharmaceutical Salts and Co-Crystals*; The Royal Society of Chemistry: London, UK, 2012; pp. 212–246. ISBN 978-1-84973-158-4.
249. Aakeröy, C.B.; Salmon, D.J. Building Co-crystals with Molecular Sense and Supramolecular Sensibility. *CrystEngComm* **2005**, *7*, 439–448. [[CrossRef](#)]
250. Cruz-Cabeza, A.J. Acid–base Crystalline Complexes and the pKa Rule. *CrystEngComm* **2012**, *14*, 6362–6365. [[CrossRef](#)]
251. Ramon, G.; Davies, K.; Nassimbeni, L.R. Structures of Benzoic Acids with Substituted Pyridines and Quinolines: Salt vs. Co-crystal Formation. *CrystEngComm* **2014**, *16*, 5802–5810. [[CrossRef](#)]
252. Shattock, T.R.; Arora, K.K.; Vishweshwar, P.; Zaworotko, M.J. Hierarchy of Supramolecular Synthons: Persistent Carboxylic Acid–Pyridine Hydrogen Bonds in Cocrystals That also Contain a Hydroxyl Moiety. *Cryst. Growth Des.* **2008**, *8*, 4533–4545. [[CrossRef](#)]
253. Tothadi, S.; Shaikh, T.R.; Gupta, S.; Dandela, R.; Vinod, C.P.; Nangia, A.K. Can We Identify the Salt–Cocrystal Continuum State Using XPS? *Cryst. Growth Des.* **2021**, *21*, 735–747. [[CrossRef](#)]

254. Swapna, B.; Nangia, A. Epalrestat–Cytosine Cocrystal and Salt Structures: Attempt To Control E,Z → Z,Z Isomerization. *Cryst. Growth Des.* **2017**, *17*, 3350–3360. [CrossRef]
255. Steiner, T.; Majerz, I.; Wilson, C.C. First O–H–N Hydrogen Bond with a Centered Proton Obtained by Thermally Induced Proton Migration. *Angew. Chem. Int. Ed.* **2001**, *4*, 2651–2654. [CrossRef]
256. Losev, E.; Boldyreva, E. The Effect of Amino Acid Backbone Length on Molecular Packing: Crystalline Tartrates of Glycine, β-alanine, γ-aminobutyric Acid (GABA) and dl-α-aminobutyric Acid (AABA). *Acta Crystallogr. Sect. C Struct. Chem.* **2018**, *74*, 177–185. [CrossRef] [PubMed]
257. Fu, X.; Li, J.; Wang, L.; Wu, B.; Xu, X.; Deng, Z.; Zhang, H. Pharmaceutical Crystalline Complexes of Sulfamethazine with Saccharin: Same Interaction Site but Different Ionization States. *RSC Adv.* **2016**, *6*, 26474–26478. [CrossRef]
258. Losev, E.A.; Boldyreva, E.V. A Salt or a Co-crystal-when Crystallization Protocol Matters. *CrystEngComm* **2018**, *20*, 2299–2305. [CrossRef]
259. Zhang, C.; Xiong, Y.; Jiao, F.; Wang, M.; Li, H. Redefining the Term of “Cocrystal” and Broadening Its Intention. *Cryst. Growth Des.* **2019**, *19*, 1471–1478. [CrossRef]
260. Braga, D.; Grepioni, F.; Shemchuk, O. Organic-inorganic Ionic Co-crystals: A New Class of Multipurpose Compounds. *CrystEngComm* **2018**, *20*, 2212–2220. [CrossRef]
261. Generally Recognized as Safe (GRAS). Available online: <http://www.fda.gov/Food/IngredientsPackagingLabeling/GRAS/> (accessed on 12 November 2020).
262. Singh Sekhon, B. Drug-drug Co-crystals. *DARU J. Pharm. Sci* **2012**, *20*, 45. [CrossRef]
263. Thipparaboina, R.; Kumar, D.; Chavan, R.B.; Shastri, N.R. Multidrug Co-crystals: Towards the Development of Effective Therapeutic Hybrids. *Drug Discov. Today* **2016**, *21*, 481–490. [CrossRef]
264. Thakuria, R.; Sarma, B. Drug-Drug and Drug-Nutraceutical Cocrystal/Salt as Alternative Medicine for Combination Therapy: A Crystal Engineering Approach. *Crystals* **2018**, *8*, 101. [CrossRef]
265. Kale, D.P.; Zode, S.S.; Bansal, A.K. Challenges in Translational Development of Pharmaceutical Cocrystals. *J. Pharm. Sci.* **2017**, *106*, 457–470. [CrossRef]
266. Almarsson, Ö.; Peterson, M.L.; Zaworotko, M. The A to Z of Pharmaceutical Cocrystals: A Decade of Fast-moving New Science and Patents. *Pharm. Pat. Anal.* **2012**, *1*, 313–327. [CrossRef]
267. Trask, A.V. An Overview of Pharmaceutical Cocrystals as Intellectual Property. *Mol. Pharm.* **2007**, *4*, 301–309. [CrossRef]
268. Desiraju, G.R. The Supramolecular Synthons in Crystal Engineering—A New Organic Synthesis. *Angew. Chem.* **1995**, *34*, 2311–2327. [CrossRef]
269. Abramov, Y.A.; Loschen, C.; Klamt, A. Rational Coformer or Solvent Selection for Pharmaceutical Cocrystallization or Desolvation. *J. Pharm. Sci.* **2012**, *101*, 3687–3697. [CrossRef]
270. Kumar, S.; Nanda, A. Approaches to Design of Pharmaceutical Cocrystals: A Review. *Mol. Cryst. Liq. Cryst.* **2018**, *667*, 54–77. [CrossRef]
271. Bernstein, J.; Davis, R.E.; Shimoni, L.; Chang, N.-L. Patterns in Hydrogen Bonding: Functionality and Graph Set Analysis in Crystals. *Angew. Chem.* **1995**, *34*, 1555–1573. [CrossRef]
272. Mehta, B.K.; Singh, S.S.; Chaturvedi, S.; Wahajuddin, M.; Thakur, T.S. Rational Coformer Selection and the Development of New Crystalline Multicomponent Forms of Resveratrol with Enhanced Water Solubility. *Cryst. Growth Des.* **2018**, *18*, 1581–1592. [CrossRef]
273. Buddhadev, S.S.; Garala, K.C. Pharmaceutical Cocrystals—A Review. *Proceedings* **2020**, *62*, 14. [CrossRef]
274. Sarkar, N.; Mitra, J.; Vittengl, M.; Berndt, L.; Aakeröy, C.B. A User-friendly Application for Predicting the Outcome of Co-crystallizations. *CrystEngComm* **2020**, *22*, 6776–6779. [CrossRef]
275. Sarkar, N.; Sinha, A.S.; Aakeröy, C.B. Systematic Investigation of Hydrogen-bond Propensities for Informing Co-crystal Design and Assembly. *CrystEngComm* **2019**, *21*, 6048–6055. [CrossRef]
276. Pindelska, E.; Sokal, A.; Kolodziejcki, W. Pharmaceutical Cocrystals, Salts and Polymorphs: Advanced Characterization Techniques. *Adv. Drug Deliv. Rev.* **2017**, *117*, 111–146. [CrossRef]
277. Qiao, Y.; Qiao, R.; He, Y.; Shi, C.; Liu, Y.; Hao, H.; Su, J.; Zhong, J. Instrumental Analytical Techniques for the Characterization of Crystals in Pharmaceutics and Foods. *Cryst. Growth Des.* **2017**, *17*, 6138–6148. [CrossRef]
278. Thipparaboina, R.; Kumar, D.; Mittapalli, S.; Balasubramanian, S.; Nangia, A.; Shastri, N.R. Ionic, Neutral, and Hybrid Acid-Base Crystalline Adducts of Lamotrigine with Improved Pharmaceutical Performance. *Cryst. Growth Des.* **2015**, *15*, 5816–5826. [CrossRef]
279. Barbas, R.; Font-Bardia, M.; Paradkar, A.; Hunter, C.A.; Prohens, R. Combined Virtual/Experimental Multicomponent Solid Forms Screening of Sildenafil: New Salts, Cocrystals, and Hybrid Salt-Cocrystals. *Cryst. Growth Des.* **2018**, *18*, 7618–7627. [CrossRef]
280. Coelho, A.A. TOPAS and TOPAS-Academic: An Optimization Program Integrating Computer Algebra and Crystallographic Objects Written in C++. *J. Appl. Crystallogr.* **2018**, *51*, 210–218. [CrossRef]
281. David, W.I.F.; Shankland, K.; Van De Streek, J.; Pidcock, E.; Motherwell, W.D.S.; Cole, J.C. DASH: A Program for Crystal Structure Determination from Powder Diffraction Data. *J. Appl. Crystallogr.* **2006**, *39*, 910–915. [CrossRef]
282. Rycerz, L. Practical Remarks Concerning Phase Diagrams Determination on the Basis of Differential Scanning Calorimetry Measurements. *J. Therm. Anal. Calorim.* **2013**, *113*, 231–238. [CrossRef]
283. Patrick Stahly, G. A Survey of Cocrystals Reported Prior to 2000. *Cryst. Growth Des.* **2009**, *9*, 4212–4229. [CrossRef]

284. Lu, E.; Rodríguez-Hornedo, N.; Suryanarayanan, R. A Rapid Thermal Method for Cocrystal Screening. *CrystEngComm* **2008**, *10*, 665–668. [[CrossRef](#)]
285. Malamatarí, M.; Ross, S.A.; Douroumis, D.; Velaga, S.P. Experimental Cocrystal Screening and Solution Based Scale-up Cocrystallization Methods. *Adv. Drug Deliv. Rev.* **2017**, *117*, 162–177. [[CrossRef](#)] [[PubMed](#)]
286. Bezerra Melo Figueirêdo, C.; Nadvorný, D.; Quintas de Medeiros Vieira, A.C.; Lamartine Soares Sobrinho, J.; Rolim Neto, P.J.; Lee, P.I.; Felts de La Roca Soares, M. Enhancement of Dissolution Rate through Eutectic Mixture and Solid Solution of Posaconazole and Benznidazole. *Int. J. Pharm.* **2017**, *525*, 32–42. [[CrossRef](#)] [[PubMed](#)]
287. Yadav, J.P.A.; Bansal, A.K.; Jain, S. Molecular Understanding and Implication of Structural Integrity in the Deformation Behavior of Binary Drug-Drug Eutectic Systems. *Mol. Pharm.* **2018**, *15*, 1917–1927. [[CrossRef](#)] [[PubMed](#)]
288. Chiou, W.L.; Riegelman, S. Pharmaceutical Applications of Solid Dispersion Systems. *J. Pharm. Sci.* **1971**, *60*, 1281–1302. [[CrossRef](#)] [[PubMed](#)]
289. Skienėh, J.M.; Sathisaran, I.; Dalvi, S.V.; Rohani, S. Co-amorphous Form of Curcumin-folic Acid Dihydrate with Increased Dissolution Rate. *Cryst. Growth Des.* **2017**, *17*, 6273–6280. [[CrossRef](#)]
290. Stevens, J.S.; Byard, S.J.; Schroeder, S.L.M. Salt or Co-Crystal? Determination of Protonation State by X-ray Photoelectron Spectroscopy (XPS). *J. Pharm. Sci.* **2010**, *99*, 4453–4457. [[CrossRef](#)]
291. Stevens, J.S.; Byard, S.J.; Schroeder, S.L.M. Characterization of Proton Transfer in Co-Crystals by X-ray Photoelectron Spectroscopy (XPS). *Cryst. Growth Des.* **2010**, *10*, 1435–1442. [[CrossRef](#)]
292. Bryce, D.L. NMR Crystallography: Structure and Properties of Materials from Solid-state Nuclear Magnetic Resonance Observables. *IUCr* **2017**, *4*, 350–359. [[CrossRef](#)]
293. Rodrigues, M.; Baptista, B.; Lopes, J.A.; Sarraguça, M.C. Pharmaceutical Cocrystallization Techniques. Advances and Challenges. *Int. J. Pharm.* **2018**, *547*, 404–420. [[CrossRef](#)]
294. Daurio, D.; Nagapudi, K.; Li, L.; Quan, P.; Nunez, F.A. Application of Twin Screw Extrusion to the Manufacture of Cocrystals: Scale-up of AMG 517-sorbic Acid Cocrystal Production. *Faraday Discuss.* **2014**, *170*, 235–249. [[CrossRef](#)]
295. Kelly, A.L.; Gough, T.; Dhumal, R.S.; Halsey, S.A.; Paradkar, A. Monitoring Ibuprofen-nicotinamide Cocrystal Formation during Solvent Free Continuous Cocrystallization (SFCC) Using near Infrared Spectroscopy as a PAT Tool. *Int. J. Pharm.* **2012**, *426*, 15–20. [[CrossRef](#)]
296. Michalchuk, A.A.L.; Hope, K.S.; Kennedy, S.R.; Blanco, M.V.; Boldyreva, E.V.; Pulham, C.R. Ball-free Mechanochemistry: In situ Real-time Monitoring of Pharmaceutical Co-crystal Formation by Resonant Acoustic Mixing. *Chem. Commun.* **2018**, *54*, 4033–4036. [[CrossRef](#)]
297. Tanaka, R.; Takahashi, N.; Nakamura, Y.; Hattori, Y.; Ashizawa, K.; Otsuka, M. In-line and Real-time Monitoring of Resonant Acoustic Mixing by Near-infrared Spectroscopy Combined with Chemometric Technology for Process Analytical Technology Applications in Pharmaceutical Powder Blending Systems. *Anal. Sci.* **2017**, *33*, 41–46. [[CrossRef](#)]
298. Am Ende, D.J.; Anderson, S.R.; Salan, J.S. Development and Scale-up of Cocrystals Using Resonant Acoustic Mixing. *Org. Process Res. Dev.* **2014**, *18*, 331–341. [[CrossRef](#)]
299. Nagapudi, K.; Umanzor, E.Y.; Masui, C. High-throughput Screening and Scale-up of Cocrystals Using Resonant Acoustic Mixing. *Int. J. Pharm.* **2017**, *521*, 337–345. [[CrossRef](#)]
300. Fleischman, S.G.; Kuduva, S.S.; McMahon, J.A.; Moulton, B.; Bailey Walsh, R.D.; Rodríguez-Hornedo, N.; Zaworotko, M.J. Crystal Engineering of the Composition of Pharmaceutical Phases: Multiple-Component Crystalline Solids Involving Carbamazepine. *Cryst. Growth Des.* **2003**, *3*, 909–919. [[CrossRef](#)]
301. Morrison, H.; Mrozek-Morrison, M.; Toschi, J.; Luu, V.; Tan, H.; Daurio, D. High throughput Bench-top Co-crystal Screening via a Floating Foam Rack/Sonic Bath Method. *Org. Process Res. Dev.* **2013**, *17*, 533–539. [[CrossRef](#)]
302. Cheney, M.L.; Weyna, D.R.; Shan, N.; Hanna, M.; Wojtas, L.; Zaworotko, M.J. Cofomer Selection in Pharmaceutical Cocrystal Development: A Case Study of a Meloxicam Aspirin Cocrystal that Exhibits Enhanced Solubility and Pharmacokinetics. *J. Pharm. Sci.* **2011**, *100*, 2172–2181. [[CrossRef](#)]
303. Frišćić, T.; Jones, W. Benefits of Cocrystallisation in Pharmaceutical Materials Science: An Update. *J. Pharm. Pharmacol.* **2010**, *62*, 1547–1559. [[CrossRef](#)] [[PubMed](#)]
304. Dalpiaz, A.; Pavan, B.; Ferretti, V. Can Pharmaceutical Co-crystals Provide an Opportunity to Modify the Biological Properties of Drugs? *Drug Discov. Today* **2017**, *22*, 1134–1138. [[CrossRef](#)] [[PubMed](#)]
305. Emami, S.; Siah-Shadbad, M.; Adibkia, K.; Barzegar-Jalali, M. Recent Advances in Improving Oral Drug Bioavailability by Cocrystals. *BioImpacts* **2018**, *8*, 305–320. [[CrossRef](#)] [[PubMed](#)]
306. Karki, S.; Frišćić, T.; Fabián, L.; Laity, P.R.; Day, G.M.; Jones, W. Improving Mechanical Properties of Crystalline Solids by Cocrystal Formation: New Compressible Forms of Paracetamol. *Adv. Mater.* **2009**, *21*, 3905–3909. [[CrossRef](#)]
307. Zhou, Z.; Li, W.; Sun, W.J.; Lu, T.; Tong, H.H.Y.; Sun, C.C.; Zheng, Y. Resveratrol Cocrystals with Enhanced Solubility and Tabletability. *Int. J. Pharm.* **2016**, *509*, 391–399. [[CrossRef](#)]
308. Grepioni, F.; Wouters, J.; Braga, D.; Nanna, S.; Fours, B.; Coquerel, G.; Longfils, G.; Rome, S.; Aerts, L.; Quere, L. Ionic Co-crystals of Racetams: Solid-state Properties Enhancement of Neutral Active Pharmaceutical Ingredients via Addition of Mg<sup>2+</sup> and Ca<sup>2+</sup> Chlorides. *CrystEngComm* **2014**, *16*, 5887–5896. [[CrossRef](#)]
309. Etter, M.C.; Choo, C.G.; Reutzel, S.M. Self-Organization of Adenine and Thymine in the Solid State. *J. Am. Chem. Soc.* **1993**, *115*, 4411–4412. [[CrossRef](#)]

310. Caira, M.R.; Nassimbeni, L.R.; Wildervanck, A.F. Selective Formation of Hydrogen Bonded Cocrystals between a Sulfonamide and Aromatic Carboxylic Acids in the Solid State. *J. Chem. Soc. Perkin Trans.* **1995**, *2*, 2213–2216. [[CrossRef](#)]
311. Friščić, T.; Fábíán, L.; Burley, J.C.; Jones, W.; Motherwell, W.D.S. Exploring Cocrystal–cocrystal Reactivity via Liquid-assisted Grinding: The Assembling of Racemic and Dismantling of Enantiomeric Cocrystals. *Chem. Commun.* **2006**, 5009–5011. [[CrossRef](#)]
312. Friščić, T.; Trask, A.V.; Jones, W.; Motherwell, W.D.S. Screening for Inclusion Compounds and Systematic Construction of Three-Component Solids by Liquid-Assisted Grinding. *Angew. Chem.* **2006**, *45*, 7546–7550. [[CrossRef](#)]
313. Friščić, T.; Jones, W. Cocrystal Architecture and Properties: Design and Building of Chiral and Racemic Structures by Solid-solid Reactions. *Faraday Discuss.* **2007**, *136*, 167–178. [[CrossRef](#)]
314. Myz, S.A.; Shakhtshneider, T.P.; Fucke, K.; Fedotov, A.P.; Boldyreva, E.V.; Boldyrev, V.V.; Kuleshova, N.I. Synthesis of Co-crystals of Meloxicam with Carboxylic Acids by Grinding. *Mendeleev Commun.* **2009**, *19*, 272–274. [[CrossRef](#)]
315. Lemmerer, A.; Esterhuysen, C.; Bernstein, J. Synthesis, Characterization, and Molecular Modeling of a Pharmaceutical Co-crystal: (2-chloro-4-nitrobenzoic Acid):(Nicotinamide). *J. Pharm. Sci.* **2010**, *99*, 4054–4071. [[CrossRef](#)]
316. Mohammad, M.A.; Alhalaweh, A.; Velaga, S.P. Hansen Solubility Parameter as a Tool to Predict Cocrystal Formation. *Int. J. Pharm.* **2011**, *407*, 63–71. [[CrossRef](#)]
317. Rehder, S.; Klukkert, M.; Löbmann, K.A.M.; Strachan, C.J.; Sakmann, A.; Gordon, K.; Rades, T.; Leopold, C.S. Investigation of the Formation Process of Two Piracetam Cocrystals during Grinding. *Pharmaceutics* **2011**, *3*, 706–722. [[CrossRef](#)]
318. Fábíán, L.; Hamill, N.; Eccles, K.S.; Moynihan, H.A.; Maguire, A.R.; McCausland, L.; Lawrence, S.E. Cocrystals of Fenamic Acids with Nicotinamide. *Cryst. Growth Des.* **2011**, *11*, 3522–3528. [[CrossRef](#)]
319. Sanphui, P.; Goud, N.R.; Khandavilli, U.B.R.; Nangia, A. Fast Dissolving Curcumin Cocrystals. *Cryst. Growth Des.* **2011**, *11*, 4135–4145. [[CrossRef](#)]
320. Nanjwade, V.K.; Manvi, F.; Shamrez, A.; Nanjwade, B. Characterization of Prulifloxacin-Salicylic Acid Complex by IR, DSC and PXRD. *J. Pharm. Biomed. Sci.* **2011**, *5*, 1–6.
321. Goud, N.R.; Gangavaram, S.; Suresh, K.; Pal, S.; Manjunatha, S.G.; Nambiar, S.; Nangia, A. Novel Furosemide Cocrystals and Selection of High Solubility Drug Forms. *J. Pharm. Sci.* **2012**, *101*, 664–680. [[CrossRef](#)]
322. Arenas-García, J.I.; Herrera-Ruiz, D.; Mondragón-Vásquez, K.; Morales-Rojas, H.; Höpfl, H. Modification of the Supramolecular Hydrogen-bonding Patterns of Acetazolamide in the Presence of Different Cocrystal Formers: 3:1, 2:1, 1:1, and 1:2 Cocrystals from Screening with the Structural Isomers of Hydroxybenzoic Acids, Aminobenzoic Acids, Hydroxy. *Cryst. Growth Des.* **2012**, *12*, 811–824. [[CrossRef](#)]
323. Padrela, L.; De Azevedo, E.G.; Velaga, S.P. Powder X-ray Diffraction Method for the Quantification of Cocrystals in the Crystallization Mixture. *Drug Dev. Ind. Pharm.* **2012**, *38*, 923–929. [[CrossRef](#)] [[PubMed](#)]
324. Alhalaweh, A.; George, S.; Basavoju, S.; Childs, S.L.; Rizvi, S.A.A.; Velaga, S.P. Pharmaceutical Cocrystals of Nitrofurantoin: Screening, Characterization and Crystal Structure Analysis. *CrystEngComm* **2012**, *14*, 5078–5088. [[CrossRef](#)]
325. Fucke, K.; Myz, S.A.; Shakhtshneider, T.P.; Boldyreva, E.V.; Griesser, U.J. How Good are the Crystallisation Methods for Co-crystals? A Comparative Study of Piroxicam. *New J. Chem.* **2012**, *36*, 1969–1977. [[CrossRef](#)]
326. Tumanov, N.A.; Myz, S.A.; Shakhtshneider, T.P.; Boldyreva, E.V. Are Meloxicam Dimers Really the Structure-forming Units in the “Meloxicam-carboxylic Acid” Co-crystals Family? Relation between Crystal Structures and Dissolution Behaviour. *CrystEngComm* **2012**, *14*, 305–313. [[CrossRef](#)]
327. Eddleston, M.D.; Arhangelskis, M.; Friščić, T.; Jones, W. Solid State Grinding as a Tool to Aid Enantiomeric Resolution by Cocrystallisation. *Chem. Commun.* **2012**, *48*, 11340–11342. [[CrossRef](#)]
328. Suresh, K.; Goud, N.R.; Nangia, A. Andrographolide: Solving Chemical Instability and Poor Solubility by Means of Cocrystals. *Chem. Asian J.* **2013**, *8*, 3032–3041. [[CrossRef](#)]
329. Losev, E.A.; Mikhailenko, M.A.; Achkasov, A.F.; Boldyreva, E.V. The Effect of Carboxylic Acids on Glycine Polymorphism, Salt and Co-crystal Formation. A Comparison of Different Crystallisation Techniques. *New J. Chem.* **2013**, *37*, 1973–1981. [[CrossRef](#)]
330. Espinosa-Lara, J.C.; Guzman-Villanueva, D.; Arenas-García, J.I.; Herrera-Ruiz, D.; Rivera-Islas, J.; Román-Bravo, P.; Morales-Rojas, H.; Höpfl, H. Cocrystals of Active Pharmaceutical Ingredients–Praziquantel in Combination with Oxalic, Malonic, Succinic, Maleic, Fumaric, Glutaric, Adipic, and Pimelic Acids. *Cryst. Growth Des.* **2013**, *13*, 169–185. [[CrossRef](#)]
331. Losev, E.A.; Boldyreva, E.V. The Role of a Liquid in “Dry” Co-grinding: A Case Study of the Effect of Water on Mechanochemical Synthesis in a “l-serine–oxalic Acid” System. *CrystEngComm* **2014**, *16*, 3857. [[CrossRef](#)]
332. Sládková, V.; Cibulková, J.; Eigner, V.; Štunc, A.; Kratochvíl, B.; Rohlíček, J. Application and Comparison of Cocrystallization Techniques on Trosipium Chloride Cocrystals. *Cryst. Growth Des.* **2014**, *14*, 2931–2936. [[CrossRef](#)]
333. Song, J.X.; Yan, Y.; Yao, J.; Chen, J.M.; Lu, T.B. Improving the Solubility of Lenalidomide via Cocrystals. *Cryst. Growth Des.* **2014**, *14*, 3069–3077. [[CrossRef](#)]
334. Sugandha, K.; Kaity, S.; Mukherjee, S.; Isaac, J.; Ghosh, A. Solubility Enhancement of Ezetimibe by a Cocrystal Engineering Technique. *Cryst. Growth Des.* **2014**, *14*, 4475–4486. [[CrossRef](#)]
335. Michalchuk, A.A.L.; Tumanov, I.A.; Drebuschak, V.A.; Boldyreva, E.V. Advances in Elucidating Mechanochemical Complexities via Implementation of a Simple Organic System. *Faraday Discuss.* **2014**, *170*, 311–335. [[CrossRef](#)]
336. Tilborg, A.; Springuel, G.; Norberg, B.; Wouters, J.; Leyssens, T. How Cocrystallization Affects Solid-state Tautomerism: Stanazolol Case Study. *Cryst. Growth Des.* **2014**, *14*, 3408–3422. [[CrossRef](#)]

337. Abourahma, H.; Shah, D.D.; Melendez, J.; Johnson, E.J.; Holman, K.T. A Tale of Two Stoichiometrically Diverse Cocrystals. *Cryst. Growth Des.* **2015**, *15*, 3101–3104. [[CrossRef](#)]
338. Fischer, F.; Scholz, G.; Batzdorf, L.; Wilke, M.; Emmerling, F. Synthesis, Structure Determination, and Formation of a Theobromine:oxalic Acid 2:1 Cocrystal. *CrystEngComm* **2015**, *17*, 824–829. [[CrossRef](#)]
339. Fernandes, J.A.; Sardo, M.; Mafra, L.; Choquesillo-Lazarte, D.; Masciocchi, N. X-ray and NMR Crystallography Studies of Novel Theophylline Cocrystals Prepared by Liquid Assisted Grinding. *Cryst. Growth Des.* **2015**, *15*, 3674–3683. [[CrossRef](#)]
340. Odiase, I.; Nicholson, C.E.; Ahmad, R.; Cooper, J.; Yufit, D.S.; Cooper, S.J. Three Cocrystals and a Cocrystal Salt of Pyrimidin-2-amine and Glutaric Acid. *Acta Crystallogr. Sect. C Struct. Chem.* **2015**, *71*, 276–283. [[CrossRef](#)]
341. Batzdorf, L.; Fischer, F.; Wilke, M.; Wenzel, K.J.; Emmerling, F. Direct in situ Investigation of Milling Reactions Using Combined X-ray Diffraction and Raman Spectroscopy. *Angew. Chem.* **2015**, *54*, 1799–1802. [[CrossRef](#)]
342. Fischer, F.; Joester, M.; Rademann, K.; Emmerling, F. Survival of the Fittest: Competitive Co-crystal Reactions in the Ball Mill. *Chem. Eur. J.* **2015**, *21*, 14969–14974. [[CrossRef](#)]
343. Stepanovs, D.; Jure, M.; Kuleshova, L.N.; Hofmann, D.W.M.; Mishnev, A. Cocrystals of Pentoxifylline: In Silico and Experimental Screening. *Cryst. Growth Des.* **2015**, *15*, 3652–3660. [[CrossRef](#)]
344. Li, A.Y.; Xu, L.L.; Chen, J.M.; Lu, T.B. Solubility and Dissolution Rate Enhancement of Triamterene by a Cocrystallization Method. *Cryst. Growth Des.* **2015**, *15*, 3785–3791. [[CrossRef](#)]
345. Saikia, B.; Bora, R.; Khatioda, R.; Sarma, B. Hydrogen Bond Synthons in the Interplay of Solubility and Membrane Permeability/Diffusion in Variable Stoichiometry Drug Cocrystals. *Cryst. Growth Des.* **2015**, *15*, 5593–5603. [[CrossRef](#)]
346. Jung, S.; Choi, I.; Kim, I.W. Liquid-assisted Grinding to Prepare a Cocrystal of Adefovir Dipivoxil Thermodynamically Less Stable Than Its Neat Phase. *Crystals* **2015**, *5*, 583–591. [[CrossRef](#)]
347. Mannava, M.K.C.; Suresh, K.; Nangia, A. Enhanced Bioavailability in the Oxalate Salt of the Anti-Tuberculosis Drug Ethionamide. *Cryst. Growth Des.* **2016**, *16*, 1591–1598. [[CrossRef](#)]
348. Lin, H.L.; Huang, Y.T.; Lin, S.Y. Spectroscopic and Thermal Approaches to Investigate the Formation Mechanism of Piroxicam-saccharin Co-crystal Induced by Liquid-assisted Grinding or Thermal Stress. *J. Therm. Anal. Calorim.* **2016**, *123*, 2345–2356. [[CrossRef](#)]
349. Fischer, F.; Heidrich, A.; Greiser, S.; Benemann, S.; Rademann, K.; Emmerling, F. Polymorphism of Mechanochemically Synthesized Cocrystals: A Case Study. *Cryst. Growth Des.* **2016**, *16*, 1701–1707. [[CrossRef](#)]
350. Chadha, R.; Rani, D.; Goyal, P. Novel Cocrystals of Gliclazide: Characterization and Evaluation. *CrystEngComm* **2016**, *18*, 2275–2283. [[CrossRef](#)]
351. Fischer, F.; Wenzel, K.J.; Rademann, K.; Emmerling, F. Quantitative Determination of Activation Energies in Mechanochemical Reactions. *Phys. Chem. Chem. Phys.* **2016**, *18*, 23320–23325. [[CrossRef](#)]
352. Sopyan, I.; Fudholi, A.; Muchtaridi, M.; Puspitasari, I. A Novel of Cocrystallization to Improve Solubility and Dissolution Rate of Simvastatin. *Int. J. PharmTech Res.* **2016**, *9*, 483–491.
353. Fischer, F.; Schmidt, M.U.; Greiser, S.; Emmerling, F. The Challenging Case of the Theophylline-benzamide Cocrystal. *Acta Crystallogr. Sect. C Struct. Chem.* **2016**, *72*, 217–224. [[CrossRef](#)] [[PubMed](#)]
354. Tantardini, C.; Arkhipov, S.G.; Cherkashina, K.A.; Kil'Met'Ev, A.S.; Boldyreva, E.V. Crystal Structure of a 2:1 Co-crystal of Meloxicam with Acetylenedicarboxylic Acid. *Acta Crystallogr. Sect. E Crystallogr. Commun.* **2016**, *72*, 1856–1859. [[CrossRef](#)] [[PubMed](#)]
355. Fischer, F.; Lubjuhn, D.; Greiser, S.; Rademann, K.; Emmerling, F. Supply and Demand in the Ball Mill: Competitive Cocrystal Reactions. *Cryst. Growth Des.* **2016**, *16*, 5843–5851. [[CrossRef](#)]
356. Kulla, H.; Greiser, S.; Benemann, S.; Rademann, K.; Emmerling, F. In situ Investigation of a Self-accelerated Cocrystal Formation by Grinding Pyrazinamide with Oxalic Acid. *Molecules* **2016**, *21*, 917. [[CrossRef](#)]
357. Dai, X.L.; Li, S.; Chen, J.M.; Lu, T.B. Improving the Membrane Permeability of 5-Fluorouracil via Cocrystallization. *Cryst. Growth Des.* **2016**, *16*, 4430–4438. [[CrossRef](#)]
358. Du, S.; Wang, Y.; Wu, S.; Yu, B.; Shi, P.; Bian, L.; Zhang, D.; Hou, J.; Wang, J.; Gong, J. Two Novel Cocrystals of Lamotrigine with Isomeric Bipyridines and in situ Monitoring of the Cocrystallization. *Eur. J. Pharm. Sci.* **2017**, *110*, 19–25. [[CrossRef](#)]
359. Cho, M.Y.; Kim, P.; Kim, G.Y.; Lee, J.Y.; Song, K.H.; Lee, M.J.; Yoon, W.; Yun, H.; Choi, G.J. Preparation and Characterization of Aripiprazole Cocrystals with Coformers of Multihydroxybenzene Compounds. *Cryst. Growth Des.* **2017**, *17*, 6641–6652. [[CrossRef](#)]
360. Gopi, S.P.; Banik, M.; Desiraju, G.R. New Cocrystals of Hydrochlorothiazide: Optimizing Solubility and Membrane Diffusivity. *Cryst. Growth Des.* **2017**, *17*, 308–316. [[CrossRef](#)]
361. Chadha, R.; Rani, D.; Goyal, P. Supramolecular Cocrystals of Gliclazide: Synthesis, Characterization and Evaluation. *Pharm. Res.* **2017**, *34*, 552–563. [[CrossRef](#)]
362. Cugovčan, M.; Jablan, J.; Lovrić, J.; Cinčić, D.; Galić, N.; Jug, M. Biopharmaceutical Characterization of Praziquantel Cocrystals and Cyclodextrin Complexes Prepared by Grinding. *J. Pharm. Biomed. Anal.* **2017**, *137*, 42–53. [[CrossRef](#)]
363. Michalchuk, A.A.L.; Tumanov, I.A.; Konar, S.; Kimber, S.A.J.; Pulham, C.R.; Boldyreva, E.V. Challenges of Mechanochemistry: Is in situ Real-Time Quantitative Phase Analysis Always Reliable? A Case Study of Organic Salt Formation. *Adv. Sci.* **2017**, *4*, 1700132. [[CrossRef](#)]
364. Zeng, Q.Z.; Ouyang, J.; Zhang, S.; Zhang, L. Structural Characterization and Dissolution Profile of Mycophenolic Acid Cocrystals. *Eur. J. Pharm. Sci.* **2017**, *102*, 140–146. [[CrossRef](#)]

365. Samie, A.; Desiraju, G.R.; Banik, M. Salts and Cocrystals of the Antidiabetic Drugs Gliclazide Tolbutamide and Glipizide: Solubility Enhancements through Drug-coformer Interactions. *Cryst. Growth Des.* **2017**, *17*, 2406–2417. [[CrossRef](#)]
366. Kulla, H.; Greiser, S.; Benemann, S.; Rademann, K.; Emmerling, F. Knowing When to Stop—Trapping Metastable Polymorphs in Mechanochemical Reactions. *Cryst. Growth Des.* **2017**, *17*, 1190–1196. [[CrossRef](#)]
367. Drozd, K.V.; Manin, A.N.; Churakov, A.V.; Perlovich, G.L. Novel Drug-drug Cocrystals of Carbamazepine with: Paraminosalicylic Acid: Screening, Crystal Structures and Comparative Study of Carbamazepine Cocrystal Formation Thermodynamics. *CrystEngComm* **2017**, *19*, 4273–4286. [[CrossRef](#)]
368. Kulla, H.; Wilke, M.; Fischer, F.; Röllig, M.; Maierhofer, C.; Emmerling, F. Warming up for Mechanochemistry—Temperature Development in Ball Mills during Synthesis. *Chem. Commun.* **2017**, *53*, 1664–1667. [[CrossRef](#)] [[PubMed](#)]
369. Fischer, F.; Fendel, N.; Greiser, S.; Rademann, K.; Emmerling, F. Impact Is Important—Systematic Investigation of the Influence of Milling Balls in Mechanochemical Reactions. *Org. Process Res. Dev.* **2017**, *21*, 655–659. [[CrossRef](#)]
370. Plata-Vargas, E.; De la Cruz-Hernández, C.; Dorazco-González, A.; Fuentes-Noriega, I.; Morales-Morales, D.; Germán-Acacio, J.M. Synthesis of Metforminium Succinate by Melting. Crystal Structure, Thermal, Spectroscopic and Dissolution Properties. *J. Mex. Chem. Soc.* **2017**, *61*, 197–204. [[CrossRef](#)]
371. Aljohani, M.; Pallipurath, A.R.; McArdle, P.; Erxleben, A. A Comprehensive Cocrystal Screening Study of Chlorothiazide. *Cryst. Growth Des.* **2017**, *17*, 5223–5232. [[CrossRef](#)]
372. Nisar, M.; Sung, H.H.Y.; Puschmann, H.; Lakerveld, R.; Haynes, R.K.; Williams, I.D. 11-Azaartemisinin Cocrystals with Preserved Lactam: Acid Heterosynthons. *CrystEngComm* **2018**, *20*, 1205–1219. [[CrossRef](#)]
373. Peach, A.A.; Hirsh, D.A.; Holmes, S.T.; Schurko, R.W. Mechanochemical Syntheses and <sup>35</sup>Cl Solid-state NMR Characterization of Fluoxetine HCl Cocrystals. *CrystEngComm* **2018**, *20*, 2780–2792. [[CrossRef](#)]
374. Nisar, M.; Wong, L.W.Y.; Sung, H.H.Y.; Haynes, R.K.; Williams, I.D. Cocrystals of the Antimalarial Drug 11-azaartemisinin with Three Alkenoic Acids of 1:1 or 2:1 Stoichiometry. *Acta Crystallogr. Sect. C Struct. Chem.* **2018**, *74*, 742–751. [[CrossRef](#)] [[PubMed](#)]
375. Hussain, E.; Kumar, R.; Choudhary, M.I.; Yousuf, S. Crystal Engineering of Naturally Occurring Seselin to Obtain Cocrystal with Enhanced Anti-Leishmanial Activity, Hirshfeld Surface Analysis, and Computational Insight. *Cryst. Growth Des.* **2018**, *18*, 4628–4636. [[CrossRef](#)]
376. Tumanova, N.; Tumanov, N.; Fischer, F.; Morelle, F.; Ban, V.; Robeyns, K.; Filinchuk, Y.; Wouters, J.; Emmerling, F.; Leyssens, T. Exploring Polymorphism and Stoichiometric Diversity in Naproxen/Proline Cocrystals. *CrystEngComm* **2018**, *20*, 7308–7321. [[CrossRef](#)]
377. Do Amaral, L.H.; do Carmo, F.A.; Amaro, M.I.; de Sousa, V.P.; da Silva, L.C.R.P.; de Almeida, G.S.; Rodrigues, C.R.; Healy, A.M.; Cabral, L.M. Development and Characterization of Dapsone Cocrystal Prepared by Scalable Production Methods. *AAPS PharmSciTech* **2018**, *19*, 2687–2699. [[CrossRef](#)]
378. Darwish, S.; Zeglinski, J.; Krishna, G.R.; Shaikh, R.; Khraishah, M.; Walker, G.M.; Croker, D.M. A New 1:1 Drug-Drug Cocrystal of Theophylline and Aspirin: Discovery, Characterization, and Construction of Ternary Phase Diagrams. *Cryst. Growth Des.* **2018**, *18*, 7526–7532. [[CrossRef](#)]
379. Batool, F.; Ahmad, M.; Minhas, M.U.; Khalid, Q.; Idrees, H.A. Fabrication of Glipizide-glycolic Acid Cocrystals for Solubility Enhancement and Their in vitro Evaluation. *Lat. Am. J. Pharm.* **2018**, *37*, 1828–1836.
380. Belenguer, A.M.; Lampronti, G.I.; De Mitri, N.; Driver, M.; Hunter, C.A.; Sanders, J.K.M. Understanding the Influence of Surface Solvation and Structure on Polymorph Stability: A Combined Mechanochemical and Theoretical Approach. *J. Am. Chem. Soc.* **2018**, *140*, 17051–17059. [[CrossRef](#)]
381. Nugrahani, I.; Utami, D.; Permana, B.; Ibrahim, S. Development of the NSAID-L-proline Amino Acid Zwitterionic Cocrystals. *J. Appl. Pharm. Sci.* **2018**, *8*, 57–63. [[CrossRef](#)]
382. Gunnam, A.; Suresh, K.; Nangia, A. Salts and Salt Cocrystals of the Antibacterial Drug Pefloxacin. *Cryst. Growth Des.* **2018**, *18*, 2824. [[CrossRef](#)]
383. Takata, N.; Tanida, S.; Nakae, S.; Shiraki, K.; Tozuka, Y.; Ishigai, M. Tofogliflozin Salt Cocrystals with Sodium Acetate and Potassium Acetate. *Chem. Pharm. Bull.* **2018**, *66*, 1035–1040. [[CrossRef](#)] [[PubMed](#)]
384. Tumanova, N.; Tumanov, N.; Robeyns, K.; Fischer, F.; Fusaro, L.; Morelle, F.; Ban, V.; Hautier, G.; Filinchuk, Y.; Wouters, J.; et al. Opening Pandora’s Box: Chirality, Polymorphism, and Stoichiometric Diversity in Flurbiprofen/Proline Cocrystals. *Cryst. Growth Des.* **2018**, *18*, 954–961. [[CrossRef](#)]
385. Emami, S.; Adibkia, K.; Barzegar-Jalali, M.; Siah-Shadbad, M. Piroxicam Cocrystals with Phenolic Coformers: Preparation, Characterization, and Dissolution Properties. *Pharm. Dev. Technol.* **2019**, *24*, 199–210. [[CrossRef](#)] [[PubMed](#)]
386. Kuang, W.J.; Ji, S.C.; Xu, S.M.; Lan, P.; Liao, A.P.; Zhou, J.Y.; Zhang, J.Y. Thermodynamic and Crystallization of Lamotrigine Cocrystal. *Cryst. Growth Des.* **2019**, *19*, 6603–6610. [[CrossRef](#)]
387. Panzade, P.; Rath, P.; Somani, P. Nevirapine Pharmaceutical Cocrystal: Design, Development and Formulation. *Drug Deliv. Lett.* **2019**, *9*, 240–247. [[CrossRef](#)]
388. Luo, Y.; Chen, S.; Zhou, J.; Chen, J.; Tian, L.; Gao, W.; Zhang, Y.; Ma, A.; Li, L.; Zhou, Z. Luteolin Cocrystals: Characterization, Evaluation of Solubility, Oral Bioavailability and Theoretical Calculation. *J. Drug Deliv. Sci. Technol.* **2019**, *50*, 248–254. [[CrossRef](#)]
389. Fernandes, R.P.; do Nascimento, A.L.C.S.; Carvalho, A.C.S.; Teixeira, J.A.; Ionashiro, M.; Caires, F.J. Mechanochemical Synthesis, Characterization, and Thermal Behavior of Meloxicam Cocrystals with Salicylic Acid, Fumaric Acid, and Malic Acid. *J. Therm. Anal. Calorim.* **2019**, *138*, 765–777. [[CrossRef](#)]

390. Li, X.; Yu, G.; Chen, X.; He, L.; Zhou, Z.; Ren, Z. Investigating the Solubilization Effect of Oxcarbazepine by Forming Cocrystals. *CrystEngComm* **2019**, *21*, 4718–4729. [[CrossRef](#)]
391. Linberg, K.; Ali, N.Z.; Etter, M.; Michalchuk, A.A.L.; Rademann, K.; Emmerling, F. A Comparative Study of the Ionic Cocrystals NaX ( $\alpha$ -D-Glucose)<sub>2</sub> (X = Cl, Br, I). *Cryst. Growth Des.* **2019**, *19*, 4293–4299. [[CrossRef](#)]
392. Roca-Paixão, L.; Correia, N.T.; Affouard, F. Affinity Prediction Computations and Mechanochemical Synthesis of Carbamazepine Based Cocrystals. *CrystEngComm* **2019**, *21*, 6991–7001. [[CrossRef](#)]
393. Mazur, L.; Materek, I.; Bond, A.D.; Jones, W. Multicomponent Crystal Forms of a Biologically Active Hydrazone with Some Dicarboxylic Acids: Salts or Cocrystals? *Cryst. Growth Des.* **2019**, *19*, 2663–2678. [[CrossRef](#)]
394. Myz, S.A.; Mikhailovskaya, A.V.; Mikhailenko, M.A.; Bulina, N.V.; Kuznetsova, S.A.; Shakhtshneider, T.P. New Crystalline Betulin-based Materials: Improving Betulin Solubility via Cocrystal Formation. *Mater. Today Proc.* **2019**, *12*, 82–85. [[CrossRef](#)]
395. Surov, A.O.; Vasilev, N.A.; Churakov, A.V.; Stroh, J.; Emmerling, F.; Perlovich, G.L. Solid Forms of Ciprofloxacin Salicylate: Polymorphism, Formation Pathways, and Thermodynamic Stability. *Cryst. Growth Des.* **2019**, *19*, 2979–2990. [[CrossRef](#)]
396. Kulla, H.; Michalchuk, A.A.L.; Emmerling, F. Manipulating the Dynamics of Mechanochemical Ternary Cocrystal Formation. *Chem. Commun.* **2019**, *55*, 9793–9796. [[CrossRef](#)]
397. Kumari, N.; Bhattacharya, B.; Roy, P.; Michalchuk, A.A.L.; Emmerling, F.; Ghosh, A. Enhancing the Pharmaceutical Properties of Pirfenidone by Mechanochemical Cocrystallization. *Cryst. Growth Des.* **2019**, *19*, 6482–6492. [[CrossRef](#)]
398. Batool, F.; Ahmad, M.; Usman Minhas, M.; Khan, F.M.; Idrees, H.A.; Khalid, Q. Use of Glutaric Acid to Improve the Solubility and Dissolution Profile of Glipizide through Pharmaceutical Cocrystallization. *Acta Pol. Pharm. Drug Res.* **2019**, *76*, 103–114. [[CrossRef](#)]
399. Holanda, B.B.C.; Alarcon, R.T.; Gaglieri, C.; de Souza, A.R.; Castro, R.A.E.; Rosa, P.C.P.; Tangerino, D.J.A.; Bannach, G. Thermal Studies, Degradation Kinetic, Equilibrium Solubility, DFT, MIR, and XRPD Analyses of a New Cocrystal of Gemfibrozil and Isonicotinamide. *J. Therm. Anal. Calorim.* **2019**, *136*, 2049–2062. [[CrossRef](#)]
400. Martins, I.C.B.; Al-Sabbagh, D.; Meyer, K.; Maiwald, M.; Scholz, G.; Emmerling, F. Insight into the Structure and Properties of Novel Imidazole-based Salts of Salicylic Acid. *Molecules* **2019**, *24*, 4144. [[CrossRef](#)]
401. Ouiyangkul, P.; Tantishaiyakul, V.; Hirun, N. Exploring Potential Cofomers for Oxyresveratrol Using Principal Component Analysis. *Int. J. Pharm.* **2020**, *587*, 119630. [[CrossRef](#)]
402. Cruz, R.M.; Boleslavská, T.; Beránek, J.; Tieger, E.; Twamley, B.; Santos-Martinez, M.J.; Dammer, O.; Tajber, L. Identification and Pharmaceutical Characterization of a New Itraconazole Terephthalic Acid Cocrystal. *Pharmaceutics* **2020**, *12*, 741. [[CrossRef](#)]
403. De Almeida, A.C.; Torquetti, C.; Ferreira, P.O.; Fernandes, R.P.; dos Santos, E.C.; Kogawa, A.C.; Caires, F.J. Cocrystals of Ciprofloxacin with Nicotinic and Isonicotinic Acids: Mechanochemical Synthesis, Characterization, Thermal and Solubility Study. *Thermochim. Acta* **2020**, *685*, 178346. [[CrossRef](#)]
404. Mikhailovskaya, A.V.; Myz, S.A.; Bulina, N.V.; Gerasimov, K.B.; Kuznetsova, S.A.; Shakhtshneider, T.P. Screening and Characterization of Cocrystal Formation between Betulin and Terephthalic Acid. *Mater. Today Proc.* **2020**, *25*, 381–383. [[CrossRef](#)]
405. Shemchuk, O.; D'Agostino, S.; Fiore, C.; Sambri, V.; Zannoli, S.; Grepioni, F.; Braga, D. Natural Antimicrobials Meet a Synthetic Antibiotic: Carvacrol/Thymol and Ciprofloxacin Cocrystals as a Promising Solid-State Route to Activity Enhancement. *Cryst. Growth Des.* **2020**, *20*, 6796–6803. [[CrossRef](#)]
406. Lv, W.-T.; Liu, X.-X.; Dai, X.-L.; Long, X.; Chen, J.-M. A 5-fluorouracil-kaempferol drug-drug Cocrystal: Ternary Phase Diagram, Characterization and Property Evaluation. *CrystEngComm* **2020**, *22*, 8127–8135. [[CrossRef](#)]
407. Abidi, S.S.A.; Garg, U.; Azim, Y.; Alam, M.; Gupta, A.K.; Pradeep, C.P.; Azum, N.; Asiri, A.M. Spectroscopic, Structural, DFT and Molecular Docking Studies on Novel Cocrystal Salt Hydrate of Chromotropic Acid and Its Antibiofilm Activity. *Arab. J. Sci. Eng.* **2020**, *46*, 353–364. [[CrossRef](#)]
408. Wróblewska, A.; Śniechowska, J.; Kaźmierski, S.; Wielgus, E.; Bujacz, G.D.; Młostoń, G.; Chworos, A.; Suwara, J.; Potrzebowski, M.J. Application of 1-hydroxy-4,5-dimethyl-imidazole 3-oxide as Cofomer in Formation of Pharmaceutical Cocrystals. *Pharmaceutics* **2020**, *12*, 359. [[CrossRef](#)] [[PubMed](#)]
409. Kulkarni, A.; Shete, S.; Hol, V.; Bachhav, R. Novel Pharmaceutical Cocrystal of Telmisartan and Hydrochlorothiazide. *Asian J. Pharm. Clin. Res.* **2020**, *13*, 104–112. [[CrossRef](#)]
410. Aljohani, M.; McArdle, P.; Erxleben, A. Influence of Excipients on Cocrystal Stability and Formation. *Cryst. Growth Des.* **2020**, *20*, 4523–4532. [[CrossRef](#)]
411. Nikam, V.J.; Patil, S.B. Pharmaceutical Cocrystals of Nebivolol Hydrochloride with Enhanced Solubility. *J. Cryst. Growth* **2020**, *534*, 125488. [[CrossRef](#)]
412. Roselló, Y.; Benito, M.; Bagués, N.; Martínez, N.; Moradell, A.; Mata, I.; Galcerà, J.; Barceló-Oliver, M.; Frontera, A.; Molins, E. 9-Ethyladenine: Mechanochemical Synthesis, Characterization, and DFT Calculations of Novel Cocrystals and Salts. *Cryst. Growth Des.* **2020**, *20*, 2985–2997. [[CrossRef](#)]
413. Guerain, M.; Derollez, P.; Roca-Paixão, L.; Dejoie, C.; Correia, N.T.; Affouard, F. Structure Determination of a New Cocrystal of Carbamazepine and DL-tartaric Acid by Synchrotron Powder X-ray Diffraction. *Acta Crystallogr. Sect. C Struct. Chem.* **2020**, *76*, 225–230. [[CrossRef](#)]
414. Campillo-Alvarado, G.; Keene, E.A.; Swenson, D.C.; MacGillivray, L.R. Repurposing of the Anti-HIV Drug Emtricitabine as a Hydrogen-bonded Cleft for Bipyridines via Cocrystallization. *CrystEngComm* **2020**, *22*, 3563–3566. [[CrossRef](#)]

415. Fandiño, O.E.; Reviglio, L.; Linck, Y.G.; Monti, G.A.; Marcos Valdez, M.M.; Faudone, S.N.; Caira, M.R.; Sperandeo, N.R. Novel Cocrystals and Eutectics of the Antiprotozoal Tinidazole: Mechanochemical Synthesis, Cocrystallization, and Characterization. *Cryst. Growth Des.* **2020**, *20*, 2930–2942. [[CrossRef](#)]
416. De Almeida, A.C.; Ferreira, P.O.; Torquetti, C.; Ekawa, B.; Carvalho, A.C.S.; dos Santos, E.C.; Caires, F.J. Mechanochemical Synthesis, Characterization and Thermal Study of New Cocrystals of Ciprofloxacin with Pyrazinoic Acid and p-aminobenzoic Acid. *J. Therm. Anal. Calorim.* **2020**, *140*, 2293–2303. [[CrossRef](#)]
417. Panzade, P.; Shendarkar, G. Design and Preparation of Zaltoprofen-nicotinamide Pharmaceutical Cocrystals via Liquid Assisted Grinding Method. *Indian J. Pharm. Educ. Res.* **2019**, *53*, S563–S570. [[CrossRef](#)]
418. Seera, R.; Guru Row, T.N. Evaluation of Cocrystallization Outcomes of Multicomponent Adducts: Rapid Fabrication to Achieve Uniform Particle Size Distribution Using Thermal Inkjet Printing. *Cryst. Growth Des.* **2020**, *20*, 4667–4677. [[CrossRef](#)]
419. Topić, F.; Friščić, T. No Regioselectivity for the Steroid  $\alpha$ -face in Cocrystallization of Exemestane with Aromatic Cocrystal Formers Based on Phenanthrene and Pyrene. *Can. J. Chem.* **2020**, *98*, 386–393. [[CrossRef](#)]
420. Yuan, Z.J.; Dai, X.L.; Huang, Y.L.; Lu, T.B.; Chen, J.M. Cocrystals of Penciclovir with Hydroxybenzoic Acids: Synthesis, Crystal Structures, and Physicochemical Evaluation. *Cryst. Growth Des.* **2020**, *20*, 4108–4119. [[CrossRef](#)]
421. Singh, M.; Bhowal, R.; Vishwakarma, R.; Chopra, D. Assessing the Impact on Aqueous Solubility of Berberine Chloride via Co-crystallization with Different Stoichiometric Ratios of Pyromellitic Dianhydride. *J. Mol. Struct.* **2020**, *1200*, 127086. [[CrossRef](#)]
422. Dai, X.L.; Yao, J.; Wu, C.; Deng, J.H.; Mo, Y.H.; Lu, T.B.; Chen, J.M. Solubility and Permeability Improvement of Allopurinol by Cocrystallization. *Cryst. Growth Des.* **2020**, *20*, 5160–5168. [[CrossRef](#)]
423. Bhattacharya, B.; Das, S.; Lal, G.; Soni, S.R.; Ghosh, A.; Reddy, C.M.; Ghosh, S. Screening, Crystal Structures and Solubility Studies of a Series of Multidrug Salt Hydrates and Cocrystals of Fenamic Acids with Trimethoprim and Sulfamethazine. *J. Mol. Struct.* **2020**, *1199*, 127028. [[CrossRef](#)]
424. Surov, A.O.; Vasilev, N.A.; Voronin, A.P.; Churakov, A.V.; Emmerling, F.; Perlovich, G.L. Ciprofloxacin Salts with Benzoic Acid Derivatives: Structural Aspects, Solid-state Properties and Solubility Performance. *CrystEngComm* **2020**, *22*, 4238–4249. [[CrossRef](#)]
425. Jia, J.-L.; Dai, X.-L.; Che, H.-J.; Li, M.-T.; Zhuang, X.-M.; Lu, T.-B.; Chen, J.-M. Cocrystals of Regorafenib with Dicarboxylic Acids: Synthesis, Characterization and Property Evaluation. *CrystEngComm* **2021**, *23*, 653–662. [[CrossRef](#)]
426. Goldyn, M.R.; Larowska, D.; Bartoszak-Adamska, E. Novel Purine Alkaloid Cocrystals with Trimesic and Hemimellitic Acids as Cofomers: Synthetic Approach and Supramolecular Analysis. *Cryst. Growth Des.* **2021**, *21*, 396–413. [[CrossRef](#)]
427. Wang, J.; Dai, X.-L.; Lu, T.-B.; Chen, J.-M. Temozolomide–Hesperetin Drug–Drug Cocrystal with Optimized Performance in Stability, Dissolution, and Tableability. *Cryst. Growth Des.* **2021**, *21*, 838–846. [[CrossRef](#)]